Cholinergic modulation of distinct types of perisomatic region targeting interneurons and their involvement in carbachol-induced fast network oscillation in the CA3 region of the hippocampus

Ph.D. Dissertation

Gergely Szabó

Semmelweis University

János Szentágothai Doctoral School of Neurosciences

Supervisor: Norbert Hájos Ph.D., D.Sc.

Institute of Experimental Medicine
Hungarian Academy of Sciences
Laboratory of Network Neurophysiology

Official Reviewers of the Ph.D. Dissertation:

Gábor Czéh Ph.D., D.Sc.
Zita Puskár Ph.D.

Members of the Theoretical Examination Board:

Béla Halász Ph.D., D.Sc. - Chairman
József Kiss MD., Ph.D., D.Sc.
György Karmos MD., Ph.D.

Budapest
2012

TABLE OF CONTENTS

ABBREVIATIONS

5HT-3 receptor: 5-hydroxy-triptamine receptor type 3

AAC: axo-axonic cell

ACh: acetyl-choline

ACSF: artificial cerebrospinal fluid

AF/DX116: M2 receptor preferring antagonist

AIS: axon initial segment

BP: band pass

CA: cornu Ammonis

CB1R: cannabinoid receptor type I

CCh: carbachol

CCK: cholecystokinin

CR: calretinin

CTAP: D -Phe-Cys-Tyr- D -Trp-Arg-Thr-Pen-Thr-NH_2; MOR antagonist

DAMGO: [D-Ala^2,N-Me-Phe^4,Gly^5-ol]enkephalin acetate, MOR agonist

DG: dentate gyrus

DSI: depolarization induced suppression of inhibition

EC: entorhinal cortex

ECoG: electro-corticogram

EEG: electro-encephalogram

eGFP: enhanced green fluorescent protein

EPSP: excitatory postsynaptic potential

FSBC: fast spiking basket cell

GABA: γ-aminobutyric acid

GAD65: glutamate decarboxylase-65

GIRK: G protein-activated inwardly rectifying K^+ current

HIPP cell: hilar perforant path-associated cell

IPSC: inhibitory postsynaptic current

ISI: interneuron-selective interneuron

KCC2: K^+-Cl^-cotransporter type 2

KO: knockout

LFP: local field potential

LIA: large irregular activity

LTP: long term potentiation

M1-5 receptor: muscarinic acetylcholine receptor type 1-5

mAChR: muscarinic acetylcholine receptor

mEPSC: miniature excitatory postsynaptic current

MFA cell: mossy fiber associated cell

mGluR: metabotropic glutamatergic receptor

mIPSC: miniature inhibitory postsynaptic current

MOR: μ-opioid receptor

MS-DBB: medial septum-diagonal band of Broca

nAChR: nicotinic acetylcholine receptor

NBQX: 2,3-dihydroxy-6-nitro-7-sulfamoyl-benzo[f]quinoxaline-2,3-dione; an AMPA receptor antagonist

NGS: normal goat serum

O-LM cell: oriens-lacunosum-moleculare cell

PB: phosphate buffer

PET: positron emission tomography

PV: parvalbumin

QX-314: [2(triethylamino)-N-(2,6-dimethylphenyl) acetamine; a voltage dependent Na^+ channel blocker

RCA neuron: recurrent collateral-associated neuron

REM: rapid eye movement

RLM cell: radiatum-lacunosum moleculare cell

RSA: rhythmic slow activity

RSBC: regular spiking basket cell

SCA cell: Schaffer collateral-associated cell

SD: standard deviation

SEM: standard error of mean

SOM: somatostatin

Str: stratum

SWR: sharp wave-associated high-frequency ripples

T50 value: the width of currents at the half of the peak amplitude

TTX: tetrodotoxin

uIPSC: unitary inhibitory postsynaptic current

VGLUT: vesicular glutamate transporter

VIP: vasoactive intestinal polypeptide

WT: wild type

I. INTRODUCTION

In cortical structures only every fifth neuron is GABAergic (Somogyi et al., 1998), yet these cells significantly influence information processing in neuronal networks (Miles et al., 1996; Pouille and Scanziani, 2004). Based on the target preference the cortical GABAergic cells can be divided to cells innervating the perisomatic region of principal neurons and to cells targeting their dendrites. Perisomatic region targeting inhibitory cells can effectively modulate the generation of sodium-dependent action potentials, being able to determine the output of principal cells. On the other hand, dendrite targeting neurons are believed to be responsible for the control of the efficacy and plasticity of glutamatergic inputs received by dendritic domains (Cobb et al., 1995; Miles et al., 1996; Lovett-Barron et al., 2012). The investigations discussed in this thesis focused on the former neurons.

Perisomatic region targeting interneurons can be classified into two neurochemically distinct categories, namely to the group of the calcium binding protein *parvalbumin* (PV)-expressing cells and to the group of neurons that do not contain parvalbumin, but express the *type I cannabinoid receptors* (CB1R) on their axon terminals (Freund and Katona, 2007). The cell group containing parvalbumin consists of basket cells with fast spiking phenotype (FSBCs) that innervate the somata and the proximal dendrites of pyramidal cells as well as axo-axonic or chandelier cells (AACs) targeting the axon initial segments (AIS) of pyramidal neurons. GABAergic cells expressing CB1Rs involve basket cells with regular spiking phenotype (RSBCs) innervating the soma-near membrane surface of pyramidal cells.

Cholinergic neuromodulation is known to exert potent effects on different cognitive functions like attention (Deco and Thiele, 2009), learning (Hasselmo, 2006) and REM sleep (Heister et al., 2009). Since GABAergic interneurons are reported to be the target of cholinergic modulation in many ways (Hájos et al., 1998; Fukudome et al., 2004; Neu et al., 2007; Lawrence, 2008), it might be possible that acetylcholine released from the fibers with basal forebrain origin to distinct cortical areas exerts its effect, at least partly, through the influence of GABAergic interneurons. Although several investigations have been carried out regarding the cholinergic receptor composition in interneurons and their sensitivity to cholinergic receptor agonists, the effect of cholinergic receptor activation and its mechanisms have not been tested specifically on distinct types of perisomatic region targeting interneurons.

Since perisomatic region targeting interneurons are capable of synchronizing the firing of large cell assemblies (Cobb et al., 1995), these GABAergic cells may have a pivotal role in generating oscillatory activities in cortical networks. Indeed, recent studies have shown the participation of parvalbumin containing interneurons in the generation of oscillations at gamma (30-80 Hz) frequencies (Cardin et al., 2009; Fuchs et al., 2007), which oscillatory activities often coincide with sensory encoding, neuronal assembly formation, or memory storage and retrieval (Sederberg et al., 2003; Tiitinen et al., 1993; Montgomery and Buzsáki, 2007). Previous studies, however, have not separated the function of FSBCs and AACs in the generation of gamma oscillations and have not clarified the potential involvement of RSBCs in the oscillogenesis either. The main goal of this thesis was to investigate the effects of cholinergic receptor activation on the properties of perisomatic region targeting interneurons and to reveal their contribution to the generation of cholinergically induced fast network oscillations. These investigations were carried out in a cortical network, in the hippocampus. In the following chapters I will outline the main findings and experiences that paved the road for the experimental work that will be presented in the thesis.

Reviewing the literature

I/1. Role of hippocampus in memory functions and spatial navigation

The hippocampus and its related structures are one of the most extensively studied areas of the nervous system. This is partly due to its well defined three laminar structure, which shows complex organization together with relatively simple feature compared to other cortical brain regions. Furthermore, the structure of this archicortical brain region is similar in all mammals, in addition, it has several common features with the medial cortex of the reptiles (Northcutt, 1981; Rodriguez et al., 2002; López et al., 2003). These properties together with the unambiguous relation to such basic cognitive functions like learning and memory or spatial navigation rendered the hippocampus to be a popular experimental model of neurobiologists.

The potential role of the hippocampus in certain memory functions has emerged in the middle of the past century, when it was clarified that the damage of the hippocampus and other temporal lobe structures leads to memory loss. The most well known precedent is

related to Henry Gustav Molaison (1926–2008), famously known as H.M., an American memory disorder patient, who was widely studied from late 1957 until his death. In 1953 H.M. had a radical surgery to stop his uncontrollable epileptic seizures. He had an almost complete removal of hippocampi as well as the surrounding cortical structures involving a part of the amygdalar nuclei on both sides (Scoville and Milner, 1957; Corkin et al., 1997). After his surgery the seizures almost ceased but the operation also caused an unexpected result: he lost the capability to remember new facts about people, places or things after a few seconds. His severe anterograde amnesia accompanied him along his life (Corkin, 2002).

Besides the case of H.M. several studies have come out investigating amnesic patients. These studies reported similar memory deficits with more localized lesions in the hippocampus itself, or in its surrounding areas, such as the parahippocampal cortices, the entorhinal region or in the perirhinal cortical areas (Rempel-Clower et al., 1996; Aggleton and Saunders, 1997; Buffalo et al., 1998). Such human neuropsychiatric observations served as a basis for memory storing theories, suggesting that the function of the hippocampus is to create and store specific memories, which later can be recalled with appropriate (modified or partial) recalling stimuli. Furthermore, the hippocampus may participate in a so called memory consolidation process, during which the repeated reactivation of the memories stored in the hippocampus leads to the reorganization of memory-representations in the neocortex (Káli and Acsády, 2003). As a result, those memories that could originally be recalled only by the hippocampus, progressively become independent on it, and finally may build into the already existing unit of neocortical knowledge stored in the neocortex (Goshen et al., 2011).

Not all kinds of memories are influenced by the hippocampus. Those types of memories that do not require the long-term storage and retrieval of factual events are usually not damaged in amnesia. Typically the short-term or working memory as well as the so called *implicit* or *non-declarative* memories including sensory or motor skills, classical operant conditioning and the so called priming remain intact in patients with hippocampal dysfunctions. On the other hand, those memories that are related to specific facts, persons or happenings, mostly intentionally recollected information of previous experiences, are believed to require the participation of hippocampal formation and are typically damaged in amnesia. We refer to this type of memory as *explicit* or *declarative memory* (since the encoded information can be explicitly declared) and it consists of two

subtypes, episodic and semantic memory. Episodic memory consists of the recollection of singular events of one's life, events that can be recalled as personal experiences. Semantic memory can be defined as factual information from one's past that cannot be necessarily bound to a given event; a knowledge of historical events and figures, knowledge of handling objects, meaning of words and concepts. To date it is a debated question whether episodic and semantic memories are similarly involved in amnesia. According to certain theories the temporal lobe areas including the hippocampus contribute equally to the processing of all kind of declarative memories (Squire, 1992; Squire and Zola, 1998). An alternative view is that the hippocampus is necessary for remembering ongoing life's experiences (episodic memory), but not necessary for the acquisition of factual knowledge (semantic memory; Tulving and Markowitsch, 1998). This idea was proposed by Vargha-Khadem and her colleagues on the basis of their study of three young people suffering from anterograde amnesia caused by hippocampal damage soon after their birth. Although these patients had severely impaired episodic memory, the acquisition of factual knowledge typical of their age was normal (Vargha-Khadem et al., 1997). The finding that in anterograde amnesia it is quite possible for episodic memory to be more severely impaired than semantic memory suggests that semantic memory can occur independently of episodic memory. Taken together, the hippocampus (together with anatomically related structures) is principally essential for episodic memory (Káli and Acsády, 2003).

Ability of navigation in space is another special feature that is attached to hippocampal function. As it is known for some decades, the firing frequency of certain hippocampal pyramidal cells markedly increases, when the animal enters to a given area of its environment. We refer to this area as a *place field* and to the corresponding cell as a *place cell* (O'Keefe and Dostrovsky, 1971). The discovery of place cells led to the "cognitive mapping" theory (O'Keefe and Nadel, 1978), which claims that the hippocampus functions as a cognitive mapping system by creating the spatial representation of the animal's location relative to its environment. Such a cognitive map would serve to plan the most appropriate track to the place, where the animal wants to go. The most frequently used tool to test spatial navigational skills of experimental animals is the Morris water maze, where the animal has to find a hidden platform to climb out, while swimming in opaque water. The time spent in the water negatively correlates to the extent of spatial representation. Rats learn quickly the location of the platform, even if it is under the water. However, in an experiment, when the hippocampi were partly isolated from their

connections by cutting the fornices, the rats were unable to find the platform (Morris et al., 1982). In another experiment the hippocampi were transiently inactivated in rats before the learning phase or during the retrieval phase in the maze. The researchers found that the hippocampus is necessary either to learn or retrieve information regarding the location of the platform (Riedel et al., 1999).

Spatial navigation skills have been demonstrated to be related to the hippocampus also in humans. It has long been known that spatial orientation presents difficulty to people with hippocampal damage. When amnesic patients with bilateral hippocampal lesions were studied, they were found to have no information about the spatial environments they contacted after the injury, however, they had precise information about the environment, where they had grown up (Teng and Squire, 1999; Rosenbaum et al., 2000). The involvement of the hippocampus in spatial navigation has also been shown in a line of studies of taxi drivers in London. When structural MRIs of taxi drivers' brain were compared to control subjects, they were found to have significantly larger posterior hippocampi (Maguire et al., 2000). Interestingly, when taxi drivers were compared to bus drivers, who have to follow a constrained set of routes all day, the authors found that taxi drivers had greater gray matter volume in mid-posterior hippocampi, suggesting that higher spatial knowledge requires higher computational power of the hippocampus (Maguire et al., 2006). In another study of the same group positron emission tomography (PET) was used to examine the brain function in London taxi drivers with many years of experience, while they recalled complex routes around the city. Compared with baseline this resulted in activation of a network of brain regions, including the right hippocampus (Maguire et al., 1997).

Contextual learning is also a typical feature that can be linked to the hippocampus. For example, it is known for several learning tasks that during the recall the response is much stronger, if the experiment is achieved at the same environment (same context), where the learning has taken place. With lesioned hippocampus this effect could not be observed (Good and Honey, 1991). Fear learning, a phenomenon that is closely linked to the function of amygdalar nuclei, also has a contextual component, which was shown to require intact hippocampus (contextual fear conditioning, Kim and Fanselow, 1992).

In this section I outlined the basic hippocampal functions. Before I would review the literature of the possible cellular mechanisms behind these functions and the network oscillations it is necessary to delineate the structure and anatomy of the hippocampus.

I/2. Hippocampal anatomy: structure, connections, cell types

As I mentioned above, the hippocampus is a quite conservative formation, the basic hippocampal architecture is common to all mammals, yet, it nonetheless demonstrates substantial species differences. Since our experiments have been carried out in mice, I disregard to review these differences and restrict to discuss only the anatomy of the rodent hippocampus.

Hippocampal connectivity, principal cells

The hippocampus is a part of the middle arc of the limbic system. The crescent-shaped, bilateral structure is localized between the neocortex and the diencephalon (Fig. 1). Through the *fimbria* it is reciprocally connected to subcortical areas and to the contralateral hippocampus by the commissural fibers. The only neocortical input originates from the entorhinal cortex, we refer to this as *perforant path*; the neocortical output mostly consists of indirect or direct projections back to the entorhinal cortex through the subiculum or straight to the entorhinal cortex, respectively (Fig. 2).

Besides its reciprocal connections with the entorhinal cortex, the hippocampus (CA1 region, see later) gives rise to projections to the perirhinal and postrhinal cortices as well as to prefrontal cortex and also to the amygdaloid complex. With the exception of the prefrontal cortex, these areas all project back to the hippocampus (CA1) (Andersen et al., 2007). The *hippocampus proper* consists of three subdivisions, named after the *Cornu Ammonis* by Lorente de Nó: CA3, CA2, and CA1. The connected areas together compose the *hippocampal formation* constituting a functional unit, which includes the dentate gyrus, the subiculum, the presubiculum, the parasubiculum, and the entorhinal cortex. Hippocampal connectivity has a characteristic feature, which differs markedly from the connections organized in the neocortex. Whereas commonly the neocortical regions are reciprocally connected (Felleman and Van Essen, 1991), this is not true for the connectivity of the hippocampal formation, since as first described by Ramón y Cajal (1893), these connections are predominantly unidirectional (Fig. 2).

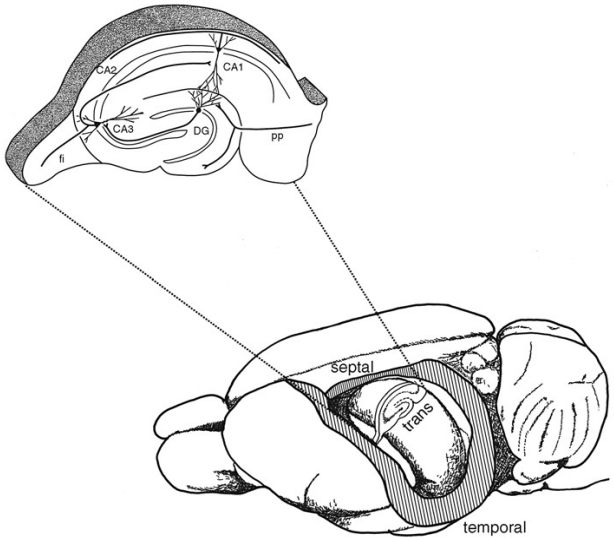

Figure 1. Line drawing of the localization of the hippocampal formation in the rat brain. Cross-section of the hippocampal formation depicts the basic *in situ* connectivity of the trisynaptic circuit, septotemporal and transverse axes are also indicated. (Adapted from Andersen et al., 2007.)

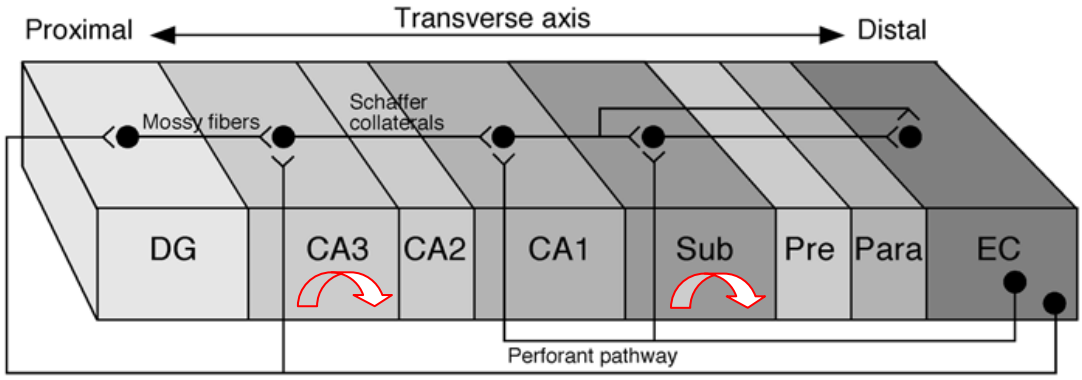

Figure 2. Scheme of the connections of the different subregions of the hippocampal formation. The information flow through the hippocampus. The hippocampus possesses bidirectional communication with the EC. Layer II cells of the entorhinal cortex (EC) project to the dentate gyrus (DG) and to the CA3 region of the hippocampus via the perforant path. Layer III neurons of the EC project to the CA1 region of the hippocampus via the temporoammonic pathway. The axons of the granule cells in the DG forming mossy fibers innervate the CA3 cells. Besides their dense local recurrent collaterals (indicated by arrows), CA3 pyramidal cells innervate the CA1 neurons via the Schaffer collaterals. Pyramidal cells of the CA1 field of the hippocampus and the subiculum project back to the layer V-VI of the EC. (Adapted from Andersen et al., 2007, modified.)

The afferent and efferent connections of the hippocampal formation mostly consist of glutamatergic fibers originating from the *principal cells*, which neurons compose the

85% of the neuronal population in the brain region. The first step in the intrinsic hippocampal circuit is traditionally considered to be the cells in layer II of the entorhinal cortex, due to the fact that much of the neocortical input reaching the hippocampal formation does so through the entorhinal cortex (Andersen et al., 2007). The pyramidal cells of layer II of the entorhinal cortex that project to the dentate gyrus give rise to the major hippocampal input pathway called the perforant path. The dentate gyrus does not project back to the entorhinal cortex.

The principal cells of the dentate gyrus, called the granule cells, give rise to axons called *mossy fibers* synapsing on pyramidal cell dendrites in the CA3 field of the hippocampus. Mossy fibers do not innervate granule cells but make synapses on the dendrites of the so called *mossy cells*, which cells are localized in the polymorphic layer of the dentate gyrus (hilus). Mossy cells are glutamatergic and project back to the molecular layer of dentate gyrus and innervate granule cell dendrites both ipsi- and contralaterally. These cells thus seem to be the major source of the glutamatergic associational/commissural projection to the dentate gyrus (Andersen et al., 2007).

Similarly to the dentate gyrus, the principal cells of the CA3 region do not project back to the granule cells. The output of CA3 pyramidal cells composes the major input of CA1 pyramidal cells, these fibers are called *Schaffer collaterals* and are also nonreciprocal. Likewise, CA1 pyramidal cells project unidirectionally to the subiculum or back to the entorhinal cortex. The entorhinal cortex also project to the CA1, but this projection originates from layer III cells and not from layer II, the origin of perforant path. This projection (so called temporo-ammonic pathway) follows a topographical organization: the lateral entorhinal area projects to the distal portion of the CA1 (close to the subiculum), while those fibers that originate in the medial entorhinal area innervate the proximal portion (close to CA2). It has been recently demonstrated that layer III entorhinal cortical cells also project to the CA2 region, thus layer II and layer III entorhinal cortical inputs converge on CA2 pyramidal neurons (Chevaleyre and Siegelbaum, 2010).

The sequential information flow in the hippocampus introduced above is also known as the *trisynaptic circuit,* involving the entorhinal cortex-dentate-gyrus; dentate gyrus-CA3; CA3-CA1 connections (Fig. 1). The specific features of these connections and the participating hippocampal fields will be discussed in details in the following section together with introducing the here localized interneurons.

Interneurons

Besides principal cells the remaining 15 % of hippocampal neurons are mainly GABAergic neurons (i.e. releasing γ-aminobutyric acid as the main neurotransmitter). These inhibitory cells are usually defined as interneurons, since the majority of them are local-circuit neurons, although some types with commissural or even extrahippocampal projections are also known. Whereas the glutamatergic cells in the hippocampus show relative homogeneity, interneurons have been found to be much more diverse. By way of example, in a study of CA1 interneurons 21 different types of GABAergic neuron were collected (Klausberger and Somogyi, 2008; Fig. 3).

The categories of interneurons based on morphological characteristics and certain neurochemical marker expressions are fairly similar in all hippocampal regions. Thus, the interneuron repertoire of the CA1 region shown by the review of Klausberger and Somogyi (2008) might be more or less valid to all the hippocampal fields; the homologous cell types of CA1 interneurons often can be found in the CA3, or in the dentate gyrus, even if they have different nomenclature.

The morphological classification of interneurons considers mainly their dendritic and axonal arborization. The dendritic localization provide information about the inputs, whereas the location of axonal terminals shows the outputs of interneurons, allowing us to predict their potential role played in neuronal networks.

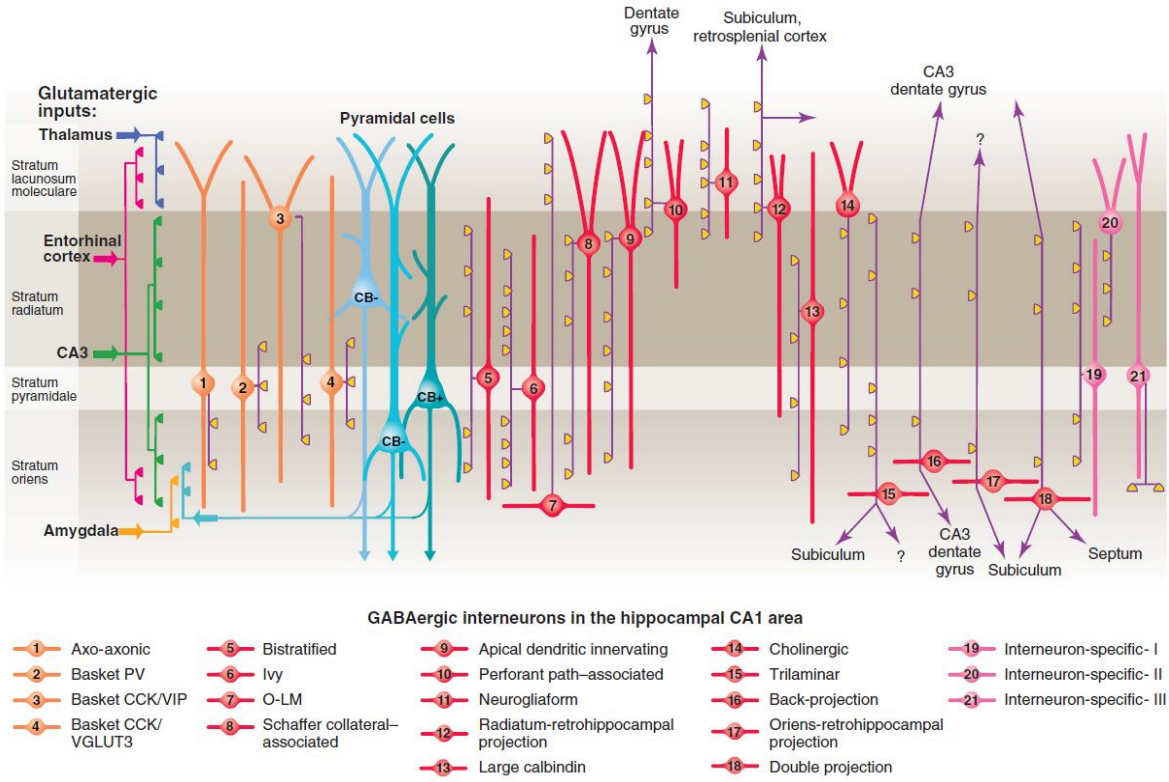

Figure 3. Interneuron diversity in the CA1 region of the hippocampus. In 2008 at least 21 different interneuron types were identified by Klausberger and Somogyi. Three types of pyramidal cells were also distinguished based on localization and immunopositivity for the calcium binding protein calbindin. The main targets of glutamatergic inputs are shown on the left. The somata and dendrites of interneurons synapsing on pyramidal cells (blue) are orange, and those innervating mainly other interneurons are pink. Axons are purple; the main synaptic terminations are yellow. Axon terminals originating from different interneuron types innervate the perisomatic region (left) and either the Schaffer collateral/commissural or the entorhinal pathway termination zones (right), respectively. VIP, vasoactive intestinal polypeptide; VGLUT, vesicular glutamate transporter; O-LM, oriens lacunosum moleculare. Source: Klausberger and Somogyi, 2008.

The comparison of morphological categories based on neurochemical markers produces further distinctions that may reveal differences in neuronal function. For instance, as we will see, the presence or absence of the Ca^{2+} binding protein parvalbumin assigns basically different functions to morphologically similar cell types.

Based on their axonal arborization hippocampal inhibitory cells can be classified into four main groups:

1) **perisomatic region targeting cells**, with axons terminating on the perisomatic region of the target neurons;
2) **dendrite targeting neurons** that innervate the dendritic regions of their target cells;
3) **interneuron-selective interneurons** that synapse on other inhibitory cells;
4) **long-range projecting GABAergic cells** that project their axons to other brain regions.

Perisomatic region targeting interneurons, which are the main subject of interest of the thesis, play critical role in regulating the action potential generation in principal cells. Only single inhibitory postsynaptic potentials (IPSPs) produced by perisomatic region targeting interneurons were shown to be able to suppress repetitive firing of pyramidal cells (Miles et al., 1996).

Perisomatic region targeting interneurons are largely similar in all cortical areas including the hippocampus. All types, that can be distinguished based on either morphology or neurochemical markers, occur in the dentate gyrus and also in the cornu Ammonis. Perisomatic region of pyramidal cells is defined as a domain of plasma membrane, which includes the cell body, the axon initial segment, and the proximal apical and basal dendrites (Freund and Katona 2007). This region is targeted by at least three types of inhibitory neurons, the fast spiking basket cells (FSBC), the regular spiking basket cells (RSBC) and the axo-axonic cells (AAC).

Basket cells by forming a “basket” around the somata of pyramidal neurons give rise to multiple contacts on their membrane (Colonnier, 1968; Freund and Buzsáki, 1996). In contrast, AACs specifically target the axon initial segments (AIS) of pyramidal cells (Somogyi, 1977). Whereas basket cells innervate not only principal cells but also other interneurons, AACs exclusively target principal cells (Somogyi et al., 1982).

The two basket cell types have characteristically different expression patterns of certain types of receptors, transmitters or modulators (Freund, 2003). For instance, RSBCs are predominantly immunopositive for cholecystokinin and express CB1Rs, whereas FSBCs are known to express the Ca^{2+} buffering protein parvalbumin (PV) (Pawelzik et al., 2002). RSBCs show regular spiking phenotype and are able to integrate consecutive independent excitatory inputs, which make them fire. In contrast, FSBCs show fast spiking phenotype and respond reliably to subtle and repetitive excitation with precisely timed action potentials (Glickfeld and Scanziani, 2006).

A special perisomatic region targeting neuron type of the CA3 region is called mossy fiber associated (MFA) neuron. Typically, these cells have axons coaligned with the mossy fibers. Their dendrites are located in the strata radiatum and oriens, the axons are terminated on the proximal apical dendritic shafts, and to a lesser degree, on the somata of pyramidal cells being in a position to selectively suppress the dentate gyrus input (Gulyás et al., 1993; Vida and Frotscher, 2000). The boutons of MFA cells are sensitive to CB1R activation (Losonczy et al., 2004). MFA cells show quite similar neurochemical and physiological properties to RSBCs (Szabó GG, Papp O, Hájos N, unpublished observations).

AACs also tend to show fast spiking phenotype and express PV. These cells are particularly in a position to effectively control pyramidal cell firing by targeting the site of action potential generation, i.e. on the AIS (Somogyi, 1977; Somogyi et al., 1982). In spite of their GABAergic nature, in certain conditions their postsynaptic effect were reported to be excitatory, because of the low levels of K^+ - Cl^- cotransporter (KCC2) in the AIS (Szabadics et al., 2006). Since then, the hyperpolarizing or depolarizing nature of AACs is still a debated question waiting to be resolved (Glickfeld et al., 2009; Woodruff et al., 2010).

Dendrite targeting interneurons compose the majority of inhibitory input in the hippocampus. For instance, in the CA1 region 92% of GABAergic synapses terminates the dendritic region of pyramidal cells (Megiás et al., 2001). The axonal endings of the dendrite targeting interneurons usually terminate on those dendritic membrane surfaces of principal cells, where the specific glutamatergic inputs are received. Therefore they are believed to be responsible for the control of the efficacy and plasticity of excitatory inputs targeting the same dendritic region (Miles et al., 1996).

As mentioned above, the layer II entorhinal cortical input through the perforant path arrives to the dentate gyrus. These fibers synapse on the dendritic spines of the granule cells in the so called *molecular layer*. The granule cells themselves compose a compact layer called the *granule cell layer*. The third layer of the dentate gyrus is the *hilus or polymorphic layer*, which localized next to the CA3 region (Fig. 1). A variety of dendrite targeting interneurons can be found in all the three layers. Similarly to the CA regions, all the dendritic surfaces of granule cells are covered by the axon terminals of different types of dendrite targeting cells (Freund and Buzsáki, 1996). This arrangement probably allows to control all the excitatory inputs received by granule cells (entorhinal afferents, commissural/associational afferents, mossy fiber collaterals). Since the thesis focuses on the CA3 region these interneurons will not be characterized in details, but their organization is well noticable on Figure 4.

The granule cell axons leaving the dentate gyrus enter the CA3 region forming a bunch of fibers, called mossy fibers because of their special synaptic terminals innervating the CA3 pyramidal neurons. The single large boutons of mossy fibers synapsing on the complex branched spines together give rise to the so-called thorny excrescences (Hamlyn, 1962). Because of the lack of myelin the layer formed by this special contact can be visualized in fresh tissue, thus it was named as *stratum lucidum*. This layer is unique to the CA3, the other two CA regions do not have stratum lucidum, since they do not receive mossy fiber input. The somata of the principal cells constitute the *pyramidal cell layer*. CA3 pyramidal cells have typically larger somata compared to the CA2 or CA1 region. The apical dendrites of CA3 pyramidal cells span three strata: *the stratum lucidum, the stratum radiatum and the stratum lacunosum moleculare*. The basal dendrites extend into *stratum oriens* towards the *alveus*. CA3 region consists three subregions: CA3c, b and a (from the hilus towards the CA1, respectively).

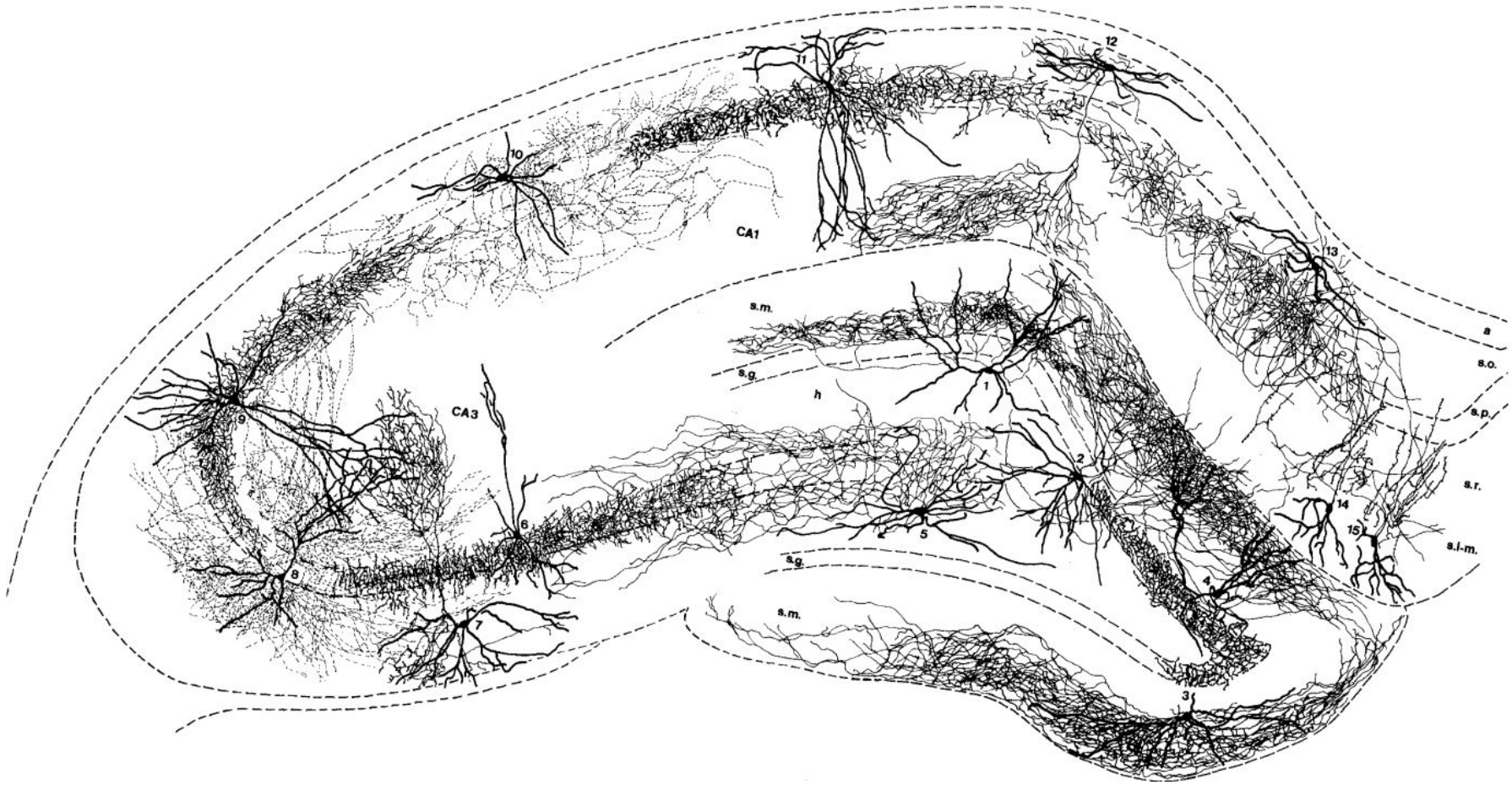

Figure 4. Drawing of different types of interneurons of the hippocampal formation based on camera lucida reconstructions in rodents. Thick lines represent the dendritic trees, thin ones indicate axons. Note that the different interneurons innervate all the dendritic and perisomatic regions of both granule and pyramidal cells. Most interneurons of the dentate gyrus shown here are not mentioned in the text. 1: HICAP (*hilar commissural-associational pathway related)* cell. 2: HIPP *(hilar perforant path-associated)* cell. 3: MOPP (*molecular layer perforant path-associated)* cell. 4: VIP-containing basket cell. 5: Trilaminar cell of CA3c. 6: Axo-axonic (or chandelier) cell. 7: 0-LM cell of CA3. 8: Bistratified cell of CA3. 9 Basket cell with axon in CA3 and CAl. 10: Bistratified cell of CA1. 11: Basket cell of CA1. 12: OLM cell of CA1. 13: Horizontal trilaminar cell of CA1. 14,15: IS-2 (interneuron selective) VIP-containing cells. a, alveus; s.o., s.p., s.r., s.1-m., strata oriens, pyramidale, radiatum, and lacunosum-moleculare of the hippocampus; s.m., s.g., h, strata moleculare, granulosum, and hilus of the dentate gyrus. Adapted from Freund and Buzsáki, 1996.

The dendrite targeting interneurons localized here show marked heterogeneity similarly to other parts of the hippocampus. Here I briefly summarize these interneurons with a particular interest to the differences compared to the well documented CA1 region (Klausberger and Somogyi, 2008; Fig. 3.).

The somata and dendrites of *Oriens-lacunosum-moleculare cells* (OLM cells) are localized in the stratum oriens and their axonal arbor in the stratum lacunosum moleculare (McBain et al., 1994; Sík et al., 1995; Maccaferri and McBain, 1996). They innervate the apical tufts of the pyramidal cell dendrites, being able to influence the excitation caused by entorhinal cortical inputs on pyramidal cells. OLM cells express the neuropeptide somatostatin, a metabotropic glutamate receptor type mGluR1α (Baude et al., 1993) and parvalbumin (PV) (Klausberger et al., 2003). *Bistratified cells* are mostly located with their cell bodies within or close to the pyramidal layer and synapse onto oblique and basal dendrites of pyramidal cells (Buhl et al., 1994; Klausberger et al., 2004). Similarly to the previously introduced fast spiking basket cells, it expresses PV and shows fast spiking phenotype (Klausberger et al., 2004). OLM and bistratified cells occur both in CA3 and CA1 region.

CA3 (and also CA2) region characteristically possesses extended recurrent collaterals originating from the pyramidal cell axons. These collaterals form dense associational connections in the stratum radiatum and stratum oriens (Li et al., 1994). Probably the GABAergic regulation of these excitatory inputs is partly achieved by the *recurrent collateral associated* (RCA) neurons, which cells are located in the stratum radiatum and project its axons to the dendritic regions of pyramidal cells in the stratum radiatum. Similarly, the *radiatum-lacunosum moleculare* (RLM) *cells,* with their somata located in the stratum radiatum and their axonal arbor in the stratum lacunosum moleculare, probably participate in the control of incoming information through the perforant path. Both cell types are CB1R immunopositive (Szabó GG, Papp O and Hájos N, unpublished observations).

The CA2 subfield is a narrow zone of cells interposed between CA3 and CA1 regions. Similarly to CA3, CA2 has pyramidal cells with large cell bodies but is not innervated by mossy fibers like CA1. Its role in hippocampal computation remained elusive, and its presence in the hippocampus is often neglected, however recent studies suggest that the participation of CA2 in hippocampal circuitry has to be reconsidered (Chevalyre and Siegelbaum, 2010; for a review see Jones and McHugh, 2011). The

interneuronal composition of CA2 area seems to be also quite unique (Mercer et al., 2010; Mercer et al., 2012), but far less data are available regarding inhibitory cells compared to the CA3 or the CA1 region.

Following the route of information flow through the trisynaptic circuit the next station is the CA1 region. Pyramidal cells of the CA3 and CA2 project to the CA1. The fibers of CA3 pyramidal cell axons reaching CA1 compose the Schaffer collaterals and organized in a three-dimensional, topographical fashion.

Similarly to CA3, the input-specified interneurons occur also in CA1. The so called *perforant path-associated cells* innervate the apical dendritic tufts of the pyramidal cells. The cell bodies of these cells can mostly be found at the border of the strata radiatum and lacunosum-moleculare, their dendrites can reach all layers or remain in the stratum lacunosum-moleculare (Hájos and Mody, 1997; Klausberger et al., 2005). To the target area of CA3 input the so called *Schaffer collateral-associated* (SCA) *cells* are partnered. These interneurons synapse on the oblique dendrites and to a lesser extent also on the basal dendrites of pyramidal cells. The somata of this cell group are mainly located in the stratum radiatum, their dendrites reach all layers (Hájos and Mody, 1997; Cope et al., 2002; Pawelzik et al., 2002). Additionally, Klausberger also defines a category of the so called *apical dendrite innervating cells* having quite similar morphology to SCA cells, but innervating mostly the main apical shaft instead of the oblique dendrites (Klausberger et al., 2005).

Specific interneurons, such as *neurogliaform cells* and *ivy cells* can also be found both in the CA3 and CA1 region (Price et al., 2005; Szabadics and Soltész, 2009; Price et al., 2005). Neurogliaform cells uniquely produce slow $GABA_A$ and $GABA_B$ receptor-mediated responses on their target cell, release GABA by volume transmission and show gap junctional coupling to each other (Price et al., 2005; Simon et al., 2005; Zsiros and Maccaferri, 2005; Szabadics et al., 2007; Zsiros et al., 2007; Oláh et al., 2009). Neurogliaform cells can usually be found in the stratum lacunosum moleculare and target the apical tufts of the principal cells (Price et al., 2008). Ivy cells are similar to neurogliaform cells in many aspects but are located in the strata pyramidale or radiatum and innervate the oblique and basal dendrites of pyramidal cells (Fuentealba et al., 2008).

In contrast to the different inhibitory cells introduced so far, in the hippocampus such interneurons also exist that specifically innervate other interneurons. These cells are called **interneuron-selective interneurons**. Their group may be divided to at least three

different subclasses and a typical common feature of them is their immunopositivity for the Ca^{2+} binding protein calretinin and/or the vasoactive intestinal polypeptide (VIP)(Acsády et al., 1996a; Acsády et al., 1996b; Freund and Buzsáki, 1996; Gulyás et al., 1996).

In the hippocampus not all the GABAergic cells are local-circuit neurons. Several types of inhibitory neurons have projections to other brain areas, these cells are refered to as long-range **projecting GABAergic cells**. Long-range GABAergic connections are supposed to be well suited to coordinate the timing of activity between brain regions (Buzsáki and Chrobak, 1995). The most studied remote target of the hippocampal GABAergic projecting neurons is the medial septum. These *hippocampo-septal cells* can be found in all parts of the hippocampus: in the CA1 region they are mainly located in the stratum oriens; in the CA3 region, they are scattered throughout all the layers; and in the dentate gyrus (DG), they are exclusively located in the hilar area (Totterdell and Hayes, 1987; Jinno and Kosaka, 2002; Gulyás et al., 2003). It has to be mentioned that the hippocampus also receives GABAergic inputs from the medial septum, thus these two areas are reciprocally connected (Raisman, 1966; Takács et al., 2008). Furthermore, septal GABAergic neurons specifically innervate hippocampal GABAergic neurons (Freund and Antal, 1988; Gulyás et al., 1991). Another group of projecting neurons projects to the subiculum. These cells were described mostly in the CA1 stratum oriens (Losonczy et al., 2002; Ferraguti et al., 2005). Moreover, a GABAergic projection from the CA1 region to the retrosplenial cortices were also reported (Jinno and Kosaka, 2002; Van Groen and Wyss, 2003; Jinno et al., 2007). And finally, Attila Sík and his colleagues also described a long-range, cross-regional inhibitiory cell projecting from the CA1 region back to the CA3 and hilar regions (Sík et al., 1994). More recently such somatostatin (SOM) expressing interneurons have also been identified in the CA1 region and also in the dentate gyrus which project back to the medial entorhinal cortex. Additionally, PV expressing GABAergic neurons in the medial entorhinal cortex have been shown to project back to the hippocampus and target on other interneurons, indicating bidirectional entorhinal-hippocampal connectivity (Melzer et al., 2012).

Subcortical connectivity of the hippocampus

Similarly to all cortical areas the hippocampus receives extended subcortical afferents. From the brain stem all the ascending monoaminergic pathways reach the

hippocampal regions. The hippocampus receives noradrenergic input from the locus coeruleus (Jones and Moore, 1977; Moore and Bloom, 1979), serotoninergic fibers from the medial and dorsal raphe nuclei (Freund et al., 1990a; Freund, 1992) and dopaminergic input from the ventral tegmental area (Scatton et al., 1980). All types of monoaminergic molecules released from these fibers were demonstrated to act on cortical principal neurons and influence glutamate release at the presynaptic sites (Scanziani et al., 1993; Aghajanian and Marek, 1999; Chu et al., 2010). Furthermore, neuromodulatory signals from the supramammillary and tuberomammillary nuclei of the hypothalamus reach the CA2 area and also the dentate gyrus (Panula et al., 1989; Maglóczky et al., 1994).

Often the effects of monoamines are not directly exerted on principal cells but transmitted by hippocampal interneurons. For instance, RSBCs that express 5-hydroxy-triptamine-3 (5HT-3) receptors (Morales and Bloom, 1997; Ferezou et al., 2002) are innervated by serotonergic afferents (Freund et al., 1990b), thus they might be able to convey the information carried by the raphe nucleus to all the neurons that are controlled by the basket cells (Papp et al., 1999). Moreover, Varga and his colleagues have recently demonstrated that fibers originating from the median raphe nucleus produce not only a slow modulatory effect but a rapid activation of hippocampal interneurons by glutamate/serotonin co-transmission (Varga et al., 2009).

The most dominant and most studied subcortical input to the hippocampus originates from the medial septum-diagonal band of Broca (MS-DBB), which is a mixed fiber system containing both cholinergic afferents and also reciprocal GABAergic projections (Mosko et al., 1973; Baisden et al., 1984; Amaral and Kurz, 1985; Freund and Antal, 1988; Tóth and Freund, 1992; Tóth et al., 1993). Since the main subject of the current thesis is the cholinergic modulation of interneurons and fast network oscillations, I will introduce this subcortical input and its effect on the hippocampus more detailed. The GABAergic component of MS-DBB input will be presented in the section introducing the generation of the theta (4-8 Hz) rhythm.

Fifty to 75% of the cells in the MS-DBB that project to the hippocampal formation are cholinergic (Andersen et al., 2007). Most of these cholinergic fibers are diffuse and rough in topographical organization (Záborszky et al., 1999). The nature of neurotransmission between these fibers and hippocampal cells is not fully explored or remained controversial (reviewed by Sarter et al., 2009). Several studies concluded that the great majority of cholinergic terminals make synaptic specializations only rarely and rather

influence their targets by volume transmission (Chedotal et al., 1994; Umbriaco et al., 1994; Descarries and Mechawar, 2000; Mechawar et al., 2000). In some studies, septal cholinergic fibers were shown to establish contacts with both principal neurons and interneurons on their cell bodies, dendritic shafts and spines (Frotscher and Léránth, 1985, 1986). Additonally, a few intrahippocampal cholinergic cells were also described (Frotscher et al., 1986). These cholinergic cells also express CR and/or VIP, thus may belong to the interneuron-selective category (Freund and Buzsáki, 1996). In a recent study the authors using molecular-anatomical approaches have demonstrated that the subcellular distribution of the muscarinic receptor type 1 (M1 receptor), which is the most predominant subtype of muscarinic cholinergic receptors (mAChRs) in the hippocampus, suggest that these receptors are likely to be activated by volume transmission (Yamasaki et al., 2010).

Cholinergic neuromodulation has complex effects on both glutamatergic and GABAergic neurons in the hippocampus exerted by the binding of acetylcholine (ACh) either to ionotropic nicotinic receptors (nAChRs) or mAChRs at pre- and postsynaptic locations. Hippocampal principal neurons do not express functional nAChRs at anatomically detectable levels (Frazier et al., 1998b; Frazier et al., 2003), however, physiological studies suggested the existence of the α7 subunit containing nAChRs on glutamatergic terminals in the hippocampus (Gray et al., 1996; Albuquerque et al., 2009). Regarding the mAChRs, with the exception of M5, all subtypes are expressed in the hippocampus (Levey et al., 1995). While the M1 and M3 types are widely expressed in pyramidal cells, the M2 and M4 receptors are expressed mostly in interneurons (Levey et al., 1995).

Acetylcholine on pyramidal cells usually induces membrane depolarization via the activation of M1 and M3 receptors, both are G_q -linked mAChRs (Young et al., 2005; Gulledge and Kawaguchi, 2007), although mAChR activation might also cause hyperpolarizing effects on the membranes of pyramidal cells (Gulledge and Kawaguchi, 2007). G_q activation leads to closure of various types of potassium channels (Krnjevic et al., 1971; Nakajima et al., 1986; Guerineau et al., 1994), as a result, depolarizes the membrane of pyramidal neurons and increases membrane resistance (Cole and Nicoll, 1984). In the neocortex this effect has been demonstrated to be clearly due to the activation of M1 receptors (Gulledge et al., 2009). Beside the effect on excitability mAChRs have also been shown to influence the glutamate release from Schaffer collaterals in the CA1

region suggesting a presynaptic locus of action, which is mediated by M4 receptors (Dasari and Gulledge, 2011).

Moving to the interneuron populations the number of potential targets of cholinergic action is increasing. Hippocampal interneurons can be influenced by activation of nAChRs. Both pharmacological (Jones and Yakel, 1997) and synaptic activation (Frazier et al., 1998a) of nAChRs produce a brief and fast depolarization or inward current due to their ionotropic nature. Different interneuron types show great variability regarding their responsiveness to nicotinic receptor agonists. According to a study carried out in the CA1 region, interneurons with axons ramifying throughout dendritic layers respond with fast depolarization mediated by α7-subunit containing nACh receptors. Interneurons located in the stratum oriens with axons ramifying in the stratum lacunosum moleculare (OLM cells) display a dual-component response with an initial fast phase mediated by α7-subunit containing nAChRs followed by a non- α7 nAChR-subunit dependent depolarizing phase. Perisomatic region targeting interneurons were found to be insensitive to nAChR agonists (McQuiston and Madison, 1999b).

Activation of mAChRs influences inhibitory transmission in a similarly complex manner. For instance, as it has been demonstrated, pharmacological activation of mAChRs increases the frequency and amplitude of spontaneous IPSCs (Pitler and Alger, 1992a), whilst at the same time depresses monosynaptically evoked IPSCs and the frequency of miniature IPSCs (Behrends and Ten Bruggencate, 1993). This means that mAChRs may affect the function of interneurons at least at two different loci: influence the firing rate by shifting the membrane potential (postsynaptic effect); and control the release of GABA by acting on presynaptically localized receptors.

Regarding the postsynaptic effects of mAChRs, CA1 interneurons have been shown to exhibit a wide range of responses to muscarinic receptor agonists; while some interneurons hyperpolarize, others exhibit a biphasic response, or do not respond. Muscarinic receptor activation increases the excitability of the majority of interneurons in all layers of the CA1 region by shifting the membrane potential to more positive values (Parra et al., 1998; McQuiston and Madison, 1999a). In the interneurons localized in the stratum oriens, these depolarizing effects have been shown to be due to the action of M1 and M3 receptors (Lawrence et al., 2006). Regarding other layers of the CA1, membrane potential of regular spiking basket cells (RSBCs) and Schaffer collateral associated neurons has been demonstrated to be controlled via M3 mAChRs, whereas the parvalbumin (PV)

expressing fast spiking basket cells (FSBCs) solely via M1 mAChRs (Cea-del Rio et al., 2010; Cea-del Rio et al., 2011).

Also the transmitter release from GABAergic terminals is controlled by mAChRs. In these processes usually the M2 and M4 receptors participate. In perisomatic region targeting interneurons M2 receptors have been shown to be expressed at the parvalbumin positive axon endings (Hájos et al., 1998), where they can effectively reduce GABA release (Fukudome et al., 2004) via triggering G protein-activated inwardly rectifying K+ (GIRK) currents (Ben-Chaim et al., 2003).

An indirect action of muscarinic receptor agonists that affect presynaptic GABA release is also known. Activation of postsynaptically localized M1/M3 receptors on pyramidal cell membrane may trigger the release of endogenous cannabinoid molecules (endocannabinoids), which binding to CB1Rs effectively inhibits the release of GABA from cholecystokinin (CCK) expressing terminals (Fukudome et al., 2004; Lawrence, 2007; Neu et al., 2007).

Taken together, the massive variety of targets where acetylcholine might exert its effect suggests that if we want to make predictions about the functions of such a complex phenomenon like cholinergically-induced network oscillations, it is crucial to know how the different elements of the network behave during cholinergic receptor activation.

I/3. Network activity patterns correlate with hippocampal function

Oscillatory activities in the hippocampus and their potential roles in higher order cognitive functions

The encoding capacity of cortical regions becomes several fold higher, if the information to be stored is based not only on the firing frequency (rate coding), but also on the relative temporal position of action potentials (phase coding). Therefore, precise timing of action potentials at the subsecond range is likely to be essential for information processing in neuronal networks (Káli and Acsády, 2003). But what could serve as a time signal for the neuronal activity to be organized around? To arrange neuronal activities in a proper order, the nervous system generates sub-threshold membrane potential fluctuations by which many cells will be close to the firing threshold at the same time, thus enabling the

synchronization of large cell assembles. Hence, not only the firing frequency of a given cell, but also the time relative to the fluctuating activity of cell populations might carry specific information. The alternating firing and non-firing periods of cell populations produce synchronized synaptic potentials through the surface membranes of targeted neurons, which are manifested as oscillatory pattern on the electroencephalogram (EEG) or electrocorticogram (ECoG) (Buzsáki, 2006).

The functions of the hippocampus have been thoroughly examined in living animals, either in anesthetized or in freely-moving conditions. These *in vivo* experiments revealed that the oscillatory activities observed in the hippocampal field potential are correlated to the animal's behavior. In rodents, theta (4–10 Hz) oscillations typically occur during exploratory behavior and rapid eye movement sleep (Grastyán et al., 1959; Vanderwolf, 1969; Soltész and Deschénes, 1993). Sharp wave-associated high-frequency ripples (SWRs, 120–200 Hz) of 100ms duration occur during slow-wave sleep, awake inactivity, and consummatory behaviors (Buzsáki et al., 1983). Additionally, in awake brain, oscillations at gamma frequencies (30–100 Hz) can also be observed embedded in theta activity, following sharp-waves as well as gamma rhythm may follow or precede epileptic activity (Traub et al., 1996; Bragin et al., 1997; Traub et al., 2001; Buzsáki et al., 2003) (Fig. 5).

These hippocampus related activity patterns can also be recorded in humans. For instance, hippocampal rhythmic slow activity (RSA) rhythm during rapid eye movement (REM) sleep has been reported to occur in humans (Bódizs et al., 2001). Although human RSA activity shows lower frequency (1.5-3 Hz) compared to the theta recorded in rodents, it is considered to be the counterpart of the mammalian theta (Bódizs et al., 2001; Buzsáki, 2002; Buzsáki et al., 1986). Nevertheless, it has to be mentioned that such activity has been recorded in the human hippocampus during virtual movement that has fallen into the theta range (4-8 Hz; Caplan et al., 2003; Ekstrom et al., 2005). SWRs may be observed also in humans, particularly during non-REM but also during REM sleep and awake (Staba et al., 2004), together with interictal epileptic spikes (Bragin et al., 1999), or temporally associated to sleep spindles (Clemens et al., 2007). Hippocampal gamma rhythm can be recorded during short-term memory tasks or memory recall in humans (Fell et al., 2001; Sederberg et al., 2003).

These behavior related network activities reflect the underlying mechanisms of information processing in the hippocampus, so investigating the origin of these network

activities may help understanding hippocampal function. In the following section the current knowledge regarding the mechanisms behind these phenomena and their role in hippocampal computation will be briefly summarized.

Theta rhythm and sharp waves – possible functions

Theta rhythm has been shown to be particularly prominent in association with voluntary movement (Vanderwolf, 1969; Whishaw and Vanderwolf, 1973), including free running and rearing (O'Keefe and Nadel, 1978). These activities are collectively termed as exploratory behavior, during which the animal gains new information about the environment. Considerable research has also focused on the correlation of theta rhythm with learning and memory (Berry and Thompson, 1978; Winson, 1978). Lesions of the medial septum and fornix reduce hippocampal theta power (Rawlins et al., 1979) and cause impairments in a number of memory-guided tasks, for instance in spatial reversal in a T-maze. These impairments appear specific to recent, episodic memory, since fornix lesions do not impair the initial learning of a goal location, but impair the learning of reversal (M'Harzi et al., 1987).

These and similar observations have contributed to the widely accepted hypothesis that theta activity represents the first phase of storing episodic memories: during theta the environment to be learned is represented in the hippocampus, which may induce a weak and transient potentiation of connectivity in a subgroup of CA3 pyramidal cells. This would be the *memory acquisition* stage (Buzsáki, 1989). The next step is the *memory consolidation* process, when the weakly changed synaptic weights are consolidated. This process takes place during sharp wave ripple oscillations (SWRs) (Buzsáki, 1986) (Fig. 5). SWRs having 50-150 msec duration usually occur embedded in the non-rhythmic irregular pattern of the hippocampal field potential, which is called large irregular activity or LIA. LIA interrupted by SWR activity can be observed during eating, grooming and slow wave sleep. SWRs are the result of the synchronous discharges of numerous pyramidal cells, which, according to Buzsáki's theory, might be sufficient to induce long term synaptic modifications in the neurons of the CA3 region and in their targets in CA1. Hence, the memory trace initiated during theta oscillation will be imprinted into the hippocampal network by SWRs.

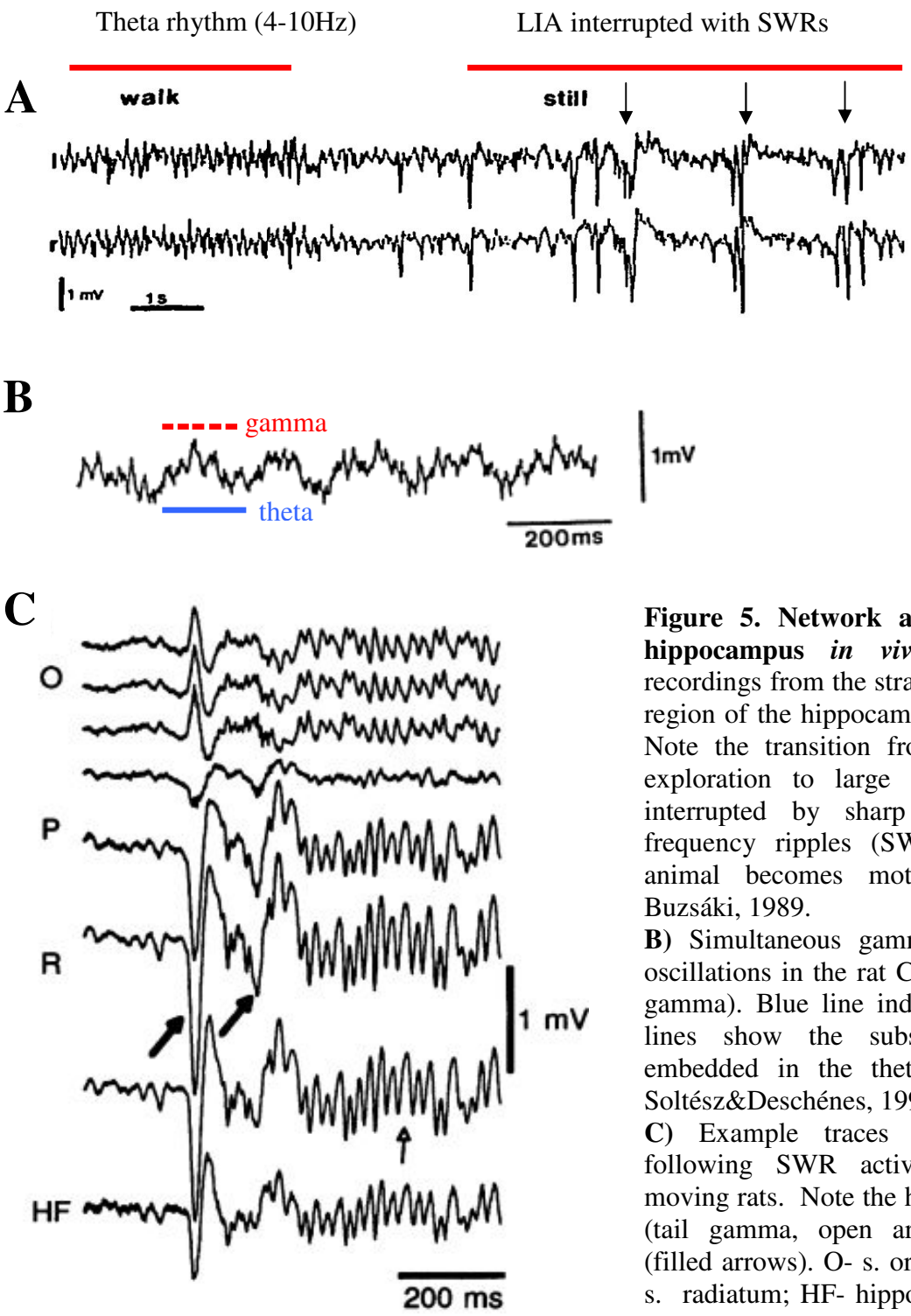

Figure 5. Network activity patterns in the hippocampus *in vivo*. A) Field potential recordings from the stratum radiatum in the CA1 region of the hippocampus of both hemispheres. Note the transition from theta rhythm during exploration to large irregular activity (LIA) interrupted by sharp wave-associated high-frequency ripples (SWRs; arrows) when the animal becomes motionless. Adopted from Buzsáki, 1989.
B) Simultaneous gamma and theta frequency oscillations in the rat CA1 region (theta –nested gamma). Blue line indicates a theta cycle, red lines show the subsequent gamma cycles embedded in the theta cycle. Adopted from Soltész&Deschénes, 1993.
C) Example traces of gamma oscillations following SWR activity recorded in freely moving rats. Note the high frequency oscillation (tail gamma, open arrows) following SWRs (filled arrows). O- s. oriens; P-s. pyramidale; R-s. radiatum; HF- hippocampal fissure. Adopted from Traub et al, 1996.

The idea that SWRs could be capable of inducing long term modifications of synaptic contacts is largely based on studies on *long term synaptic plasticity* including the widely known phenomenon called *long term potentiation* or LTP. LTP has been first described in the dentate gyrus of the rabbit (Bliss and Lomo, 1973). Since this study, it has been reported in many brain areas and by using many experimental protocols. LTP is a long-lasting enhancement in signal transmission between two neurons that results from their coinciding activity (Bliss and Gardner-Medwin, 1973). Several methods exist to evoke long-lasting changes in glutamatergic synapses, but the easiest way to induce LTP is to stimulate many incoming fibers with high frequency impulses at the same time to ensure sufficient synaptic input to evoke action potentials postsynaptically (Cooke and Bliss, 2006). Since SWRs reflect synchronous discharge of bulk of pyramidal cells, during SWRs similar processes may take place as during LTP induction protocols. Supporting this idea, during SWRs Ca^{2+} mediated action potentials have been reported to be generated in the dendrites of CA1 pyramidal cells, which may contribute to the changes of synaptic weights (Kamondi et al., 1998). Besides its role in memory consolidation, SWRs may participate in the information transfer to the neocortex, during which the memory traces produced by hippocampal networks are transported to the neocortex in order to be permanently stored (Chrobak and Buzsáki, 1996; Skaggs and McNaughton, 1996; Nádasdy et al., 1999; Goshen et al., 2011).

As mentioned above, the encoding capacity might be much higher, if the timing of action potentials also carries specific information. A particularly striking example for the importance of the timing of pyramidal cell firing relatively to theta rhythm is the phenomenon called *phase precession* (O'Keefe and Recce, 1993). Place cells respond to particular regions of the environment termed as place field. O'Keefe's observation was that as the rat traversed the place field of a place cell, the phase of firing of that cell relative to the ongoing theta oscillation systematically changed. A place cell, while the animal moving through its place field, fires systematically at earlier theta phase during the subsequent theta cycles till the animal leaves the place field. Consecutive experiments have led to the idea that phase precession reflects the cued recall of upcoming places in a known environment (Jensen and Lisman, 1996; Tsodyks et al., 1996). Thus, the *rate code,* which expresses the location of the animal in space will be completed with a *phase code*, which serves as an additional temporal dimension expressing whether the encoded place field belongs to the

left or to the forthcoming places that the animal will reach. Such a mechanism might be involved in the storage of episodic memories, which often involve complex sequences of events (Lisman and Buzsáki, 2008).

Theta rhythm and sharp waves –mechanisms

In general, when considering the mechanisms behind oscillations, it is fundamental to distinguish *current* generation and *rhythm* generation. Current generator refers to the transmembrane currents giving rise to the deflections of field potential with a given magnitude, whereas rhythm generator refers to the mechanism that determines the pattern and frequency of oscillatory activities. In the case of theta, extracellular field deflections are assumed to be generated by the summed activity of IPSPs and EPSPs on the somata and dendrites of principal cells, respectively. The interplay between coherent excitatory (from perforant path) and inhibitory (septal connections and local feed-forward inhibition) inputs reaching hippocampal pyramidal cells, functioning as current generators (dipoles), might produce the unique properties of theta pattern appearing on field potential (Buzsáki, 2002).

The origin of theta rhythm genesis is still a question of debate. Several brain regions have been identified to be responsible for, or at least contribute, to the pacemaking activity involved theta oscillation. The rhythm generating properties are usually attributed to interneuron-principal cell networks. For instance, at least three hippocampal interneuron types have riveted particular attention regarding the hippocampal theta rhythm generation. *Perisomatic region targeting interneurons* are thought to be important in the timing of action potential generation of pyramidal cells during theta oscillation. Basket and axo-axonic cells discharging rhythmically in the gamma range on the descending phase of pyramidal layer theta provide rhythmic hyperpolarization on the perisomatic region of pyramidal cells. As a consequence, dendritic region will be periodically isolated from somatic regions due to the periodic activation of these interneurons. Another group of interneurons that have been suggested to be involved in hippocampal theta rhythm targets the dendritic region of pyramidal cells. Specifically, *OLM and HIPP* (hilar perforant path-associated) cells innervate the zones where the entorhinal inputs are terminated on pyramidal cells and granule cells, respectively. Since current flow through the distal dendrites of principal cells is a determining event in generating theta waves, inhibitory control of these inputs might play a crucial role in the regulation of theta rhythm. The third

class of cells involved in theta rhythm generation are the long range *projecting GABAergic cells* that innervate the medial septum. As mentioned earlier, the hippocampus possesses reciprocal inhibitory connections with this brain region. Septally projecting GABAergic cells discharge rhythmically during theta. These cells include special types in the CA1 region that receive feedback excitation from CA1 pyramidal cells and project back to the CA3 and hilar regions. This long-range inhibition may allow precise synchronization of population activity of principal cells and also the coordination of rhythmic discharge of cells in the medial septum (Buzsáki, 2002 and references therein).

Besides hippocampal networks, extrahippocampal regions have also been connected with the generation and regulation of theta. For instance, the medial septum-diagonal band of Broca (MS-DBB) complex has been shown to play a particularly important role in these processes (Lawson and Bland, 1993; Vértes and Kocsis, 1997). Lesion or inactivation of MS-DBB neurons abolishes theta rhythm in all cortical areas, thus it has been suggested to be the ultimate rhythm generator of theta (Petsche et al., 1962). In agreement with this, it has been demonstrated that a subpopulation of MS-DBB GABAergic neurons serves as pacemakers of hippocampal theta (Hangya et al., 2009). As mentioned in the chapter dealing with subcortical inputs, the MS-DBB, besides its reciprocal GABAergic connection, provides the hippocampus with extended cholinergic fibers. Based on the sensitivity of theta rhythm to cholinergic agents an atropine-sensitive and an atropine-insensitive component of theta can be distinguished (Kramis et al., 1975). The former type is typical in the anesthetized animal, while the latter can be observed in the awake, walking animal. Though muscarinic receptor blockers do not abolish atropine resistant theta, the shape and depth profile of this type of oscillation changes in the presence of atropine (Buzsáki et al., 1986). Thus, cholinergic influence plays a role in the generation and/or modulation of theta rhythm. The precise subjects of atropine action in these processes are unknown (Buzsáki, 2002). As we have seen in the chapter dealing with cholinergic inputs, acetylcholine arriving from MS-DBB fibers may depolarize both pyramidal neurons and interneurons, and additionally, may influence the GABA release from the terminals of certain types of interneurons, providing a variety of targets of cholinergic modulation.

The hypothalamic supramammillary nucleus, which is reciprocally connected to the MS-DBB (Borhegyi and Freund, 1998), is another external region that has been suggested to participate in the pacemaking of hippocampal theta (Vértes and Kocsis, 1997). Involvement of other subcortical parts in the regulation of theta, like the posterior

hypothalamic nucleus, the pontomesenchephalic tegmentum, as well as the ventral tegmental nucleus of Gudden complicates this view further (Kirk, 1998; Boucetta and Jones, 2009; Vann, 2009).

Cortical interactions of the hippocampus also play a role in the regulation of hippocampal theta. As the main neocortical input, entorhinal cortex has a great influence on hippocampal rhythms, for instance, it might be the origin of the above mentioned phase precession in the hippocampus (Maurer and McNaughton, 2007). Furthermore, contrary to the simplest model of theta generation suggesting that the MS-DBB functions as a pacemaker enforcing a global rhythm into which hippocampal and entorhinal cortical networks are entrained, numerous studies raise the possibility of local entorhinal cortical theta oscillators (Mitchell and Ranck, 1980; Brankack et al., 1993; Kocsis et al., 1999). A recent study based on simultaneous recordings both from the hippocampus and the entorhinal cortex has revealed a consistent delay between theta rhythms measured in these two structures, allowing for a considerable degree of independence of local circuit computation at the stages of entorhinal cortical-hippocampal system, instead of imposing rapidly propagating activity across regions (Mizuseki et al., 2009).

In contrast to the theta rhythm, which originates by the interplay of several brain regions, SWRs are produced in the hippocampus locally as a result of popular bursts of pyramidal cells (Buzsáki, 2006). More specifically, the origin of SWRs is the synchronous population bursts in CA3 (Ylinen et al., 1995; Csicsvári et al., 2000; Maier et al., 2003) generated by its recurrent excitatory circuit (Miles and Wong, 1987; Traub et al., 1989). These bursts propagating to the CA1 region give rise to sharp waves by depolarizing pyramidal cell dendrites (Maier et al., 2003; Ylinen et al., 1995). These inputs reach not only the pyramidal cells but also interneurons, giving rise to the ripple component of SWRs with a 150-200Hz frequency oscillating pattern (Buzsáki et al., 1992). Since SWRs originate in the hippocampus, in certain circumstances they can be studied in acute hippocampal slices, and such experimental approaches have shown that perisomatic inhibition plays a crucial role in initiating SWRs (Ellender et al., 2010). Consistently, modeling studies suggest that fast spiking inhibitory neurons are necessary to the generation of high frequency ripples (Taxidis et al., 2011).

Gamma oscillations – possible functions

In cortical areas the importance of oscillatory patterns in the gamma frequency range (30-100Hz) has been emphasized in neural processes such as sensory encoding, selective attention, neuronal assembly formation, or memory storage and retrieval (Singer, 1993; Tiitinen et al., 1993; Fries et al., 2001; Sederberg et al., 2003; Montgomery and Buzsáki, 2007). According to memory functions, gamma oscillations have been proposed to be important in changes of synaptic weights, since they could provide a temporal frame for spike timing-dependent plasticity (Paulsen and Moser, 1998).

In the hippocampus, network oscillations in the gamma range can be observed mostly superposed onto the theta rhythm during exploration (theta-nested gamma), but also occur during LIA regardless of SWRs or following them (Bragin et al., 1995; Traub et al., 1996; Buzsáki et al., 2003). As mentioned earlier, during theta, the hippocampus is in the memory acquisition stage, during which episodic memory traces are formed about sensory representations of the environment. Based on the model of Lisman and Idiart (1995; Fig. 6), it is likely, that theta-nested gamma is the manifestation of the cooperating theta and gamma oscillations, working on to create a neural code by which episodic memory traces are produced. Their model is built on the idea of neural ensembles (*items*), groups of active cells with certain spatial patterns, which patterns represent elementary units of percepts, memories or thoughts. Each item is encoded in a distributed fashion by the synaptic weights in the network, therefore they can be selectively recalled by appropriate cues. When multiple items are encoded, each item is represented by the cells that fire synchronously during a given gamma cycle. During a theta period, approximately 7±2 gamma cycles occur. When the next theta cycle begins, the sequence of items (encoded by ensembles firing together during a gamma cycle) will be replayed (Lisman and Buzsáki, 2008; Fig 6). This mechanism suggests that during acquisition and recall of episodic memories the function of gamma and theta rhythm might be the dissociation of subsequent items and the indication of the beginning and ending of the sequence of items, respectively. Consistently, based on classic studies, the capacity limit of short-term memory in humans has been established to be 7±2. Furthermore, it has been suggested that during short-term memory recall, items are serially scanned at a rate about 30ms per item (Sternberg, 1966). The model of Lisman and Idiart serves as a good explanation to these results, i.e. different

memory items are represented by sequential gamma cycles of a theta cycle, with approximately 7 gamma cycles within a theta period, moreover, with a temporal separation of gamma cycles at 30ms (Jensen and Lisman, 1998; Lisman and Buzsáki, 2008).

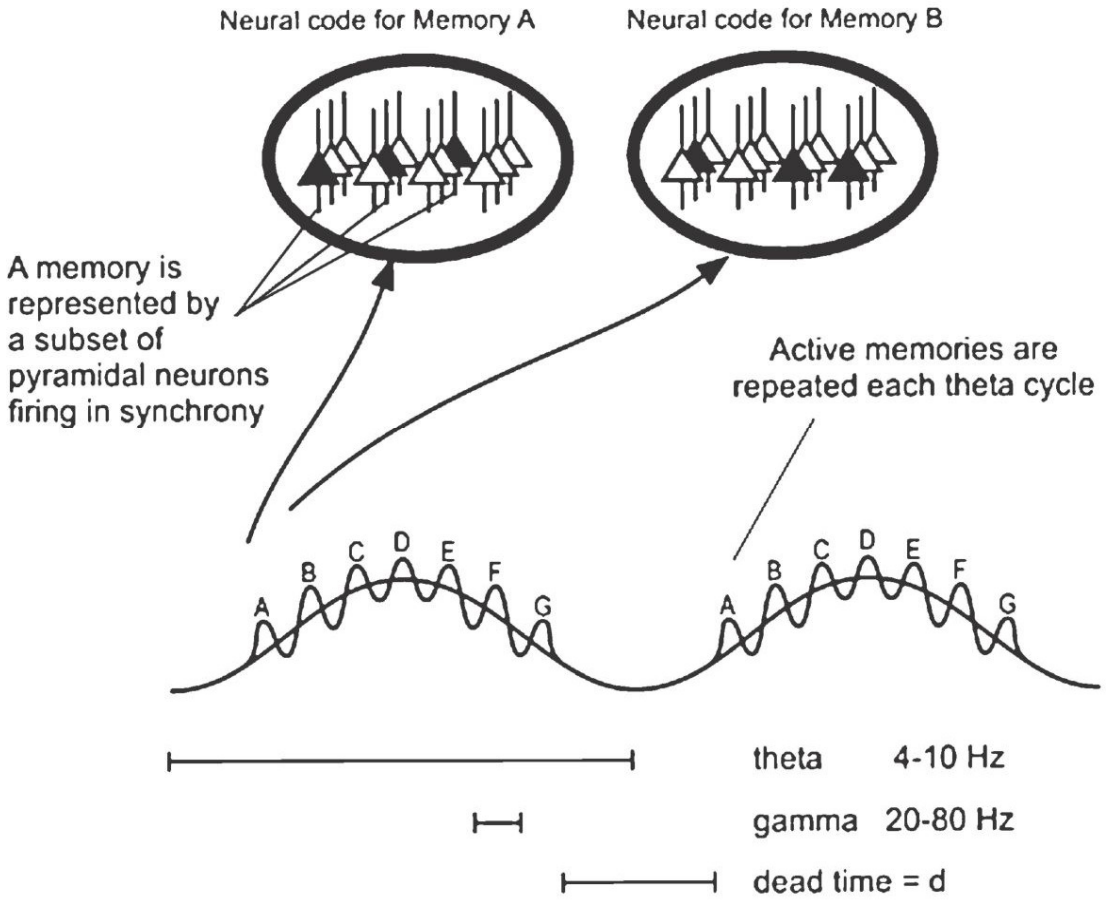

Figure 6. Hypothetical cooperation of gamma oscillation and theta rhythm in storing memories. Seven gamma cycles (A-G) are embedded in a theta cycle. Two theta cycles are shown. During different gamma cycles different ensembles of pyramidal neurons are active, representing a sequence of items during the theta cycle. The ovals above show the spatially arranged active cells (shown in black) during two subsequent gamma cycles encoding memory A and then B. Thus, the spatial code of active cells is used to encode the memory. This entire pattern can repeat on the next theta cycle. Model of Lisman&Idiart (1995), adapted from Lisman&Buzsáki, 2008.

This model implies that the time precision of firing during a gamma cycle is not important, since an ensemble of active pyramidal cells carries the encoded information. In contrast to this, an alternative model coming from the Wolf Singer's laboratory suggests that the exact timing (in millisecond range) of pyramidal cell spiking relative to the gamma phase might be crucial in coding. According to their theory, the pyramidal cells that receive the strongest excitation will fire during the gamma cycle. Consequently, the strength of pyramidal cell excitation would be translated into a phase value that corresponds to the time of occurrence of the spikes relative to the cycle period, allowing for a coding scheme similarly to the phase precession observed during theta rhythm. It has to be mentioned that evidence for the importance of action potential coding in the millisecond range during gamma cycle comes from the visual cortex, but no such data are available coming from hippocampal studies (Hopfield, 1995; Fries et al., 2007; Lisman and Buzsaki, 2008).

Gamma oscillations – mechanisms

Hippocampal gamma oscillations have been shown to be mostly originated from two independent sources. One of the oscillators is the entorhinal cortex, where gamma oscillation arises at higher frequency („fast gamma", at ~90Hz), which can spread to the dentate gyrus and to the CA regions (Bragin et al., 1995; Chrobak and Buzsáki, 1998). *In vivo* studies have revealed that the CA3 network itself is also capable of generating gamma oscillation. This rhythm is slower („slow gamma", at ~40Hz), and can be observed in animals with entorhinal cortical lesions (Bragin et al., 1995; Csicsvári et al., 2003). It has recently been shown that these two types of oscillations emerge alternating in time, i.e. excluding mutually each other, allowing for the alternating processing of information coming from the entorhinal cortex or the CA3 region (Colgin et al., 2009).

In vivo approaches have revealed that during gamma oscillation originating from the CA3 region alternating pairs of sinks and sources (dipols) occur in the strata pyramidale and radiatum of both CA3 and CA1. Current-source pairs measured in the CA1 have followed those measured in the CA3 with a systematic monosynaptic delay, indicating that the oscillatory activity originated in CA3 spreads to the CA1 region. The capability of generating gamma oscillation is likely due to the extended recurrent collateral system, which is a unique property of CA3 region in the hippocampus. Furthermore, the

synchronization of the local neuronal network is likely to be carried out by perisomatic region targeting interneurons activated by recurrent collaterals (Csicsvári et al., 2003). The importance of perisomatic inhibition in the rhythm generation has been emphasized by *in vitro* studies as well (Hájos et al., 2004; Mann et al., 2005). Moreover, some studies are also available aiming to identify the perisomatic region targeting neuron type that is crucial in the gamma genesis. Recent studies modifying the behavior of PV-containing inhibitory neurons using molecular biological techniques demonstrated the importance of these GABAergic cells in the generation of gamma oscillation (Fuchs et al., 2007; Cardin et al., 2009). However, neither approach could differentiate between the contribution of FSBCs and AACs, since both cell types express PV. In addition, the participation of CCK-expressing RSBCs in oscillogenesis has not been addressed either.

To reveal the detailed mechanisms of the generation of fast network oscillations and the identity of the involved perisomatic region targeting cells is not, or at least limitedly possible in *in vivo* conditions. To explore the mechanisms of rhythm generation *in vitro* techniques are also available, which techniques together with their restrictions may suit an appropriate tool for the investigation of these fast network rhythms and to test their sensitivity to different drugs. Oscillations in the gamma range can be observed in animals with lesioned entorhinal cortex (Bragin et al., 1995), indicating that the slow gamma might emerge within the local network of CA3. By preparing acute brain slices containing the hippocampal formation these oscillations can be induced in certain conditions. As this thesis mainly focuses on the network mechanisms of fast network oscillations close to the gamma range, I will introduce the different models that have been established to evoke and maintain gamma-like oscillations in acute brain slices.

Fast network oscillations in vitro may model rhythmic activities at the gamma frequency range in vivo

Three major types of *in vitro* oscillation models have been developed to attempt to grab the properties of gamma oscillations recorded *in vivo*. In the first model electrical stimulation was used to evoke oscillatory pattern in the CA1 region (Whittington et al., 1995). In their model the 40Hz oscillation emerges owing to the release of glutamate in response to electrical stimulation. The glutamate activates the mGluRs of interneurons, inducing a synchronous firing of the interneuronal network interconnected through

chemical and electrical synapses. This repetitive firing may entrain pyramidal cell discharges, although fast excitatory transmission was shown to be not required for the generation. The oscillation takes 100-300ms long (Whittington et al., 1995). This transient oscillatory activity might reflect to the conditions which occur in the hippocampus following sharp waves, when the synchronous discharge of CA3 pyramidal cells produce glutamate release in CA1, contributing to the generation of transient gamma oscillation following SWR activity (Traub et al., 1996). By the application of mGluR agonists similar oscillation can be maintained persistently both in CA3 (Pálhalmi et al., 2004) and in CA1 (Boddeke et al., 1997) regions, but whereas the oscillation in CA1 doesn't require intact excitatory transmission, in the case of the oscillation induced in CA3, participation of both pyramidal cells and GABAergic interneurons are crucial (Pálhalmi et al., 2004). This difference might reflect the different anatomical connectivity of CA3 and CA1 subfields.

The second *in vitro* gamma oscillation model was introduced in 1998 by the lab of Prof. Ole Paulsen (Fisahn et al., 1998). They used the cholinergic receptor agonist carbachol (CCh, 20μM) to induce oscillation at around 30Hz in the CA3 region which could propagate to the CA1 region. This oscillation could be maintained, while CCh was present in the perfusate. Their experiments led to the model suggesting that the oscillation is the result of the repetitive discharges of CA3 pyramidal cells and local interneurons. Local collaterals of pyramidal neurons excite local inhibitory cells, which in turn inactivate the same pyramidal cells through a feed-back inhibitory loop. When the inhibition is abating, pyramidal cells are again able to generate action potential, again discharge the inhibitory cells and another gamma cycle emerges (Fisahn et al., 1998). Since this type of oscillation is generated in the network of CA3 and doesn't need the entorhinal input, it might correspond to the "slow" gamma rhythm, which can be observed embedded into the theta oscillation, when the cholinergic tone is high (Marrosu et al., 1995).

Fast network oscillatory pattern can also be generated in hippocampal slices by application of kainic acid, which is an ionotropic glutamate receptor agonist (Hájos et al., 2000). This type of oscillation might be the model of gamma rhythm recorded during those conditions, when the level of acetylcholine in the hippocampus is low, for example during LIA, although gamma oscillation occurs independent of SWR activity (Csicsvári et al., 2003).

In summary, these different oscillatory models may reflect different fast network oscillations of different functional states of the hippocampus. Studying fast network

oscillations in slice preparations may provide a good tool to investigate the cellular and network mechanisms behind these phenomena, thus may help us in getting closer to the understanding hippocampal functions.

To reveal the functional neuronal networks behind oscillatory activities it might be expedient to thoroughly investigate the basic elements of the system. Since several experimental data have shown the crucial involvement of perisomatic inhibition in gamma oscillations (Csicsvári et al., 2003; Hájos et al., 2004; Mann et al., 2005; Oren et al., 2006; Fuchs et al., 2007; Cardin et al., 2009; Oren et al., 2010), the knowledge of properties of perisomatic region targeting interneurons is essential to be expanded. It is particularly important to know how their GABA releasing properties change in special circumstances that occur during the oscillation. And finally, the behavior of these neurons during oscillations has to be revealed. These investigations compose the main skeleton of this thesis.

II. AIMS OF THESIS

The main goal of this thesis was to investigate the involvement of perisomatic region targeting interneurons in the generation of cholinergically induced fast network oscillation. Therefore two objectives were determined:

The first objective was to determine the output properties of perisomatic region targeting interneurons in the hippocampal CA3 region and to determine their sensitivity to cholinergic receptor activation. To this end, it was necessary to develop a method by which the distinct types of these interneurons can be distinguished from each other. Furthermore, we aimed to reveal the mechanisms by which the cholinergic receptor agonist exerts its action on GABA release in these cell types.

The second objective of the thesis was to investigate the contribution of these interneurons to the CCh-induced fast network oscillation. Therefore, the firing of interneurons was monitored during CCh-induced oscillations in acute hippocampal slices, then the involvement of all types of perisomatic region targeting interneurons to the maintenance of oscillation was also tested by using pharmacological tools.

III. MATERIALS AND METHODS

III/1. Experimental animals and ethical approval

All experiments were carried out in accordance with the Hungarian Act of Animal Care and Experimentation (1998, XXVIII, governmental decree 243 / 1998), and with the guidelines of the institutional ethical code, which conforms to the regulation of animal experiments by the European Union. Experimental procedures used in this study were reviewed and approved by the Department of Animal Health and Food Control, Budapest. (Permission number: 2300/003; 2301/003.)

Both sexes of transgenic mice expressing enhanced green fluorescent protein (eGFP) controlled by glutamate decarboxylase-65 (GAD65) promoter (López-Bendito et al., 2004) or PV promoter (Meyer et al., 2002) were used for the paired recording studies. For studying oscillations, transgenic mice and both sexes of C57BL/6 mice were used. In addition, μ-opioid-receptor (MOR) knock-out (KO) mice (Matthes et al., 1996) were used to test the specificity of DAMGO ([D-Ala^2,N-Me-Phe^4,Gly^5-ol]enkephalin acetate) effects, which were compared with the effects obtained in their wild type (WT) littermates. Animals were kept under a 12-12 hour light-dark cycle, water and food was available *ad libitum*. All efforts were made to minimize pain and suffering and to reduce the number of animals used.

III/2. Slice preparation for *in vitro* physiology

Mice (postnatal days 15–23) were deeply anaesthetized with isoflurane and decapitated. The brain was quickly removed and placed into ice-cold cutting solution containing (in mM): sucrose, 252; KCl, 2.5; NaH_2PO_4, 1.25; $MgCl_2$, 5; $CaCl_2$, 0.5; $NaHCO_3$, 26; and glucose, 10. The cutting solution was bubbled with 95% O_2 and 5%CO_2 (carbogen gas) for at least half an hour before use. Horizontal hippocampal slices (200–350μm thick) were prepared using a Leica VT 1000S or a VT1200S microtome (Leica, Nussloch, Germany), and kept in an interface-type holding chamber at room temperature for at least 60 min before recording in standard ACSF with the composition (in mM) NaCl,

126; KCl, 2.5; NaH_2PO_4, 1.25; $MgCl_2$, 2; $CaCl_2$, 2; $NaHCO_3$, 26; and glucose, 10. Solutions were prepared with ultra pure water and bubbled with carbogen gas.

III/3. Paired recordings

To characterize cellular interactions from identified cell pairs or other mechanisms of DAMGO actions, we cut 200–250-µm-thick slices to reduce the connectivity in the slice, since the high spontaneous activity evoked by carbachol could have influenced the analysis of synaptic events. Slices were transferred to a submersion type of recording chamber. To reduce the occurrence of spontaneous synaptic events, the flow rate was 2–3 mL / min. Experiments were performed at room temperature under visual guidance using an Olympus microscope (BX61WI; Olympus Corp., Tokyo, Japan). Fluorescence of eGFP- containing cells was excited by a monochromator at 488 nm wavelength or by standard epifluorescence using a UV lamp, and the resulting fluorescence visualized with a CCD camera (TILL photonics, Gräfelfing, Germany, or Hamamatsu Photonics, Japan). Whole-cell patch-clamp recordings were made using a Multiclamp 700B amplifier (Molecular Devices), filtered at 2 kHz, digitized at 5 kHz with a PCI-6024E board (National Instruments, Austin, TX, USA), recorded with in-house data acquisition and stimulus software (Stimulog, courtesy of Professor Zoltán Nusser, Institute of Experimental Medicine, Hungarian Academy of Sciences) and analyzed off-line using the EVAN software (courtesy of Professor István Mody, UCLA, CA). Patch pipettes were from borosilicate glass tubing with resistances of 3–6 MΩ. The intracellular solution used for the presynaptic cell contained (in mM) K-gluconate, 110; NaCl, 4; Mg-ATP, 2; HEPES, 40; and GTP, 0.3; with 0.2% biocytin; adjusted to pH 7.3 using KOH and with an osmolarity of 290 mOsm / L. The intrapipette solution used for the postsynaptic cell contained (in mM) CsCl, 80; Cs-gluconate, 60; $MgCl_2$, 1; Mg-ATP, 2; NaCl, 3; HEPES, 10; and QX-314 [2(triethylamino)-N-(2,6-dimethylphenyl) acetamine], 5; adjusted to pH 7.3 with CsOH, and with an osmolarity of 295 mOsm / L. Presynaptic interneurons were held in current-clamp mode around a membrane potential of -65 mV, and stimulated by brief current pulses (1.5 ms, 1–2 nA). Pyramidal cells were clamped at a holding potential of -65 mV. Series resistance was frequently monitored and compensated between 65–75%, and cells that changed > 25% during recording were discarded from further analysis. For the analysis of the kinetic properties of uIPSCs we used only those recordings where series resistance

changed by ≤20% (Fig. 14, Table 2). In experiments with carbachol, 5μM NBQX was occasionally added to the bath solution to reduce the high background synaptic activity.

III/4. Recording oscillations in slices

To investigate oscillations 300–350-μm-thick slices were cut. Oscillations were recorded in a dual-superfusion chamber (Supertech Ltd., Pécs, Hungary) at room temperature with a flow rate of 2–4 ml/min (Hájos et al., 2009). Oscillations were induced by bath application of 5 μM carbachol (CCh). As it has been shown that for the full development of CCh induced oscillation 10 to 15min of agonist application is needed (Hájos et al., 2009), LFPs were recorded after this time. Patch pipettes (~ 4–6 MΩ) filled with ACSF were used to monitor local field potentials and action potentials extracellularly. The field pipette was placed in stratum (str.) pyramidale of CA3. To record from identified interneuron subtypes, slices were cut from transgenic animals. EGFP- expressing neurons were identified using epifluorescence and differential interference contrast on an Olympus BX61 microscope. A second pipette was used to record spiking activity in a loose-patch configuration from the visually identified neurons. Action potentials were recorded for at least 60 s. The pipette was then withdrawn from the slice, and the same cell was patched with a new pipette filled with intrapipette solution containing the following (in mM): K-gluconate, 138; CsCl, 3; phosphocreatine, 10; ATP, 4; GTP, 0.4; HEPES, 10; QX-314, 0.2; biocytin 3 mg/ml, adjusted to pH 7.3–7.35 using KOH (285–290 mOsm/L). Whole-cell series resistance was in the range of 5–15 MΩ. Both extracellular and whole-cell recordings were performed with a Multiclamp 700B amplifier (Molecular Devices), with the exception of experiments presented in Figure 23, where field potentials were recorded with a BioAmp amplifier (Supertech). To detect EPSCs more reliably in pyramidal cells during oscillation, picrotoxin (600–650 μM) was included in the pipette solution (Nelson et al., 1994). Voltage measurements were not corrected for a junction potential. Both field and unit recordings were low-pass filtered at 2 kHz using the built-in Bessel filter of the amplifier. Data were digitized at 6 kHz with a PCI-6042E board (National Instruments) and recorded with EVAN software (courtesy of Professor István Mody, UCLA, CA). All data were analyzed off-line using custom-made programs written in MATLAB 7.0.4 and Delphi 6.0.

III/5. Measurements of evoked and miniature events

In the presence of CCh, electrically evoked or miniature IPSCs were pharmacologically isolated by bath application of 3 mM kynurenic acid to block ionotropic glutamate receptors. To isolate evoked EPSCs and to prevent epileptiform discharges in CA3, $GABA_A$ receptor-mediated currents were blocked intracellularly by including picrotoxin (600–650 μM) in the pipette solution. We experienced that 10–15 min was enough after break-in to eliminate IPSCs. To measure miniature events, 0.5 μM tetrodotoxin (TTX) was included in the bath solution to exclude action potential dependent synaptic events.

III/6. Post hoc anatomical identification of interneurons

After recordings, slices were fixed in 4% paraformaldehyde in 0.1 M phosphate buffer (PB; pH 7.4) for at least 60 min, followed by washout with PB several times, cryoprotected in 20% sucrose and repeatedly freeze–thawed (for details see Gulyás et al., 1993). Biocytin was visualized using avidin-biotinylated horseradish peroxidase complex reaction (ABC; Vector Laboratories, Burlingame, CA, USA) with nickel-intensified 3,3-diaminobenzidine as a chromogen. After dehydration and embedding in Durcupan (Fluka), neurons were identified based on their dendritic and axonal arborization and some representative cells were reconstructed with the aid of a drawing tube using a 40x objective.

III/7. Identification of FSBCs and AACs using double immunofluorescent labelling

After recordings, the slices were fixed as above, washed, cryoprotected, embedded in agar (1%) and re-sectioned at 60 μm thickness. Every third section was processed for electron microscopy where biocytin was visualized as above. The sections were then treated in 1% OsO_4, followed by 1% uranyl acetate, dehydrated in a graded series of

ethanol, and embedded in epoxy resin (Durcupan; Fluka). Ultrathin sections of 60 nm thickness were cut for electron microscopy, and the postsynaptic targets of 5–10 boutons of each examined cells were identified. The remaining sections were processed for fluorescent double immunolabelling. They were treated with 0.2 mg / mL pepsin (Cat. No.: S3002; Dako) in 0.2 M HCl at 37˚C for 5 min and were washed in 0.1 M PB similar to the procedure developed by Watanabe et al. (1998). Sections were blocked in normal goat serum (NGS; 10%) made up in Tris-buffered saline (TBS, pH = 7.4) followed by incubations in mouse anti-Ankyrin-G (1:100; Santa Cruz Biotechnology) diluted in TBS containing 2% NGS and 0.3% Triton X-100. Following several washes in TBS, Cy3-conjugated goat anti-mouse (1 : 500; Jackson) was used to visualize the immunoreaction, while Alexa488-conjugated streptavidin (1 : 500; Invitrogen) to visualize the biocytin. Sections were then mounted on slides in Vectashield (Vector Laboratories). Images were taken using an AxioImager Z1 axioscope (Carl Zeiss MicroImaging GmbH, Germany).

III/8. Data analysis and materials

Analyzing unitary inhibitory postsynaptic currents (uIPSCs). The kinetic properties of uIPSCs were investigated on averaged events that were calculated with excluding the transmission failures. The latency of synaptic transmission was calculated by subtracting the time of the action potential peaks from the start of the postsynaptic currents. This latter value was estimated by subtracting the rise time from the peak time of events calculated from the time of the action potential peaks. Calculation of asynchronous release was achieved by the comparison of the average charge (area under the curve) of all currents in a 100-ms-long time window before and after the action potential trains. Fitting of single exponential functions on the decaying phases of averaged uIPSCs and statistical analyses were performed using Origin 8.0 software (OriginLab Corporation, Northampton, MA, USA).

Calculating peak-to-peak amplitude of the oscillation. To calculate the amplitude of the oscillation, an amplitude distribution histogram was made on a 60 s, 1 Hz, high-pass filtered section of the recording. The voltage range containing 95% of the points was used as peak-to-peak amplitude.

Firing-phase calculation. A custom-written firing phase detection algorithm was used. Spikes recorded in a loose-patch mode were detected by manually setting the threshold on the unfiltered trace. The negative peak of the trough of the oscillation was considered as phase zero. However, the position of the negative trough of an oscillation depends on how the original signal is filtered. In *in vivo* studies (Buzsáki et al., 2003) for gamma detection, the field potential is filtered with a relatively narrow (30 – 80 Hz) bandpass (BP) filter. Filtering at such a low frequency distorts the shape of the gamma oscillation and makes the original asymmetric wave shape symmetric, similar to a harmonic oscillation (Fig. 17B). We therefore detected the negative peak of the oscillation on field potentials digitally bandpass filtered between 5 and 500 Hz. We chose the negative peak of the oscillation as zero, because it has functional significance. Pyramidal cells start to fire in high synchrony in this phase (Hájos et al., 2004; Mann et al., 2005; Oren et al., 2006). Also at this point, the extracellular potential rises very quickly and defines phase zero very well. If the signal is low-pass filtered at gamma frequencies (as in the *in vivo* studies), this sharp negative peak will disappear and the position of the zero phase will be influenced by potential changes throughout the full cycle as well as by variable gamma cycle length (Atallah and Scanziani, 2009), all spoiling functionally meaningful zero phase definition. The phase of individual spikes was specified by calculating the position of the unit spikes in relation to two subsequent negative phase times. Here again, care has to be taken, since the amplitude and the instantaneous frequency of the oscillation vary, and often the detection algorithm might skip one or more oscillation cycles. This would result in an erroneous shift in spiking phase toward zero. Therefore, our spike phase detection algorithm checked for the actual detected cycle length and assigned a phase to a spike only if the actual cycle length did not differ from the mean of the average cycle length by more than a chosen fraction of the SD of the cycle length. Heuristically, we found that if we chose 0.3 SD, we achieved a feasible phase calculation. If there is no oscillation length checking, as a result of the skipped cycles, firing phase is shifted toward zero. If the detection algorithm is too strict (not allowing jitter), spikes during short or long oscillatory cycles are discarded (can be rather high portion), and the phase coupling will be very high but does not represent physiological values. Since the oscillations in our experiments had a mean frequency of 15.2±0.5 Hz (n=15) at room temperature, to relate our results to *in vivo* data we mimicked the narrow BP filtering with a 5–30 Hz BP filter and also calculated the phase of the spikes this way. The cell groups showed the same overlap in their phase, but

the firing phase of the cell groups was shifted in the positive direction (due to the fact that low-pass filtering of the saw teeth-like oscillations shifted the negative peak to the negative direction).

Since most data in the first part of the study did not have a Gaussian distribution according to the Shapiro–Wilk's W test or the Kolmogorov–Smirnov test, nonparametric statistics were used. Multiple groups of data were compared using the nonparametric Kruskal–Wallis Anova test completed with comparison of samples as pairs with the Mann–Whitney U-test. For dependent samples the Wilcoxon signed-ranks test was used. $P < 0.05$ was considered a significant difference. Data are presented as mean ± SEM. In the second part of the study, unless it is indicated, a Student's paired t test was used to compare the changes in IPSC amplitude, firing characteristics, cell membrane property parameters, and oscillation power after drug application. Data are presented as mean ± SEM. The Kolmogorov–Smirnov test was used to compare two cumulative distributions. Circular statistics were used to calculate cell firing phase and phase coupling. ANOVA was used to compare multiple datasets.

All chemicals and drugs were purchased from Sigma Aldrich (St Louis, MO, USA), except AM251, AF / DX 116, TTX, CTAP (D -Phe-Cys-Tyr- D -Trp-Arg-Thr-Pen-Thr-NH_2) and DAMGO, which were purchased from Tocris Bioscience.

IV. RESULTS

Part I. Comparative studies of the output properties of perisomatic region targeting interneurons and their sensitivity to cholinergic receptor activation in the CA3 subfield of the hippocampus

This chapter describes those experiments that aimed to reveal the output properties of perisomatic region targeting interneurons, which cells are supposed to be crucial in generating fast network oscillations in CA3 hippocampal region (Csicsvári et al., 2003; Hájos et al., 2004; Mann et al., 2005; Oren et al., 2006; Fuchs et al., 2007; Cardin et al., 2009; Oren et al., 2010). To specifically investigate how these neurons affect their postsynaptic targets it was necessary to perform paired recordings between identified interneurons and pyramidal cells. Not only the effect of a single action potential, but also of action potential trains was tested in order to reveal the possible differences in short term dynamics.

Furthermore, to address the question whether the synaptic release from the terminals of these neurons changes during cholinergically induced gamma oscillation, their sensitivity to the cholinergic agonist carbachol (CCh) was tested. Moreover, I will show the results indicating that cholinergic receptor activation exerts its effect on the different types of cells through distinct mechanisms.

IV/1. Identification of different types of perisomatic region targeting interneurons

As shown in the introduction chapter, at least three different types of perisomatic region targeting interneurons may control the action potential generation of pyramidal neurons in the CA3 region: the two basket cell types, the fast spiking one expressing PV (FSBC) and the regular spiking type (RSBC), which expresses CCK and CB1R, but not PV; as well as AAC, which also has PV content. To investigate the synaptic properties of these neurons it was indispensable to unequivocally separate them from each other. On Figure 6A the camera lucida reconstructions of three biocytin loaded cells are shown. At the light microscopic level the axonal arbour of these neurons show quite similar features,

axon collaterals are localized in the pyramidal cell layer in all cases. Somatic location and dendritic orientation did not show consequent differences either. Thus, distinguishing these neurons purely based on morphology may not be achieved.

Using transgenic mice provided an opportunity to find the appropriate interneurons to record from. RSBCs were sampled in *in vitro* slices prepared from transgenic mice in which the enhanced green fluorescent protein (eGFP) expression was under the control of the GAD65 promoter. As in this mouse line PV-containing interneurons do not express eGFP in the hippocampus (López-Bendito et al., 2004), we used another transgenic mouse to selectively target the FSBCs and AACs. In this mouse line the bacterial artificial chromosome technique was used to drive the expression of eGFP only in PV-containing cells (Meyer et al., 2002), providing a tool to obtain recordings from hippocampal FSBCs and AACs (Katsumaru et al., 1988).

Firing patterns of neurons reflect, among others, to the ion channel compositions that determine the capability of action potential generation. Furthermore, the presence or absence of certain ion channels may modify the responses of neurons to hyper- or depolarizing current steps. Therefore, so called step protocols were applied to all neurons prior to the experiments, which contained a series of increasing hyper- and depolarizing current injections. This method revealed that RSBCs based on the regular spiking pattern and the significant *sag* are kept well apart from the AACs and FSBCs, which cells showed rather fast spiking phenotype and much less significant sag (Fig. 7B). All the recorded interneurons that were tested for firing characteristics were filled with biocytin to allow post hoc visualization of their morphology (Fig. 7A). Only those neurons identified as RSBCs sampled from GAD65-eGFP mice, which had an axonal arbour predominantly in the stratum pyramidale surrounding somata and had typical regular firing, were used in this study (n = 17; Daw et al., 2009).

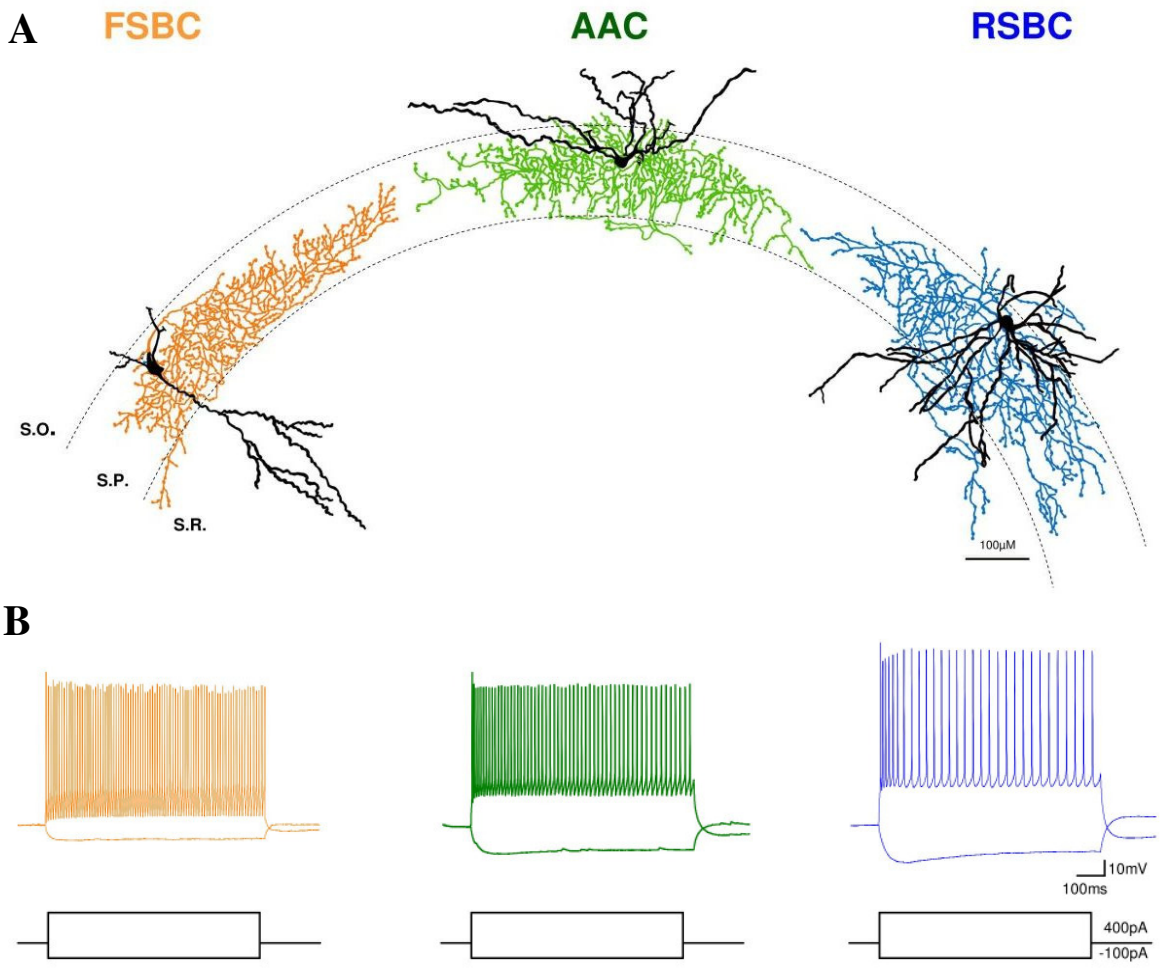

Figure 7. Electrophysiological and morphological properties of the three types of perisomatic region targeting interneurons in the CA3 region of the mouse hippocampus. A) Camera lucida reconstructions of representative biocytin-loaded neurons. Left: Fast-spiking basket cell (FSBC)(orange); middle: axo-axonic cell (AAC)(green); right: regular-spiking basket cell (RSBC)(blue). Cell bodies and dendrites of interneurons are shown in black, while axon clouds are colored. **B**) Firing characteristics of three representative cells in response to depolarizing and hyperpolarizing current steps by 400 pA and -100 pA, respectively. Color coding similarly as in **A**.

As mentioned above, AACs and FSBCs have similar morphology at the light microscopic level, possess similar firing pattern and both express PV. Therefore, separating them from each other required a new method to be developed. To distinguish FSBCs and AACs after recordings obtained in slices from PV-eGFP mice, double immunofluorescent staining was performed to visualize the biocytin-filled axon collaterals together with the axon initial segments (AISs) of neurons, which were labelled with an antibody developed against ankyrin-G. This scaffolding protein is present at high concentrations in the AIS of neurons, where it anchors several proteins, including voltage-gated sodium channels (Nav1.2 and 1.6; Jenkins and Bennett, 2001), so it is appropriate to visualize AISs at the light microscopic level (Boiko et al., 2007). We observed two clearly distinguishable patterns of labelling in the double-stained materials. There were cells with biocytin-filled axons that only rarely approached ankyrin-G-stained profiles (n = 23, Fig. 8A-C), whereas other cells had axon collaterals forming close appositions with ankyrin-G-labelled segments, often in a climbing fiber-like manner (n = 26, Fig. 8G-I). To confirm that intracellularly-labelled boutons avoiding ankyrin-G-immunoreactive elements derived from basket cells, as suggested by the morphology, electron microscopic examination was performed. In all tested cases we found that axon terminals of these neurons formed symmetrical synapses on the somata or proximal dendrites of CA3 pyramidal cells (n = 5; Fig. 8D-F), therefore these interneurons were confirmed to be basket cells. In those cases in which biocytin-filled boutons surrounded ankyrin-G-immunopositive segments, electron microscopic studies confirmed that axon terminals formed synaptic contacts on the AIS of pyramidal cells (n = 5; Fig. 8J-L); as a result, we identified these interneurons as AACs. In PV-eGFP mice, we also recorded four bistratified cells and one oriens–lacunosum moleculare cell, which was not unexpected as previous data indicated that these GABAergic cell types could express PV at low levels (Klausberger and Somogyi, 2008). These neurons were excluded from this study. Hence, using anatomical methods, we identified all the three types of perisomatic inhibitory interneurons whose synaptic outputs have been investigated.

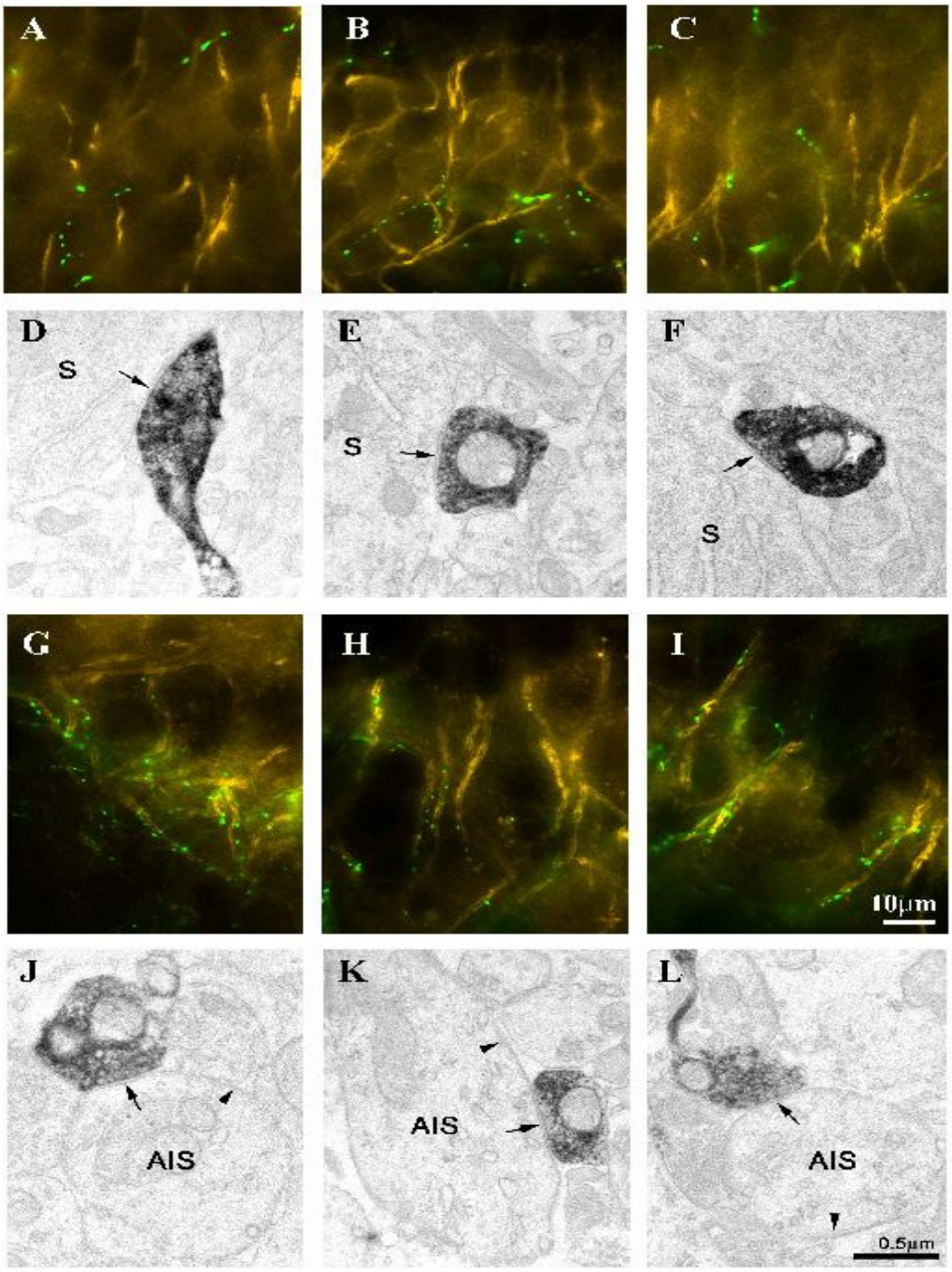

Figure 8. Separation of FSBCs and AACs based on there target selectivity. A-C) Double immunofluorescent labelling for biocytin (green) and for ankyrin G (yellow) shows no close appositions of biocytin-filled boutons with axon initial segments. **D-F)** Electron micrographs of peroxidase-labelled axon terminals of the same cells as in A-C illustrates that these boutons formed symmetrical synapses (arrows) on CA3 pyramidal cell somata (s), a characteristic for basket cells. **G-I)** Double immunofluorescent labellings as in A-C show tight appositions of biocytin-labelled boutons (green) and ankyrin G-labelled axon initial segments (yellow), suggesting that these neurons are axo-axonic cells. **J-L**) Electron micrographs of peroxidase-labelled axon endings of the same cells as in G-I confirms that these interneurons formed synapses (arrow) on axon initial segments (AISs) of CA3 pyramidal cells, indicating that the recorded neurons were axo-axonic cells. Arrowheads show undercoating, characteristic for axon initial segments.

IV/2. Characterization of basic properties of synaptic connections between perisomatic region targeting inhibitory cells and postsynaptic pyramidal neurons

In the first set of experiments we aimed to characterize the basic properties of synapses formed by the three types of perisomatic region targeting inhibitory cells on their pyramidal cell targets. To this end, uIPSCs were recorded from synaptically coupled perisomatic region targeting inhibitory cell–pyramidal neuron pairs in the CA3 region. We compared the peak amplitude (including failures), potency (excluding failures), 10–90% rise time and T50 values (i.e. the width of currents at the half of the peak amplitude) of uIPSCs. In addition, the synaptic latency of transmission (i.e. the time between the action potential peak and the beginning of the postsynaptic current) and the probability of transmission failure were also calculated (Fig. 9; Table 1). The analysis showed that the three groups are different regarding peak amplitude ($H_{2,50} = 22.36$; $P < 0.0001$), synaptic potency ($H_{2,50} = 18.8$; $P < 0.0001$), probability of failures ($H_{2,50} = 20.83$; $P < 0.0001$), T50 value ($H_{2,48} = 18.2$; $P = 0.0001$) and latency ($H_{2,49} = 14.23$; $P = 0.0008$), whereas 10–90% rise time values belonging to the three groups did not differ significantly from each other ($H_{2,49} = 4.15$; $P = 0.12$). Further statistical investigations revealed that in AAC–pyramidal cell pairs synaptic currents had the largest peak amplitude and potency, as did T50 values of postsynaptic currents; these parameters significantly differed from the values of the other two groups (Fig. 9; Table 1). Moreover, synaptic transmission of RSBCs was found to have a higher probability of failures and longer latency than either FSBCs or AACs (Fig. 9; Table 1). These results indicate that the synaptic output of the individual AACs could have the largest potential to influence the activity of pyramidal neurons in the CA3 region of the hippocampus.

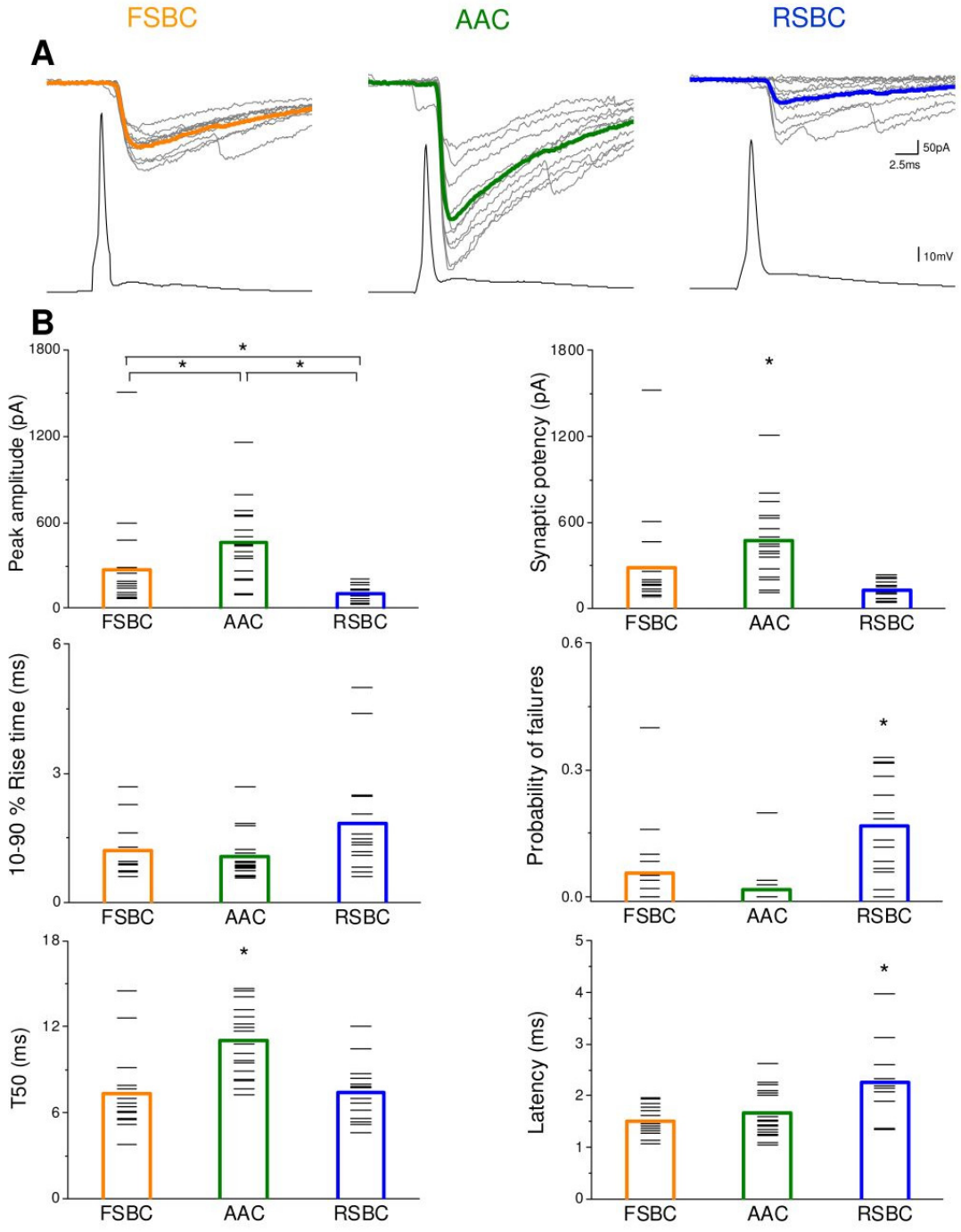

Figure 9. Basic properties of synaptic communication between perisomatic region targeting interneurons and pyramidal cells. A) Ten superimposed unitary inhibitory postsynaptic currents (uIPSCs, thin lines) evoked by single presynaptic action potentials in representative FSBC-, AAC- and RSBC- pyramidal cell pairs. Averages of uIPSCs are indicated by thick black lines. **B)** Comparison of the peak amplitude, the synaptic potency, the 10-90% rise time, the failure probability, the half-decay (T50) and the latency obtained in the three types of perisomatic inhibitory interneurons and pyramidal cell pairs. Bars show the averages, short lines show the mean values for individual cell pairs.

Table 1. Summary of uIPSC properties.

	FSBC	AAC	RSBC
Peak amplitude (pA)	274.9±84.7 (P=0.0043; n=17)	463.3±61.8 ($P<10^{-4}$; n=18)	107.1±13.9 (P=0.0496; n=15)
Potency (pA)	288.4 ± 84.3 (P=0.0059; n=17)	475.5 ± 63.8 ($P<10^{-4}$; n=18)	133.0 ± 16.2 (p=0.0759; n=15)
10-90% Rise time (ms)	1.2 ± 0.1 (P=0.364; n=17)	1.1 ± 0.1 (P=0.0504; n=18)	1.8 ± 0.3 (P=0.226; n=14)
T50 (ms)	7.3 ± 0.6 (P=0.0002; n=17)	11.0 ± 0.6 (P=0.0005; n=17)	7.4 ± 0.5 (P=0.7358; n=14)
Failure probability	0.056 ± 0.025 (P=0.0621; n=17)	0.016 ± 0.011 ($P<10^{-4}$; n=18)	0.168 ± 0.029 (P=0.002; n=15)
Latency (ms)	1.5 ± 0.1 (P= 0.3141; n=17)	1.7 ± 0.1 (P= 0.0083; n=18)	2.3 ± 0.2 (P=0.0002; n=14)

P values represent the results of the statistical comparison of FSBC vs. AAC (1st column); AAC vs. RSBC (2nd column) and RSBC vs. FSBC (3rd column), Mann-Whitney U test

IV/3. CCh reduces the amplitudes of uIPSCs in a presynaptic cell type dependent manner

Hippocampal circuits are extensively supplied by cholinergic fibers arriving from the medial septum (Wenk et al., 1975; Wainer et al., 1985). To investigate the effect of cholinergic receptor activation on the perisomatic inhibition, we obtained paired recordings during pharmacological activation of ACh receptors by bath application of CCh (2-5µM). First, we examined the postsynaptic effect of CCh in the different types of perisomatic region targeting inhibitory cells. The analysis revealed that cholinergic receptor activation similarly changed the membrane potential of all types of perisomatic inhibitory cells (H

2,26 = 4.81; P = 0.09). CCh depolarized FSBCs by 6.1 ± 1.3 mV (n = 8), AACs by 3.6 ± 2.0 mV (n = 11) and RSBCs by 6.3 ± 1.1 mV (n = 7).

Next, we investigated the presynaptic effect of CCh by looking into the properties of uIPSCs. In these sets of experiments transmission failures were included in the average uIPSCs. CCh caused a robust decrease in uIPSC amplitudes in all three types of cell pairs. In FSBC–pyramidal cell pairs and in AAC–pyramidal cell pairs, the synaptic currents were reduced to 29.9 ± 2.5% (n = 16, P < 0.0001, Fig. 10) and 27.1 ± 2.8% of control amplitude (n = 16, P < 0.0001, Fig. 10), respectively. In contrast, CCh caused an almost total suppression of neurotransmission in RSBC–pyramidal cell pairs, reducing the amplitude to 6.0 ± 3.4% of control (n = 13, P < 0.0001). Accordingly, the magnitude of the reduction in the amplitude caused by CCh proved to be dissimilar among different types of cell pairs (H 2,45 = 19.98; P < 0.0001). Whereas the magnitude of the suppression in FSBC– and AAC–pyramidal cell pairs was similar (P = 0.44), both differed significantly from the results obtained in RSBC–pyramidal cell pairs (P = 0.0001).

Next, we investigated the nature of receptors involved in the reduction in uIPSCs. In slices prepared from PV-eGFP mice, a muscarinic receptor antagonist AF/DX 116, which prefers M2-type receptors, was tested. In FSBC–pyramidal cell pairs, CCh decreased the amplitudes of uIPSCs to 28.3 ± 3.6% of control (n = 6, P = 0.03), an effect that was restored by the antagonist to 95.6 ± 19.7% of control (n = 6, P = 0.31). Similarly, in AAC–pyramidal cell pairs the amplitudes were reduced to 30.2 ± 4.0% of control by CCh (n = 8, P = 0.008), a decrease that could be reversed with AF/DX 116 to 101.6 ± 12.4% of control (n = 8, P = 0.38). As shown earlier, CCh may trigger the synthesis of endocannabinoids via M1 / M3 muscarinic receptors; these endocannabinoid signalling molecules could reduce GABA release from RSBC terminals by activating CB1Rs (Fukudome et al., 2004; Neu et al., 2007). Therefore, we tested whether the suppression of release at these synapses can be reversed by antagonizing CB1R function. In RSBC–pyramidal cell pairs, the amplitude of uIPSCs was reduced to 2.9 ± 0.7% of control (n = 6, P = 0.03), which was completely reversed by the co-application of a CB1R antagonist AM251 (104.6 ± 39.2% of control, n = 6, P = 0.84; Fig. 10).

These data demonstrate that CCh effectively decreases the GABA release from perisomatic region targeting inhibitory cells to a different extent via different mechanisms, suggesting that the network dynamics could be substantially affected by cholinergic septal

input and also via controlling the contribution of distinct cell types to perisomatic inhibition.

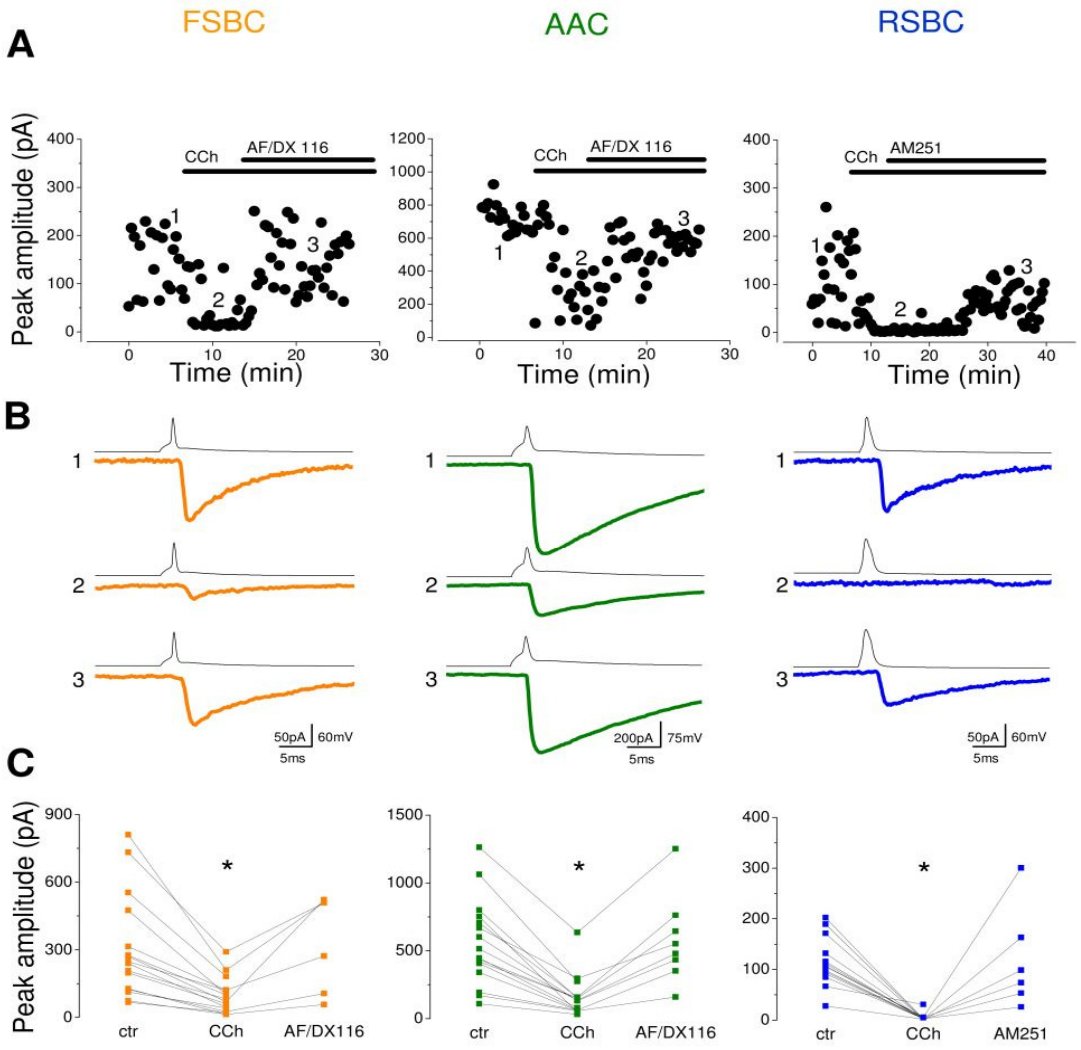

Figure 10. CCh suppresses the unitary IPSC amplitudes in a cell-type specific manner. A) Representative experiments obtained in FSBC-, AAC- and RSBC-pyramidal cell pairs. In each case, bath application of 5 µM carbachol suppressed the uIPSC amplitude. In FSBC- and AAC-pyramidal cell pairs the reduction of the peak amplitude could be recovered by an M2 receptor preferring antagonist AF/DX116 (10 µM), while a CB_1 cannabinoid receptor antagonist AM251 (1 µM) reversed the suppression of uIPSCs amplitude in RSBC-pyramidal cell pairs. **B)** Average of five uIPSCs evoked by single presynaptic action potentials taken at the labelled time points. **C)** Summary data of all pairs. Each square represents a mean value of IPSC amplitude from individual cell pairs under a given condition. Note the different scales on y axis.

IV/4. CCh changes the short-term depression of FSBC– and AAC–pyramidal cell synapses in a frequency-dependent manner

In the next set of experiments we studied the short-term changes of uIPSC amplitudes evoked by action potential trains with distinct frequencies and sought to determine the effect of CCh on the dynamics of synapses. To this end, uIPSCs were recorded in response to 10 action potentials evoked at frequencies of 1, 5, 10, 15 and 30 Hz. An example of these experiments is presented in Figure 11, where the discharges of presynaptic interneurons were elicited at 30 Hz. Synaptic currents in FSBC– and AAC–pyramidal cell pairs showed powerful depression during the trains (Fig. 11A), whereas the uIPSC amplitudes in this RSBC–pyramidal cell pair were facilitating and depressing (Fig. 11A). In contrast to FSBC– and AAC–pyramidal cell pairs, in which the typical depression of uIPSC amplitudes increased with the firing frequency of interneurons (Fig. 12), we observed that the dynamics of RSBC–pyramidal cell synapses were very heterogeneous regarding the short-term plasticity. These synapses showed depression, facilitation or facilitation–depression, which gave on average no change in the uIPSC amplitude at all tested frequencies (an example is shown for 30 Hz in Fig. 11C).

After performing the recordings in control conditions, CCh was bath applied. As expected in RSBC–pyramidal cell pairs, GABA release suffered almost full block upon cholinergic receptor activation, thus no further investigations of short-term changes of uIPSCs could be performed. In the case of PV-containing interneuron–pyramidal cell pairs, the magnitude of the depression notably decreased as a result of CCh treatment (Fig. 11B). We found that CCh altered the synaptic depression in a frequency-dependent manner. In the case of FSBC–pyramidal cell pairs the extent of the depression decreased significantly at 30 Hz ($P = 0.01$; $n = 14$) and tended to decrease at the other tested frequencies ($P = 0.05$ at 15 Hz, $P = 0.21$ at 10 Hz, $P = 0.58$ at 5 Hz and $P = 0.05$ at 1 Hz; Fig. 12A), whereas at AAC–pyramidal cell connections the synaptic depression was reduced or even eliminated at all tested frequencies ($P = 0.0003$ at 30 Hz, $P = 0.0002$ at 15 Hz, $P = 0.017$ at 10 Hz, $P = 0.015$ at 5 Hz and $P = 0.001$ at 1 Hz; $n = 17$; Fig. 12B).

These data suggest that cholinergic receptor activation not only changes the magnitude of perisomatic inhibition originated from FSBCs and AACs but also effectively regulates its short-term plasticity in a frequency-dependent manner.

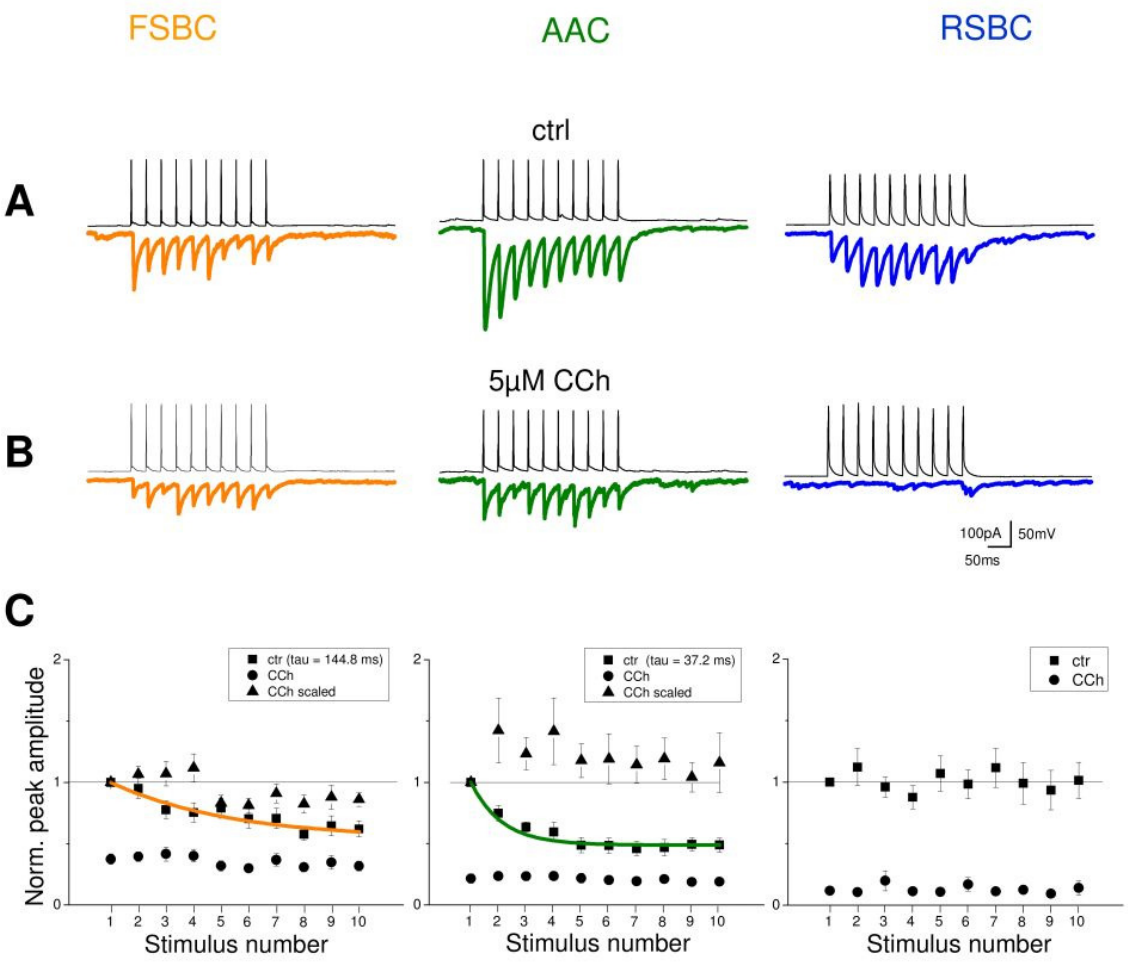

Figure 11. **Changes in short-term dynamics of transmitter release induced by CCh. A)** Representative averaged IPSCs in response to 10 action potentials at a frequency of 30 Hz in control conditions. **B)** Responses in the same pairs in the presence of 5 µM CCh. **C)** Summary of changes in release dynamics effected by CCh at 30 Hz recorded in FSBC- (n=14), AAC- (n=17) and RSBC-pyramidal cell pairs (n=14). Filled squares represent normalized peak amplitudes in control conditions, circles show the same in CCh, and triangles show data obtained in CCh that were normalized to the first IPSC amplitude in CCh. Amplitudes are plotted against time during trains. Curves represent exponential fit to control data points. Note that RSBC data was unsuitable to fit with exponential because of the lack of short term plasticity.

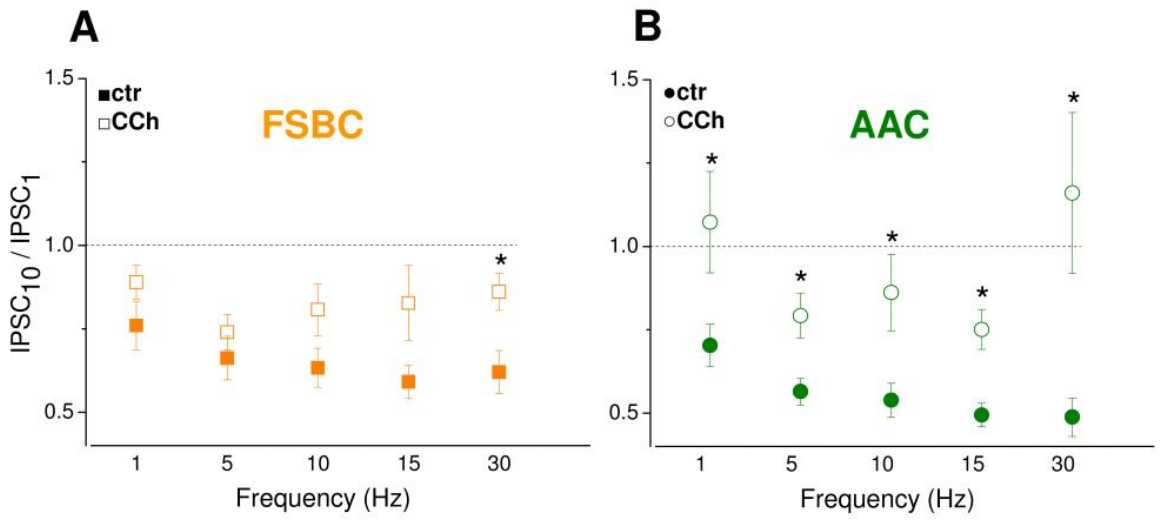

Figure 12. Short-term plasticity of synaptic transmission in fast spiking basket and axo-axonic cell -pyramidal cell pairs is frequency-dependent. A) Ratio of $IPSC_{10}/IPSC_1$ is shown at different frequency values at FSBC-pyramidal cell pairs. **B)** Same as in A, but for AAC-pyramidal cell pairs. Solid squares and circles represent control conditions, open symbols show data from CCh treated slices. All data are from 14 FSBC- and 17 AAC -pyramidal cell pairs. Asterisks represent significant changes with $p<0.05$.

IV/5. Asynchronous GABA release from RSBC terminals shows frequency dependence

Previous studies reported that CCK-containing basket cells in the dentate gyrus or in the CA1 hippocampal region were capable of asynchronous transmitter release and, thus, could generate fluctuating and long-lasting inhibitory signals (Hefft and Jonas, 2005; Daw et al., 2009). We also noticed in our experiments that the occurrence of IPSCs often increased after the action potential trains in RSBC–pyramidal cell pairs. Therefore, we investigated the magnitude of the asynchronous release as a function of the discharge frequency of the presynaptic RSBCs, and contrasted this with data obtained in FSBC– and AAC– pyramidal cell pairs. We compared the total charge transfer of spontaneous postsynaptic currents received by the pyramidal cells before and after the action potential trains elicited at different frequencies (Fig. 13). At RSBC–pyramidal cell synapses we observed robust asynchronous release that showed strong frequency dependence. While

below 10 Hz no asynchronous release could be observed, at 15 Hz (P = 0.02) and at 30 Hz (P = 0.0001, n = 14) significant increases in the charge transfer could be detected (Fig. 13).

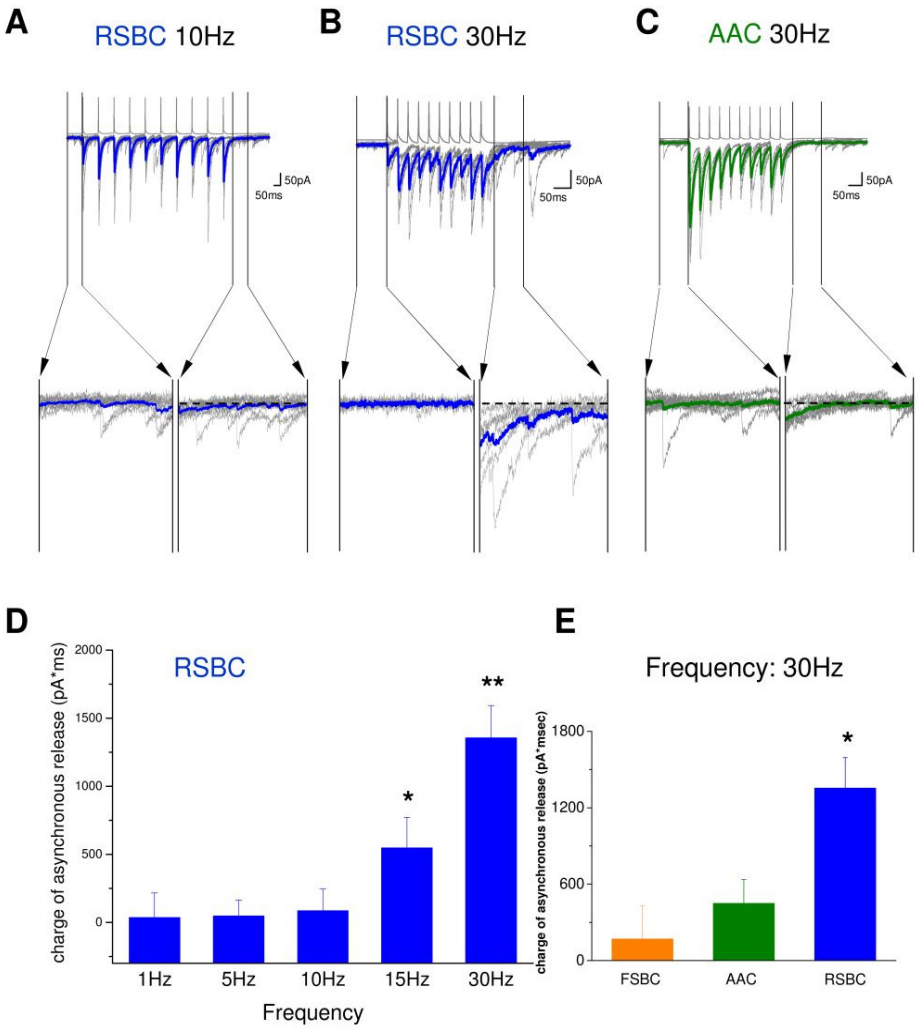

Figure 13. Asynchronous transmitter release in perisomatic region targeting inhibitory cell-pyramidal cell pairs. Examples of IPSC trains in response to 10 action potentials evoked at 10 Hz (**A**) and at 30 Hz (**B**) in an RSBC-pyramidal cell pair, and at 30 Hz in an AAC-pyramidal cell pair (**C**). Averages are shown with thick coloured lines, whereas the individual traces with grey. The magnified 100-ms-long periods before and after the action potential trains were compared to estimate the amount of asynchronous release, demonstrating the presence of asynchronous release in the RSBC-pyramidal cell pair only at 30 Hz. **D)** Summary of the frequency-dependent asynchronous release in RSBC- pyramidal cell pairs. A significant asynchronous release was found at 15 and 30 Hz (p*<0.05 and p**<0.001, respectively). **E**) Summary of asynchronous release in the three types of perisomatic inhibitory interneuron-pyramidal cell pairs at the discharge frequency of 30 Hz.

We then examined the possibility of asynchronous release at the other two types of perisomatic region targeting inhibitory cell, but we did not find any significant change in the charge transfer following action potential trains tested at 30 Hz ($P = 0.17$ for FSBCs, $n = 17$; and $P = 0.05$ for AACs, $n = 18$), confirming that neither FSBCs nor AACs release transmitter in an asynchronous manner. In addition, we tested whether the asynchronous release from RSBC terminals was also sensitive to CCh. At 30 Hz the amount of asynchronous release drastically decreased in the presence of CCh ($22.2 \pm 34.1\%$ of control charge; $P = 0.001$; $n = 14$).

These results indicate that, in contrast to FSBCs and AACs, RSBCs can release GABA asynchronously; the magnitude of this release increases with the firing frequency of the interneurons and this type of release is also suppressed by cholinergic receptor activation.

IV/6. Synaptic cross-talk between terminals of AACs may elongate the decay of synaptic currents

We observed different decay kinetics of postsynaptic currents originating from AACs than from basket cells (Fig. 9; Table 1). As we obtained our experiments at room temperature, when the neurotransmitter uptake is reduced (Binda et al., 2002), we wondered whether the slower decay of synaptic currents recorded in AAC–pyramidal cell pairs might be due to the spillover of GABA between release sites, as they are in a close proximity along the AIS of pyramidal cells (Fig. 8), providing the structural basis for synaptic cross-talk. One way to test this assumption is to compare the decay of IPSCs evoked under conditions with high release probabilities with those that were recorded under reduced release probabilities. In the latter case, GABA has a lower chance of reaching its receptors in the neighbouring synapses so the decay of IPSCs should be faster (Overstreet and Westbrook, 2003). Therefore, we determined the decay time constants (τ) by fitting an exponential to the averaged IPSCs in control conditions (i.e. with high release probability) and in the presence of CCh (i.e. with lower release probability), as CCh affects GABA

release from the terminals without directly altering GABA receptor function (Behrends and Ten Bruggencate, 1993).

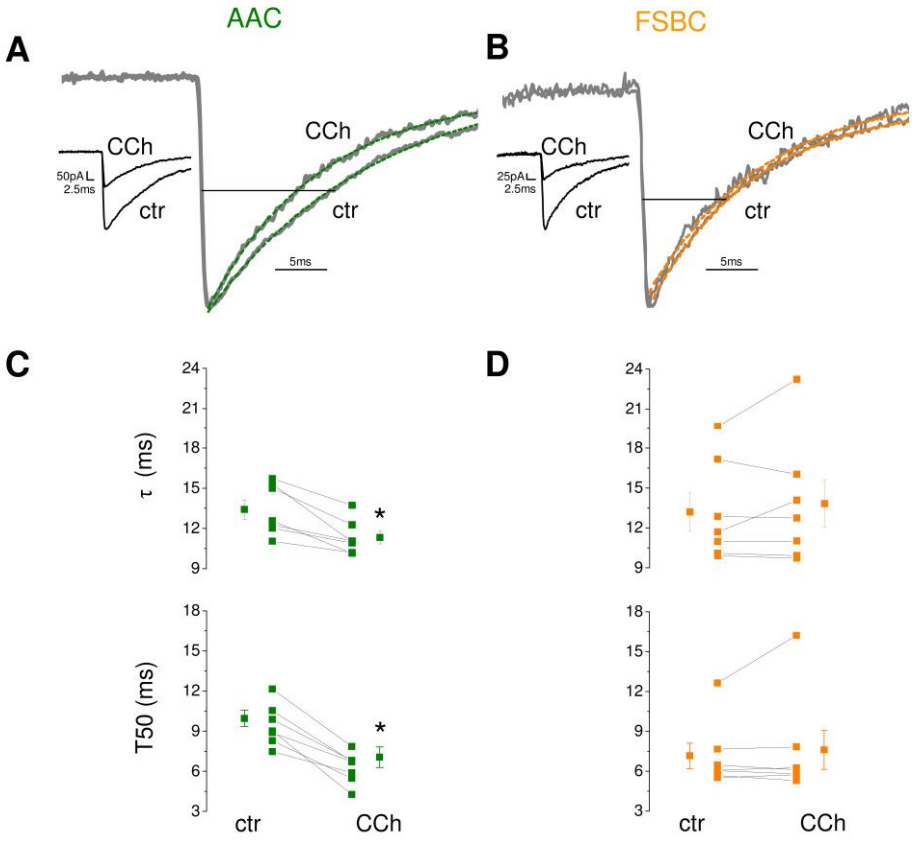

Figure 14. Differences in decay kinetics between AACs and FSBCs might be attributed to synaptic cross-talk between release sites of AACs, but not those of FSBCs. A) Two representative superimposed IPSCs originating from an AAC-pyramidal cell pair in control conditions (ctr) and in the presence of CCh. Dashed coloured lines represent the exponential fits, while horizontal line illustrates the decay width at 50% (T50) of the peak amplitude. Note that the traces are normalized in order to visualize the changes in the decay. Original traces are shown on the insert. **B)** Same as in A, but with uIPSCs originating from a FSBC cell. **C)** Summary of changes in decay time constants (τ) and T50 values at AAC-pyramidal cell pairs in response to CCh. **D)** Same as in **C**, but for FSBC-pyramidal cell pairs. Each data points represent a cell pair in the line series. Data calculated from 7 paired recordings in each case. Asterisks represent significant changes with $p<0.01$.

Table 2. Summary of uIPSC properties before and after CCh treatment.

	FSBC		AAC	
	Ctr	CCh	Ctr	CCh
Peak amplitude (pA)	367.4 ± 167.5	155.2 ± 78.7 *(P=0.0078; n=8)*	509.8 ± 103.7	116.5 ± 26.5 *(P=0.0039; n=9)*
10-90% Rise time (ms)	1.2 ± 0.2	1.9 ± 0.6 *(P=0.0391; n=8)*	0.9 ± 0.1	1.2 ± 0.3 *(P=0.0742; n=9)*
T50 (ms)	7.1 ± 1.0	7.6 ± 1.5 *(P=0.94; n=7)*	9.5 ± 0.6	6.3 ± 0.4 *(P=0.02; n=7)*
Decay τ (ms)	13.2±1.4	13.8±1.8 *(P=0.7422; n=7)*	13.4±0.7	11.3±0.5 *(P=0.0078; n=7)*
Failure probability	0.089 ± 0.049	0.194 ± 0.069 *(P=0.0625; n=8)*	0.027 ± 0.022	0.258 ± 0.064 *(P=0.0078;* n=9)
Latency (ms)	1.5 ± 0.1	1.4 ± 0.1 *(P=0.1484; (n=8)*	1.6 ± 0.2	1.8 ± 0.2 *(P=0.0977; (n=9)*

Corresponding data to the indicated number of cell pairs before and after CCh treatment were compared with Wilcoxon Signed Rank Paired test. $P<0.05$ was accepted as statistical difference, also indicated by grey shading.

We found that the decay of uIPSCs was significantly faster at AAC–pyramidal cell synapses in the presence of CCh than in control conditions (P = 0.01, n = 7, Fig. 14A and C; Table 2). Similar results were obtained by analyzing the half-width (T50) values of uIPSCs in control conditions and in the presence of CCh (P = 0.01; n = 7, Fig. 14A and C; Table 2). In contrast, both types of analysis failed to detect any difference between the

decay of uIPSCs recorded in FSBC–pyramidal cell pairs under conditions with high and low release probabilities ($P = 1.0$ and $P = 0.93$ for the comparison of τ and T50 values, respectively; $n = 7$; Fig. 14B and D; Table 2). The comparison of the uIPSC decays of AACs with that of FSBCs in the presence of CCh revealed no difference ($P = 0.46$ for τ and T values, $n = 7$ for FSBC and AACs), suggesting that kinetics of $GABA_A$ receptor operation might be similar at the two types of synapses, if they are operating independently of each other. These data are in line with the hypothesis that, when GABA uptake is compromised, synaptic cross-talk could significantly elongate the synaptic inhibition originating from AACs but not from FSBCs.

Part II. Contribution of the distinct types of perisomatic region targeting interneurons to the maintenance of ongoing cholinergically induced fast network oscillation in the CA3 region of the hippocampus

Experiments of the previous chapter revealed the output characteristics of perisomatic region targeting interneurons, namely how they release transmitter at different frequencies and whether they are able to produce long lasting inhibition by asynchronous GABA release. Furthermore, experiments with CCh showed that both their excitability and their release properties were sensitive to cholinergic receptor activation but in a different extent: in the presence of 5μM CCh the amount of release from FSBC and AAC terminals decreased but a significant portion remained intact; in contrast, GABA release from RSBC terminals totally ceased as a result of the action of endocannabinoids. Based on the latter findings a plausible consequence is arising: it is unlikely that RSBCs might participate in the synchronization of pyramidal cell firing required for generating and maintaining carbachol induced oscillation, since they do not release GABA during these conditions.

However, based on these results FSBCs and AACs may fulfill this role, since both cell types release GABA and furthermore, both are more excited in the presence of carbachol. Therefore, to figure out that either of them or both are necessary to rhythm generation, further experiments are needed. One way to test their contribution is to investigate their firing properties during oscillation and correlate it to the phase of the ongoing rhythm. Another approach might be to pharmacologically influence the function of interneurons and monitor whether any change occurs in the properties of the oscillation. In the following chapter such experiments are going to be introduced.

IV/7. Perisomatic region targeting inhibitory cell types have distinct firing characteristics during CCh-induced network oscillations

CCh (5μM) was bath applied to induce oscillatory activity, and the local field potential (LFP) was monitored extracellularly with an electrode placed in stratum pyramidale.

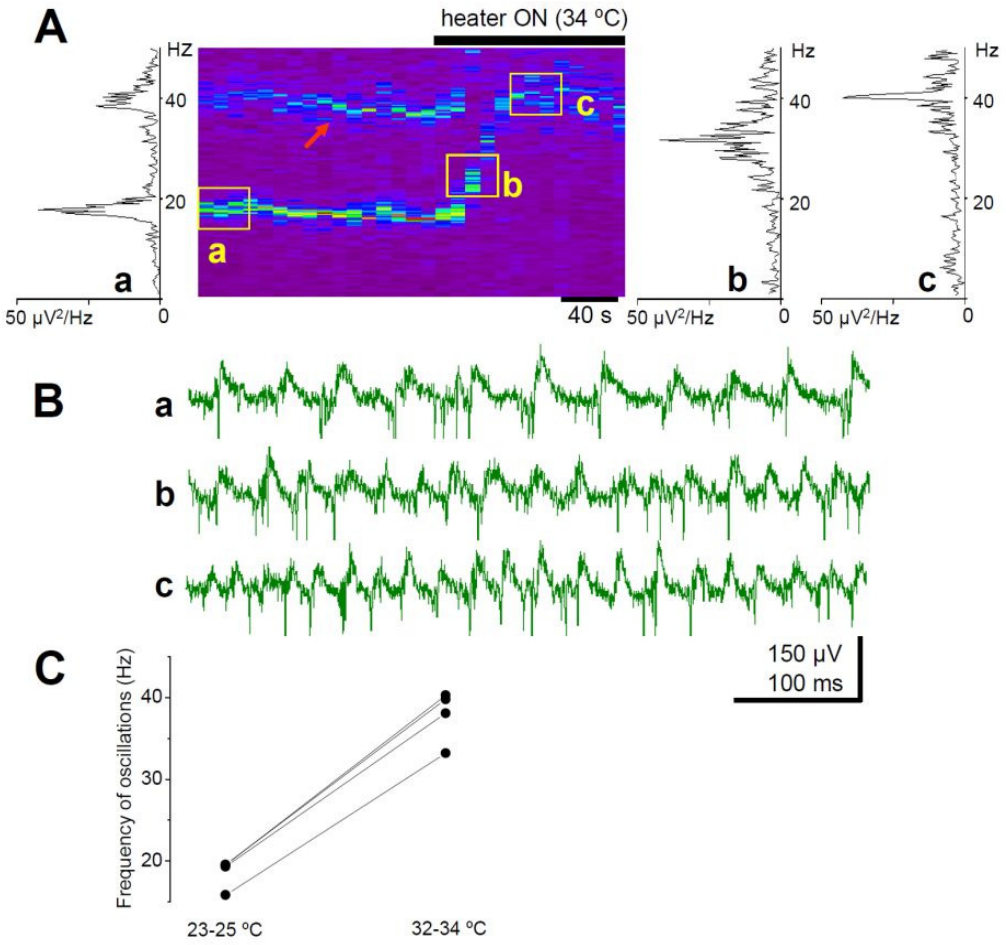

Figure 15. Changes of CCh-induced *in vitro* oscillation during continuous transition from 32-34 ºC to room temperature recorded in an submerged slice chamber. A) The colored spectrograms of 10-s-long epochs juxtaposed in time show that by increasing the bath temperature in the submerged recording chamber, the frequency of the CCh-induced oscillation increases from ~20 Hz to ~40 Hz. Warmer colors indicate peaks on the power spectra. Red arrow indicates a harmonic of ~20Hz oscillation at ~ 40 Hz. Power spectra of the oscillation are shown at different time-points (and temperatures) marked by yellow boxes before (left), during (right) and after (far right) the temperature induced acceleration of the oscillation. **B)** As shown on the unfiltered traces, by increasing the temperature, the frequency but not the amplitude nor the shape of the oscillation changes. The transition is continuous, without a break in the properties of the oscillation, suggesting that the generation mechanisms at different temperatures are identical. **C)** Summary plot showing the significant increase in the frequency of CCh-induced oscillations after changing from the room temperature (18.5 ± 0.9 Hz) to 32-34 ºC (37.8 ± 1.6 Hz, n=4, $p<0.0001$).

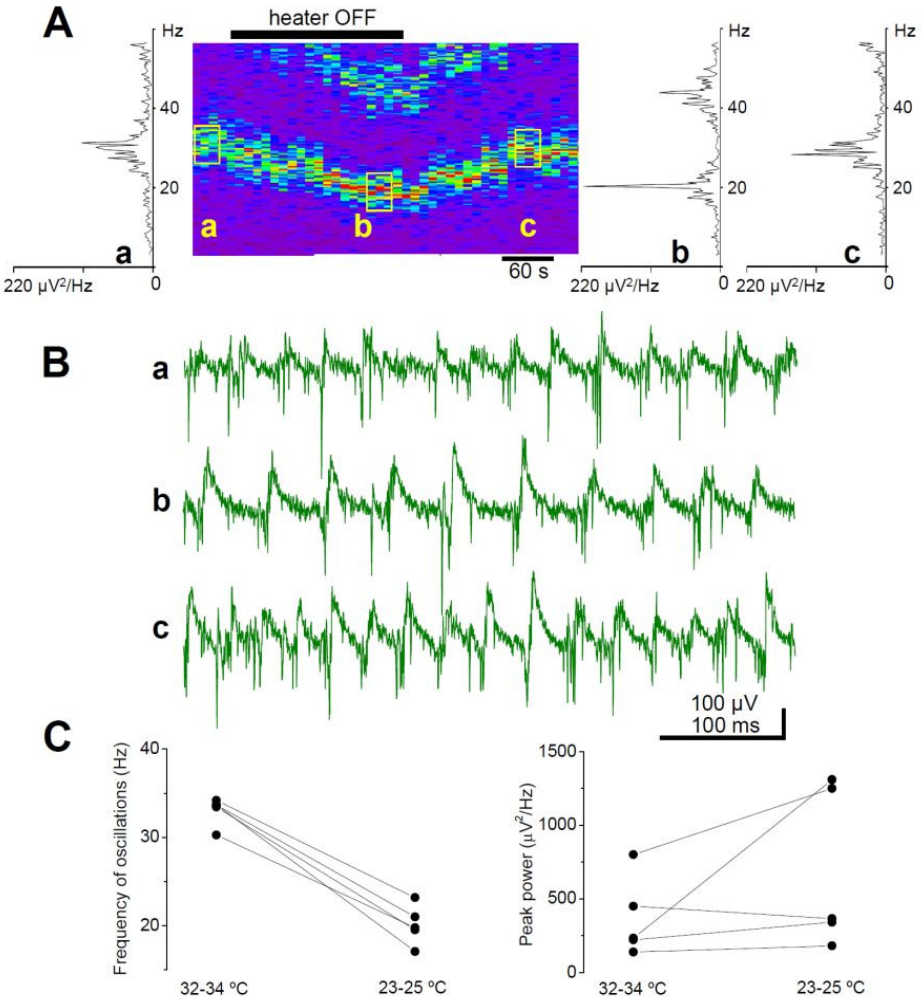

Figure 16. Changes of CCh-induced *in vitro* oscillation during continuous transition from 32-34 ºC to room temperature recorded in an interface slice chamber. A) The colored spectrograms of 10-s-long epochs juxtaposed in time show that by decreasing the bath temperature from 34 ºC to room temperature in the interface recording chamber, the frequency of the CCh-induced oscillation decreases, a change that is reversible by restoring the bath temperature. Warmer colors indicate peaks on the power spectra. Power spectra of the oscillation are shown at different time-points (and temperatures) marked by yellow boxes before (left), during (right) and after (far right) the temperature induced modulation of the oscillation. **B)** As shown on the unfiltered traces, by decreasing the temperature, the frequency decreases, which can be reversed by increasing the temperature. The transition is continuous, without a break in the properties of the oscillation, suggesting that the generation mechanisms at different temperatures are identical. **C)** Summary plot showing the significant decrease in the frequency of CCh-induced oscillations after changing from 32-34 ºC (33.1 ± 0.7 Hz) to the room temperature (20.1 ± 0.9 Hz, n=5, p<0.0001) without a change in the peak power (32-34 ºC: 368.8 ± 119.7 μV^2/Hz; room tempr.: 690.1 ± 243.1 μV^2/Hz, n=5, p=0.19).

Most *in vitro* experiments were conducted at room temperature to achieve necessary oxygenation of neurons. Under these conditions, the peak-to-peak amplitude of the CCh-induced oscillations was 147.6 ± 7.12μV with a power peak at 15.2 ± 0.5Hz (n=15). Although the frequency of CCh-induced oscillations at room temperature is in the beta frequency band (13–30 Hz), at more physiological temperatures it falls into the gamma frequency range (Fig. 15 and 16; Fisahn et al., 1998; Hájos et al., 2004). All other features of CCh-induced oscillations at room temperature and during temperature transitions resemble gamma oscillations recorded *in vitro* at 30-35°C or *in vivo* (Csicsvári et al., 2003; Mann et al., 2005; Hájos and Paulsen, 2009).

In the first set of experiments we aimed to know what firing properties characterize the three types of perisomatic region targeting interneurons in CA3 during cholinergically induced oscillatory activities. Although experiments of the previous part revealed that RSBCs do not likely to contribute to the oscillations because of the lack of GABA release during these conditions, we considered necessary to involve these cells to the following investigations (see explanation in the discussion chapter). We recorded the spontaneous firing properties of eGFP-expressing neurons in a loose-patch mode (Fig. 17 A, B). Using a whole-cell configuration, the same cell was then repatched and filled with biocytin for post hoc identification. Analysis of the results revealed that during oscillations the firing of the three cell types differed (Fig. 17 B–F, Table 3). FSBCs fired single spikes almost at each oscillation cycle, in contrast to AACs and RSBCs, which often skipped cycles (Fig. 16B, C). On average, FSBCs discharged two action potentials (i.e., doublets) in every 10^{th} cycle and AACs only occasionally fired doublets, while RSBCs very rarely did so (Fig. 17D). The phase of the action potentials (zero set to the negative peak of the oscillation recorded in stratum pyramidale) of different cell types did not prove to be a distinguishing feature, since cells fired on the ascending phase of oscillations with their preferred phase varying within overlapping ranges (Fig. 17E; 18A).

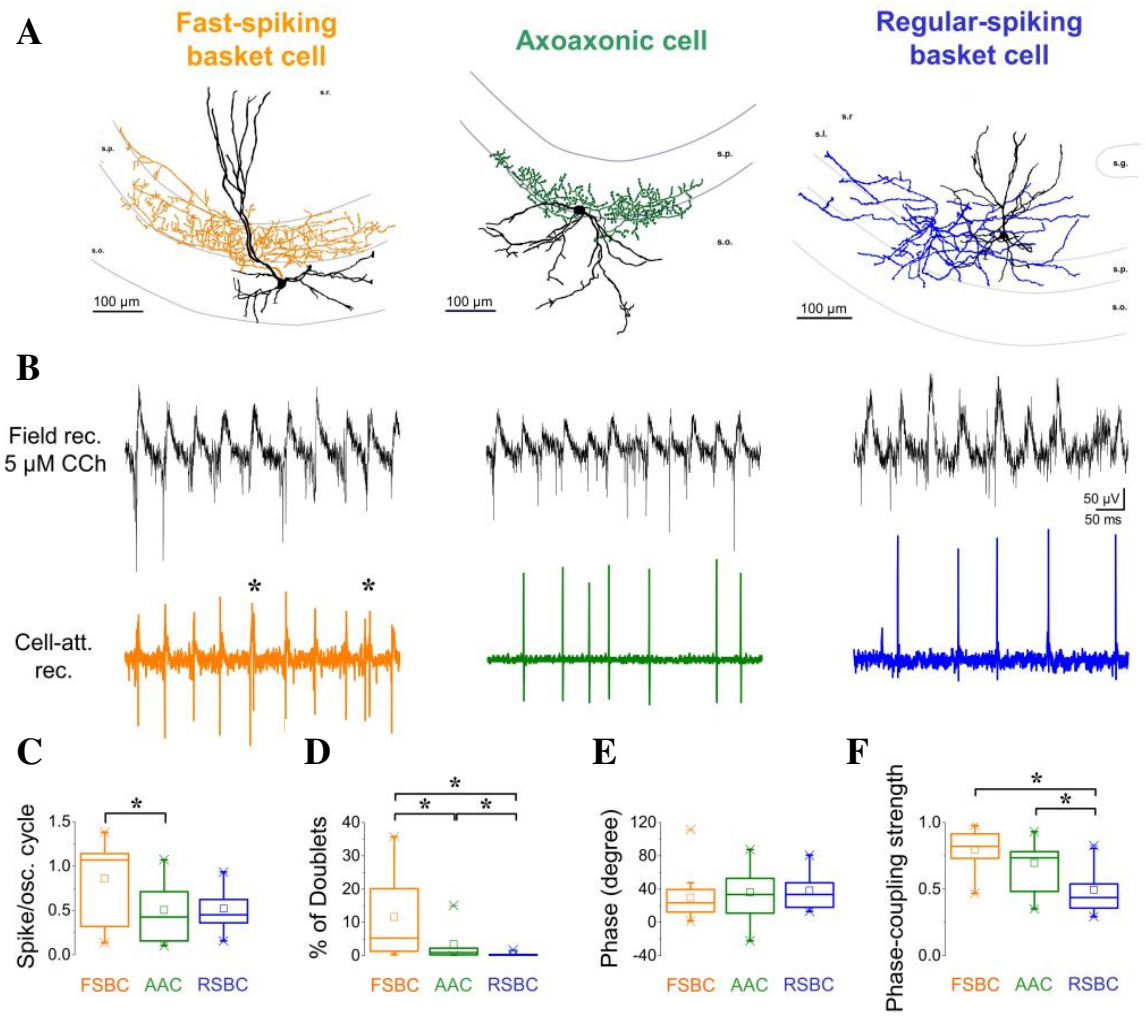

Figure 17. Subtypes of perisomatic region targeting inhibitory cells can be separated on the basis of their firing frequency, doublet incidence, and phase-coupling strength during CCh-induced network oscillations *in vitro*. A–C) Concomitant recording of field oscillations and spikes in a loose-patch mode from different perisomatic region targeting inhibitory cells (a) showed that they fire phase locked to oscillations induced by CCh (**B, C**). FSBCs (orange) often fired doublets (asterisks).**C, D,** The spikes per cycle (**C**) and the doublet ratio (**D**) were significantly higher for FSBCs (n = 13) than for AACs (n = 12, green) and RSBCs (n = 10, blue). Thus, FSBCs fired approximately once in every oscillation cycle. e, f, While the average phase of the individual cells varied around the ascending phase of the cycles (**F**) (see also Fig.18**A**) and cell types could not be separated on the basis of their firing phase (**E**), the phase coupling (**F**) of FSBCs and AACs was significantly (p = 0.001 and 0.023, respectively) higher than that of the RSBCs. Polar plots showing the firing accuracy and phase of each recorded neurons are shown in Fig. 18**A**. Here in **C–F**, and also in Fig. 26, the mean (small open square), the median (midline of the big box), the interquartile range (large box), the 5/95% values (ends of bars), as well as the minimal/maximal values (bottom and top X symbols) are shown on the charts. s.r., str. radiatum; s.l., str. lucidum; s.p., str. pyramidale; s.o., str. oriens; s.g., str. granulosum.

Table 3. Firing properties of the three types of perisomatic region targeting inhibitory cells during CCh-induced network oscillation.

	FSBC (n=13)	AAC (n=12)	RSBC (n=10)
Firing frequency (Hz)	15.01 ± 2.3	7.9 ± 1.3	9.42 ± 1.2
Spike/osc. cycle	0.86 ± 0.13	0.51 ± 0.09	0.52 ± 0.08
% of Doublets	11.6 ± 3.6	3.4 ± 1.4	0.4 ± 0.1
Phase (degree)	29.9 ± 7.8	36.3 ± 8.4	38.1 ± 6.5
Phase coupling strength	0.8 ± 0.04	0.69 ± 0.06	0.49 ± 0.06

Data are presented as mean ± SEM.

In contrast, there was a difference in the phase-coupling strength of the three cell types (Fig. 17F). FSBCs fired with high accuracy around the phase characteristic for the individual cells. The firing of AACs was less coupled to the oscillation, and RSBCs proved to be significantly less accurate in their firing than the other two cell types. In summary, during CCh-induced synchronous activities in hippocampal slices, FSBCs were the most active perisomatic region targeting inhibitory cells and often fired doublets in a cycle, and their action potentials were the most strongly coupled to the oscillation.

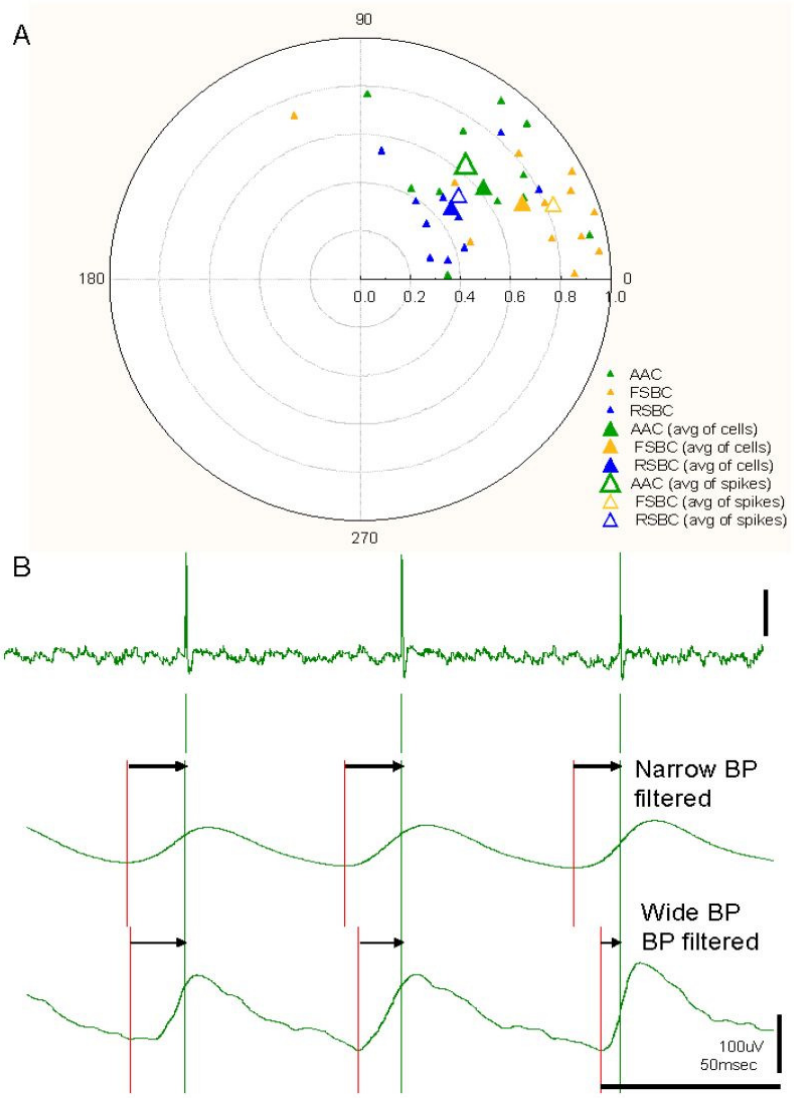

Figure 18. Firing phase and phase coupling of all recorded cells, the effect of filtering on spike phase detection. A) Firing phase of individual cells within each population scattered considerably, though their phase coupling was higher than found in *in vivo* experiments. Preferred firing phase for each perisomatic region targeting inhibitory cell group was calculated in two different ways: either the average phase and coupling of all individual cells were circularly averaged (large closed symbols), or all spikes from the same group of cells were pooled and the circular average and coupling were calculated (large open symbols). As visible on the figure the result of the two different ways of averaging gave similar phase and coupling strength for the populations and that the average phases of the populations are close to each other.

B) Filtering oscillation in different ways results in different spike phase assignment. In *in vivo* studies the field signal is band-pass filtered in a narrow range (BP, 5-30 Hz) to detect gamma oscillation. This results in a loss of high-frequency components and the signal is sinusoid rather than saw-tooth shaped. The negative peak of the sinusoid wave is shifted earlier compared to the negative peak of the wide BP filtered trace (5-500 Hz, red bars indicate detected negative peaks). Therefore the phase assigned to the detected spike (green bars, top trace) is systematically larger for the narrow BP filtered trace (middle trace) than for the wide BP filtered trace (bottom trace), as shown by the longer arrows between the red and green lines on the middle trace compared to the bottom trace. While in our study there is a shift in the firing phase of the perisomatic region targeting inhibitory cells, if detected on the basis of filtering used in *in vivo* studies versus how we filtered the oscillation, the shift is near systematic and the preferred firing phase of the cells overlaps. Regardless how firing phase was calculated, there was no significant difference in the populations' firing phase, due to the scatter of the firing preference of individual cells shown on **A**.

IV/8. DAMGO, an opioid receptor agonist reduces CCh-induced fast network oscillations via μ-opioid receptors

Morphine has been shown to be able to disrupt long-range synchrony of gamma oscillations in hippocampal slices via μ-opioid receptors (MORs) (Whittington et al., 1998). Since these types of opioid receptors are selectively expressed on PV-immunopositive axon terminals (Drake and Milner, 2002) and their activation effectively reduced GABA release from fast spiking basket cells (Glickfeld et al., 2008), activation of MORs could be a useful tool to investigate the contribution of PV-containing perisomatic region targeting inhibitory cells to oscillogenesis. Therefore, we tested whether the activation of MORs could interfere with fast network oscillation generated in our *in vitro* slices. We induced network oscillations by bath application of 5μM CCh in hippocampal slices. Addition of 1μM DAMGO to the superfusate effectively reduced the power or even fully eliminated the CCh-induced oscillations within 2–8 min both at room temperature (Fig. 20, left) and at 32-34°C (Fig 21).

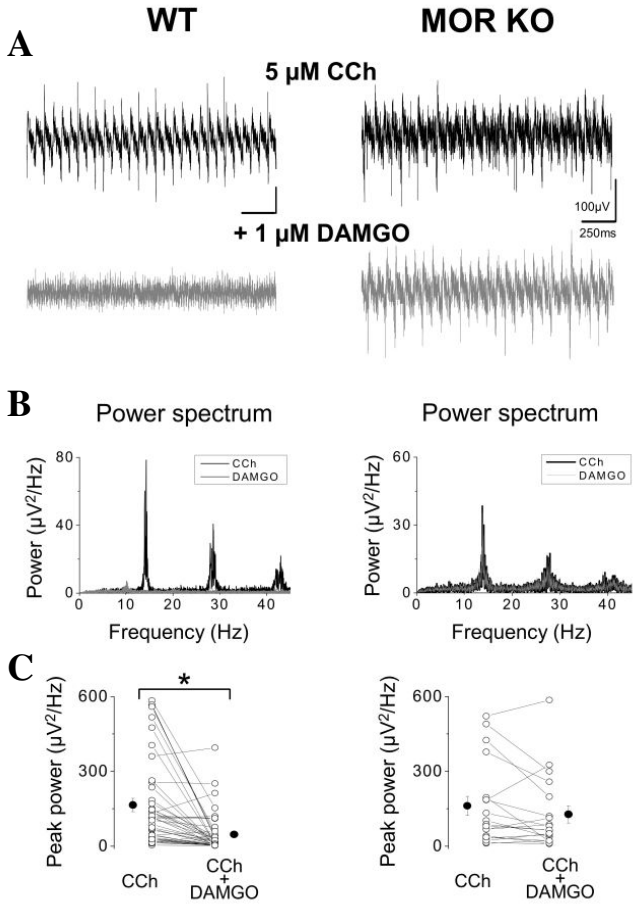

Figure 20. CCh-induced *in vitro* network oscillations can be blocked by MOR activation. A) CCh-induced oscillations (top row) were blocked by bath application of 1μM DAMGO in the WT mouse (left), but not in MOR KO animals (right), indicating the specific action of DAMGO on MORs. **B)** Power spectral density plots from the same experiment show a decrease in the power following DAMGO application in WT (left), but not in KO (right) animals. **C)** Statistical analyses demonstrated a significant drop in the peak power in the WT (left, 164.9 ± 26.7 vs 46.7 ± 11.6 μV^2/Hz; n = 44; Wilcoxon signed rank test, p< 0.0001) but not in the KO animals (right, 161.7 ± 38.2 vs 127.3 ± 34.4 μV^2/Hz; n = 19; Wilcoxon signed rank test, p = 0.15).

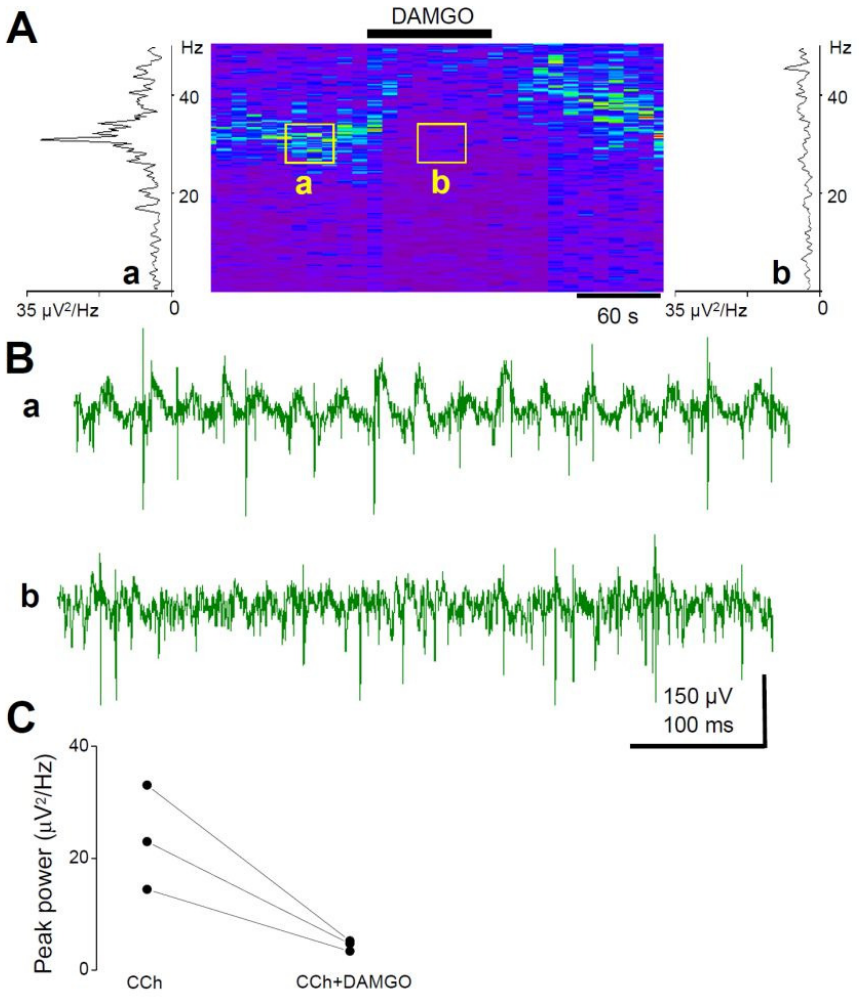

Figure 21. Cholinergically induced oscillations at 32-34 ºC can be also reversibly blocked by DAMGO application. **A)** The colored spectrograms of 10-s-long epochs versus time show that bath application of DAMGO effectively diminished the oscillation, which could be fully reversed after washing out the drug. Warmer colors indicate peaks on the power spectra. Power spectra of the oscillation are shown at different time-points marked by yellow boxes before (a, left) and after (b, middle) the DAMGO treatment. **B)** As shown on the unfiltered traces taken from the same periods, DAMGO application substantially reduced the peak amplitude, i.e. the power of the oscillation at this, physiologically more relevant temperature. **C)** Summary plot showing the significant decrease in the peak power of CCh-induced oscillations after DAMGO treatment (4.4 ± 0.5 μV^2/Hz) compared to control (23.5 ± 5.4 μV^2/Hz, n=3, p=0.05).

To test the specificity of DAMGO action, CTAP, a MOR antagonist, was applied (200 nM) for 5 min preceding DAMGO. CTAP alone did not change the parameters of the oscillation, suggesting the lack of tonic MOR activation in our slice preparations, but prevented the effect of subsequently applied DAMGO (Fig. 22). If CTAP was applied after DAMGO-induced drop in oscillation power, it could fully reverse the effect of DAMGO in 5–10 min (Fig. 22).

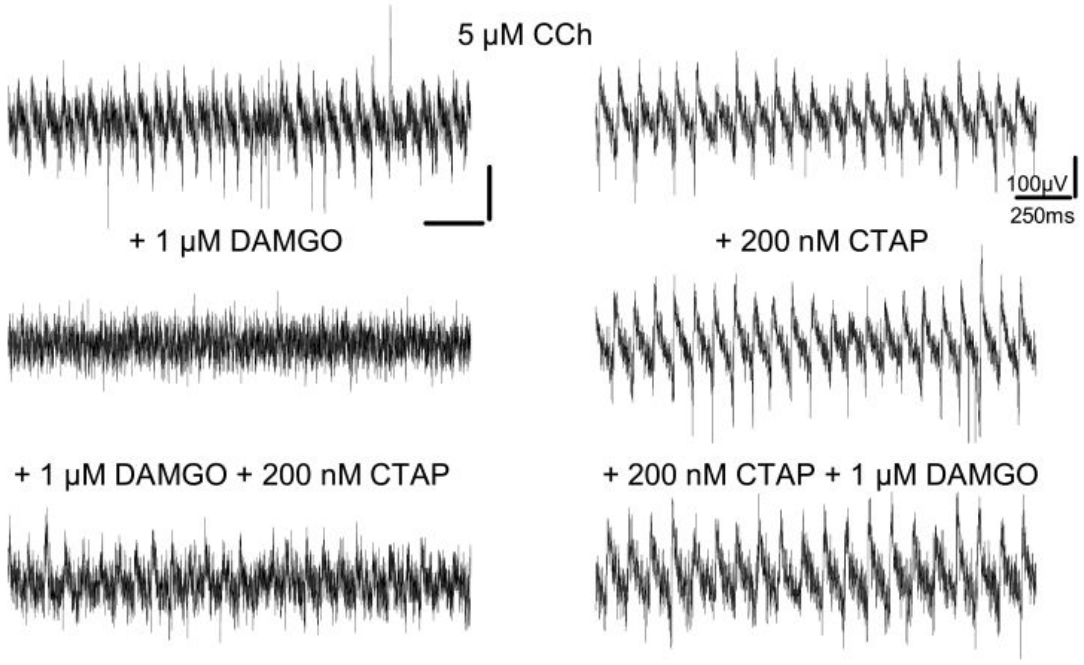

Figure 22. Effect of μ-opioid receptor activation could be reversed or occluded by bath application of a MOR antagonist, CTAP. Left: n=3, baseline: 54.07 ± 18.69 μV^2/Hz, DAMGO: 14.47 ± 3.71 μV^2/Hz, +CTAP 55.60 ± 21.87 μV^2/Hz, baseline and DAMGO+CTAP is significantly different from DAMGO p=0.035. Right: n=3, baseline: 47.57 ± 7.25 μV2/Hz, CTAP: 44.20 ± 6.51 μV2/Hz, +DAMGO 43.53 ± 3.72 μV^2/Hz, no significant difference.

To further confirm that DAMGO acted exclusively via MORs, we repeated the experiments in MOR knockout mice. We found no difference in the peak power (WT: 164.9 ± 26.3μV^2/Hz, n = 44; KO: 161.17 ± 38.2 μV^2/Hz, n = 19; Mann–Whitney test, p = 0.98) or in the frequency of network oscillations (WT: 15.1 ± 0.7 Hz, n = 44; KO: 16.5 ±

0.8Hz, n = 19; Mann–Whitney test, p = 0.12) between the KO and WT animals. In mice lacking MORs, DAMGO application had no detectable effect on the power and the frequency of the oscillations (Fig. 20, right).

Thus, these data collectively showed that DAMGO could effectively suppress CCh-induced oscillation, an effect that was mediated solely via MORs.

IV/9. μ-opioid receptor activation suppresses synaptic inhibition causing desynchronization of pyramidal cell activity

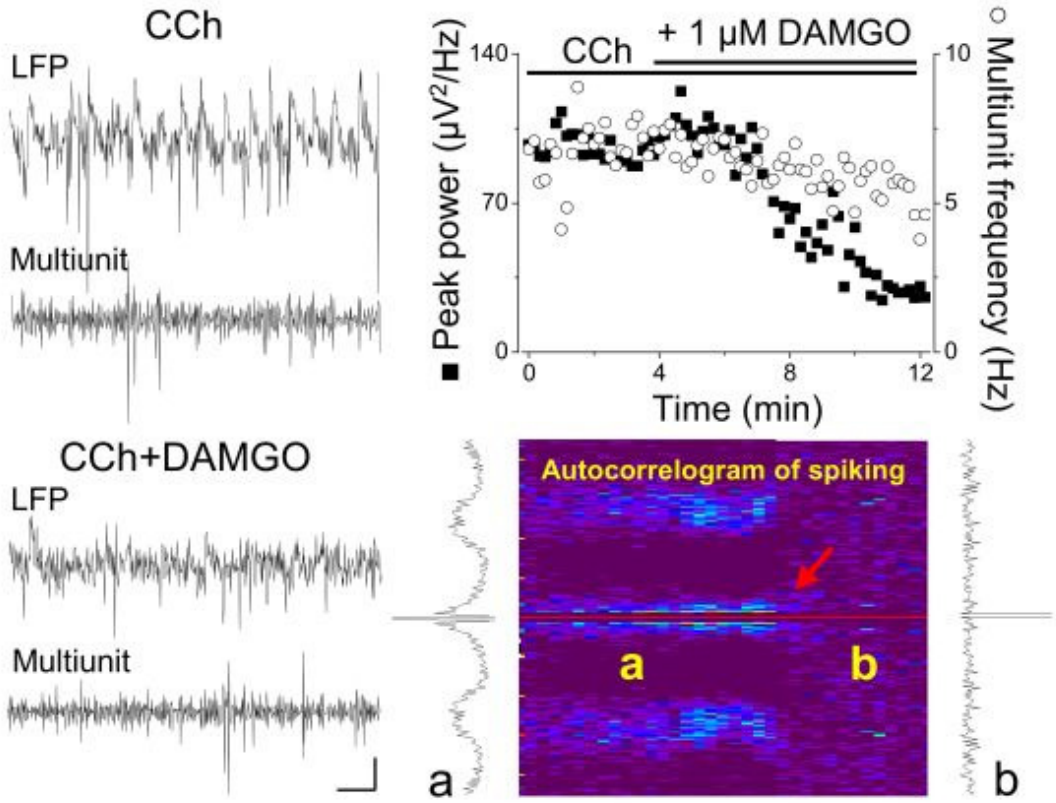

Figure 23. μ-opioid receptor activation suppresses network oscillations as a result of desynchronization of multiunit activity without changing firing frequency. The left column shows parallel recordings of field oscillations (top trace) and concomitant multiunit activity (filtered between 100 Hz and 2 kHz) during CCh-induced oscillation before and after DAMGO application. Calibration: 50 μV and 0.1 s. The time course of the same experiment is shown in the right column. While the wash-in of DAMGO caused a fast drop in the peak power of the oscillation, the frequency of multiunit activity only slightly decreased (top), but their synchronization was abolished (arrow) as indicated by the autocorrelograms (bottom).

Two different mechanisms may lead to the break down of field oscillations: decrease of the activity of neurons leads to the subsequent disappearing of the currents responsible for the generation of the rhythmic field potentials; or alternatively, the firing of neurons desynchronizes and the currents do not sum up to give a detectable field signal. To get a deeper insight into the mechanisms of how DAMGO blocks oscillations and to distinguish these two possibilities, first we recorded local field potentials in stratum pyramidale and simultaneously monitored multiunit activity that reflects mostly pyramidal cell firing (Fig. 23).While the peak power of oscillations was significantly reduced by DAMGO application (CCh: 86.4 ± 17.8μV^2/Hz; CCh plus DAMGO: 18.6 ± 5.4 Hz; n = 5, p = 0.006), the frequency of multiunit firing did not change (CCh: 26.2 ± 9.3 Hz; CCh plus DAMGO: 24.2 ± 9.1Hz; n = 5, p = 0.54), but, remarkably, unit synchrony disappeared, as shown by the multiunit autocorrelograms (Fig. 23). Though we could not identify the neurons participating in the multiunit spike assembly, they fired earlier in the oscillation phase (phase: 2.96 ± 1.13°; phase-coupling strength: 0.67 ± 0.054; n = 5) than the interneurons (Table 3), indicating that they were pyramidal cells (Hájos et al., 2004).

To clarify what might be in the background of this asynchronicity, we monitored local field potentials in stratum pyramidale as well as EPSCs and IPSCs from two pyramidal cells (Fig. 24). The originally synchronized, phase-locked, large-amplitude, compound IPSCs decreased, or, as in the experiment shown in Figure 24, largely fell below the detection threshold by DAMGO application (Fig. 24, bottom). Since the currents generating CCh-induced oscillations in the hippocampus predominantly originate from perisomatic inhibitory synapses (Mann et al., 2005; Oren et al., 2010), parallel to the IPSC amplitude decrease, the power of the oscillations also dropped, or completely disappeared (Fig. 24, top). During this transition, there was a much smaller change in the amplitude or in the frequency of EPSCs (or in the charge per cycle). However, the synchrony of the excitatory events decreased and disappeared, as shown on autocorrelograms (Fig. 24, middle).

These results together suggest that after the suppression of CCh-induced oscillations caused by DAMGO, pyramidal cell activity is mostly maintained, but their spikes are no longer phase locked to the oscillations due to the disappearance of periodic inhibitory control. Thus, the reduction of synaptic inhibition by DAMGO could decrease or abolish CCh -induced network oscillations.

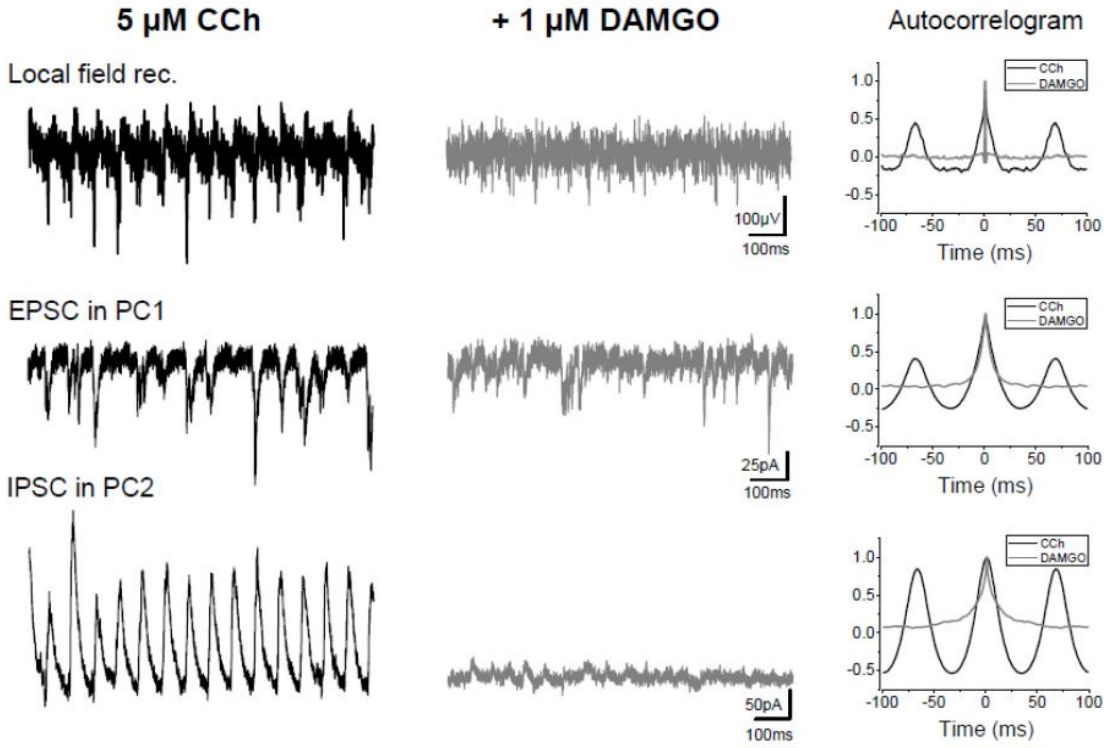

Figure 24. DAMGO application suppresses network oscillations in parallel to the decrease of IPSC amplitudes, that results in de-synchronization of EPSCs. The left column shows in black parallel recordings of field oscillations (top trace) as well as EPSCs (middle) and IPSCs (bottom) recorded from two pyramidal cells during CCh-induced oscillation. As shown on the autocorrelograms (right column), postsynaptic currents were highly synchronous and phase locked to the field oscillation. Application of DAMGO (grey traces in the middle) significantly reduced synaptic inhibition (averaged charge changed from 37.02±3.38 pC to 17.02±0.90 pC, n=5, p=0.04), and resulted predominantly in the desynchronization of EPSCs without a change in their charge (from 8.72±0.67 pC to 10.09±0.79 pC, n=5, p=0.15). As shown by the autocorrelogram, the field oscillations were also inhibited (peak power, CCh, 83.2±7.5 μV^2 /Hz; in CCh+DAMGO, 28.4±2.9 μV^2/Hz, n=5; p=0.04).

IV/10. Activation of μ-opioid receptors reduces inhibitory transmission, but leaves excitatory transmission and pyramidal cell properties intact

The finding that DAMGO reduces synaptic inhibition is in agreement with earlier results (Masukawa and Prince, 1982; Cohen et al., 1992). However, to clarify the mechanisms underlying the effect of MOR activation on oscillation, we aimed to determine whether DAMGO exerts additional effects on the elements of CA3 neuronal network. First, we tested the effects of DAMGO on the cellular properties of CA3 pyramidal cells. These neurons showed no significant change in their input resistance (in CCh: 370.0 ± 25.5 MOhm; in CCh plus DAMGO: 355.5 ± 9.83 MOhm; n = 5; p = 0.53) or in their membrane time constant (in CCh: 88.6 ± 8.58 ms; in CCh plus DAMGO: 90.5 ± 16.0 ms; n = 5; p = 0.89).

We then examined the effects of DAMGO on evoked and miniature postsynaptic currents. As shown in Figure 25, in CA3 pyramidal cells DAMGO application caused a significant reduction in the amplitude of IPSCs evoked by electrical stimulation of fibers in stratum pyramidale or at the border of strata pyramidale and lucidum. In contrast, MOR activation had no effect on EPSC amplitude evoked with the stimulation of fibers in stratum radiatum. Similarly, in CA3 pyramidal cells a decrease was detected in the frequency of miniature IPSCs following DAMGO application, without a change in their amplitude distribution. No change could be detected in the frequency or amplitude of miniature EPSCs. For more details, see Figure 26.

Last, we tested whether the excitatory input on interneurons expressing PV could be affected by DAMGO. Similarly to the results obtained in CA3 pyramidal cells, the activation of MORs had no effect on the amplitude of evoked EPSCs recorded in three FSBCs and two AACs (in CCh: 202.7 ±59.1 pA; in CCh plus DAMGO: 214.8 ± 73.3; n = 5, p = 0.72; not shown).

These results collectively demonstrated that DAMGO suppresses only inhibitory transmission, without affecting the excitatory synaptic communication and pyramidal cell excitability in the presence of CCh.

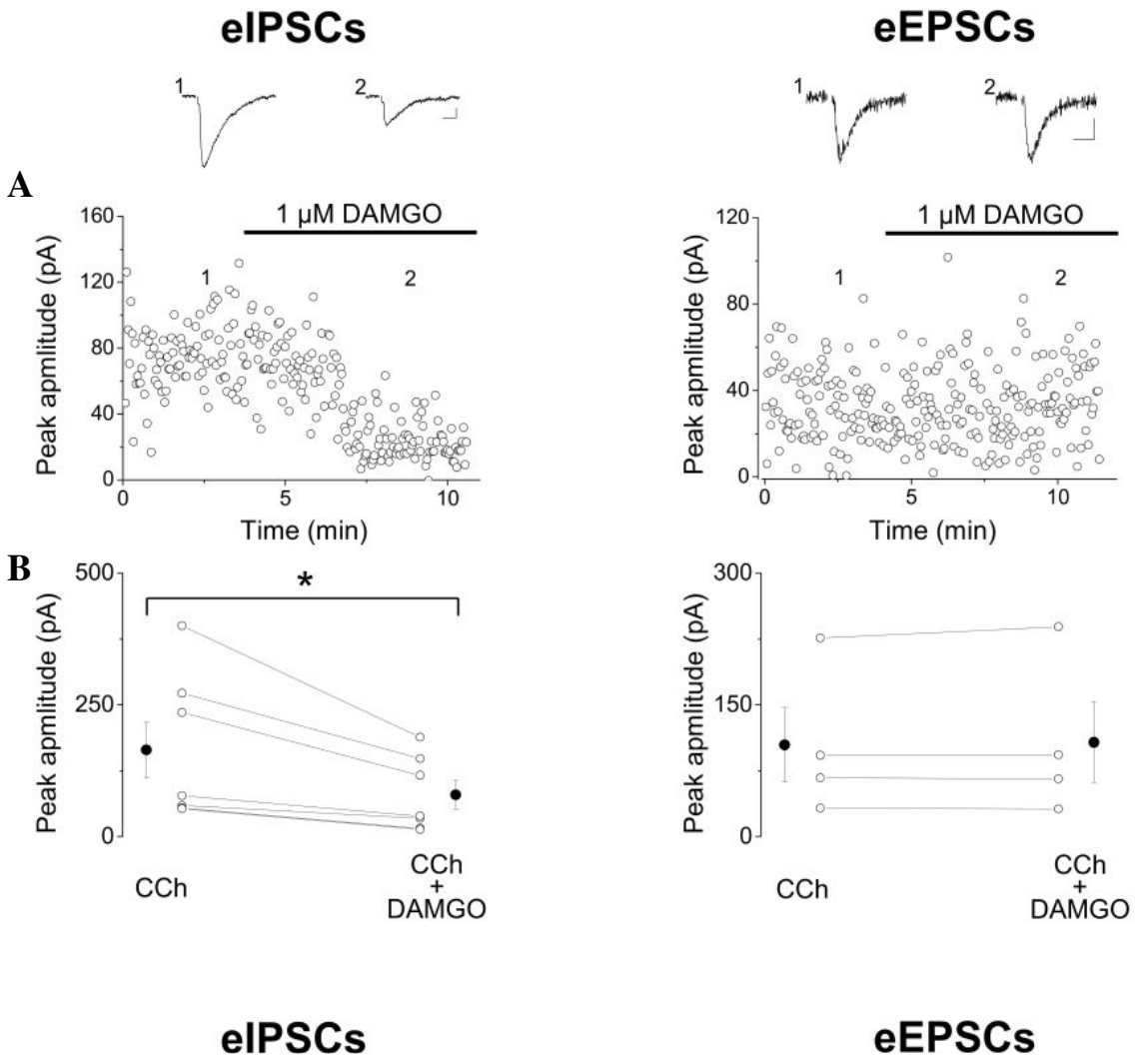

Figure 25. μ-opioid receptor activation reduces the amplitude of inhibitory, but not excitatory synaptic currents evoked by electrical stimulation in CA3 pyramidal cells. A) Two examples showing that the bath application of DAMGO reduced the peak amplitude of evoked inhibitory synaptic currents (eIPSCs), leaving unaffected the amplitude of evoked excitatory synaptic currents (eEPSCs). Recordings were done in the presence of 5 μM CCh. Example traces are averaged records of six to eight consecutive events taken at the labeled time points. The stimulus artifacts were removed from the traces. Calibration: 10 pA and 10 ms. **B)** In all tested cases, DAMGO application significantly reduced the amplitude of evoked IPSCs (left, 164.3 ± 52.38 vs 79.3 ± 26.68 pA in DAMGO, n = 7, p = 0.017) recorded from CA3 pyramidal cells elicited by electrical stimulation in stratum pyramidale or at the border of strata radiatum and lucidum. In contrast, EPSCs elicited by electrical stimulation in stratum radiatum showed no change following DAMGO application (right,104.4 ± 42.3 vs 107.2 ± 45.6 pA in DAMGO, n = 4, p = 0.45).

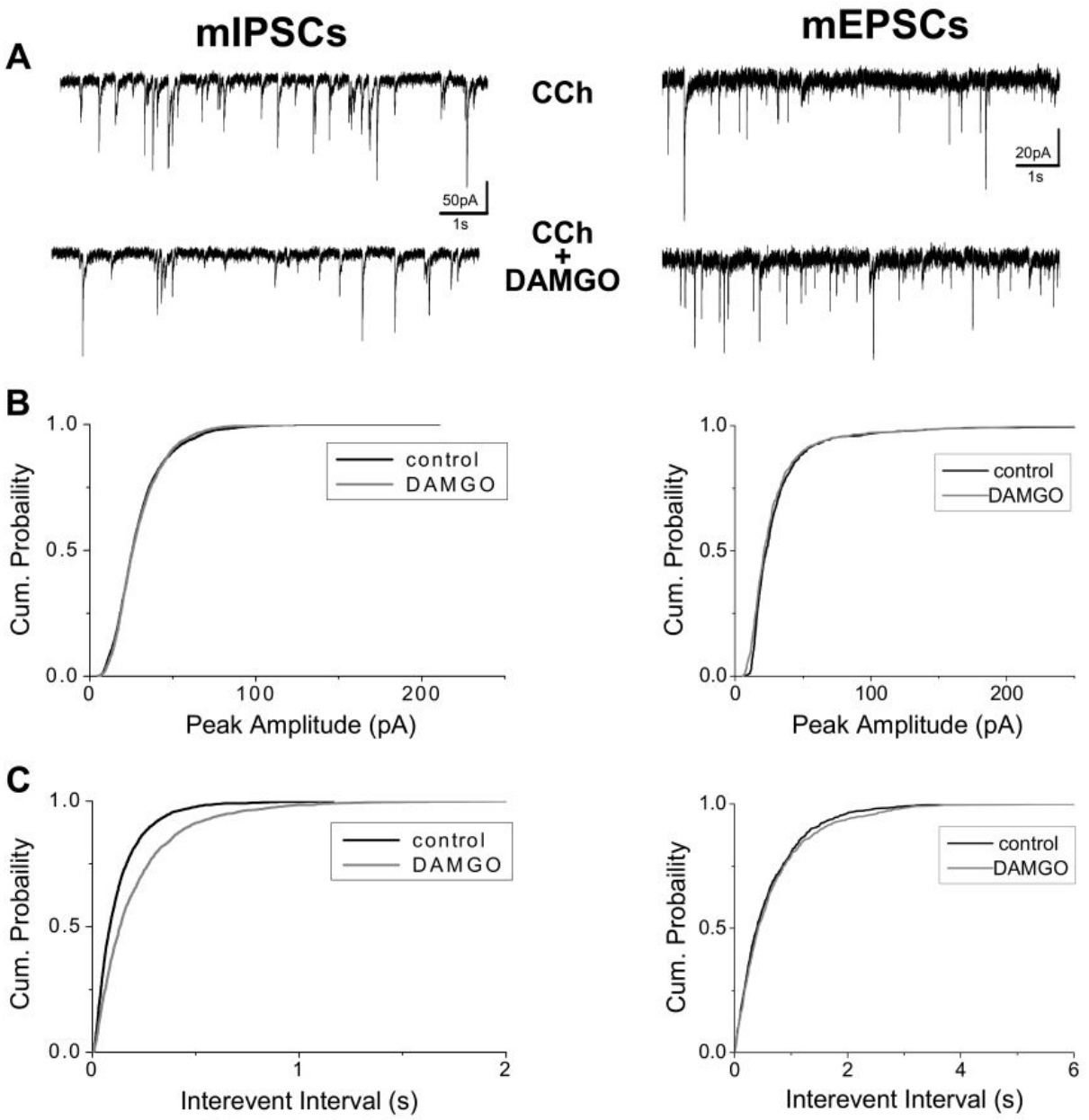

Figure 26. μ-opioid receptor activation decreases the frequency of miniature inhibitory, but not excitatory synaptic currents without affecting their amplitudes. **A)** Raw data obtained in the presence of 500 nM TTX in CA3 pyramidal cells are shown. **B)** DAMGO application in the presence of 5 μM CCh did not alter the amplitude of mIPSCs (n=7, p>0.1) or mEPSCs (n=7, p>0.1) as shown on the cumulative distributions. **C)** In contrast, the frequency of mIPSCs were decreased (n=7, p<0.001) indicated by the rightward shift on the cumulative distributions, an effect that suggests the presynaptic locus of DAMGO action. The frequency of mEPSCs was not altered (n=7, p>0.1).

IV/11. GABA release from FSBC and AAC terminals is differently affected by DAMGO application in the presence of CCh

Our pharmacological experiments strengthened the hypothesis that PV-immunopositive perisomatic region targeting inhibitory cells expressing MORs could have a role in oscillogenesis. Immunocytochemical results showed that MORs are expressed in PV-immunopositive axon terminals synapsing on the somata or on the proximal dendrites of hippocampal pyramidal cells, but in the axon endings contacting axon initial segments the presence of MORs is questionable, as stated by Drake and Milner (2002). Since RSBCs do not participate in perisomatic current generation here, these data propose that the effect of DAMGO on oscillation could be due to the reduction of GABA release predominantly, if not exclusively, from the axon terminals of FSBCs. To address the question of the extent to which IPSCs originating from the PV-expressing interneuron types might contribute to active current sources in the pyramidal cell layer (Mann et al., 2005), we performed paired whole-cell recordings from presynaptic PV-expressing interneurons and postsynaptic pyramidal cells in the CA3 region (Fig. 27A). As demonstrated in part I., CCh decreased the amplitude of uIPSCs originating from PV-expressing perisomatic region targeting interneurons, but a significant portion of release remained intact (Fig. 10). We tested whether in the presence of CCh, which is needed for the maintenance of the oscillation, a further change can be observed in response to DAMGO application. To approximate the conditions to continuous firing during ongoing oscillation, we evoked trains of 10 action potentials at a frequency that was typical of the given cell type, i.e. 15Hz and 10Hz at FSBC and AAC, respectively. Then to mimic the conditions of a steady state oscillation we measured the amplitude of the last five uIPSCs, when the possible synaptic depression in FSBC– and AAC-pyramidal cell pairs reached steady-state levels (Fig. 27B). Comparison of uIPSC amplitudes before and after DAMGO application revealed that the last five uIPSCs in FSBC–pyramidal cell pairs were significantly depressed compared to the uIPSCs measured in the presence of CCh, but there was no further reduction in uIPSC amplitudes observed in AAC–pyramidal pairs (Fig. 27A,B). Interestingly, the uIPSC amplitude of FSBCs in the mixture of CCh and DAMGO was not significantly different from the IPSC amplitude of AACs in the presence of CCh or in CCh plus DAMGO ($p = 0.15$) (Fig. 27C). These data demonstrate that in the presence of CCh DAMGO selectively suppressed GABA release from axon terminals of FSBCs, but not of AACs, and thus synaptic output

of FSBCs is the major source of the perisomatic inhibitory currents, which generates CCh - induced field oscillation.

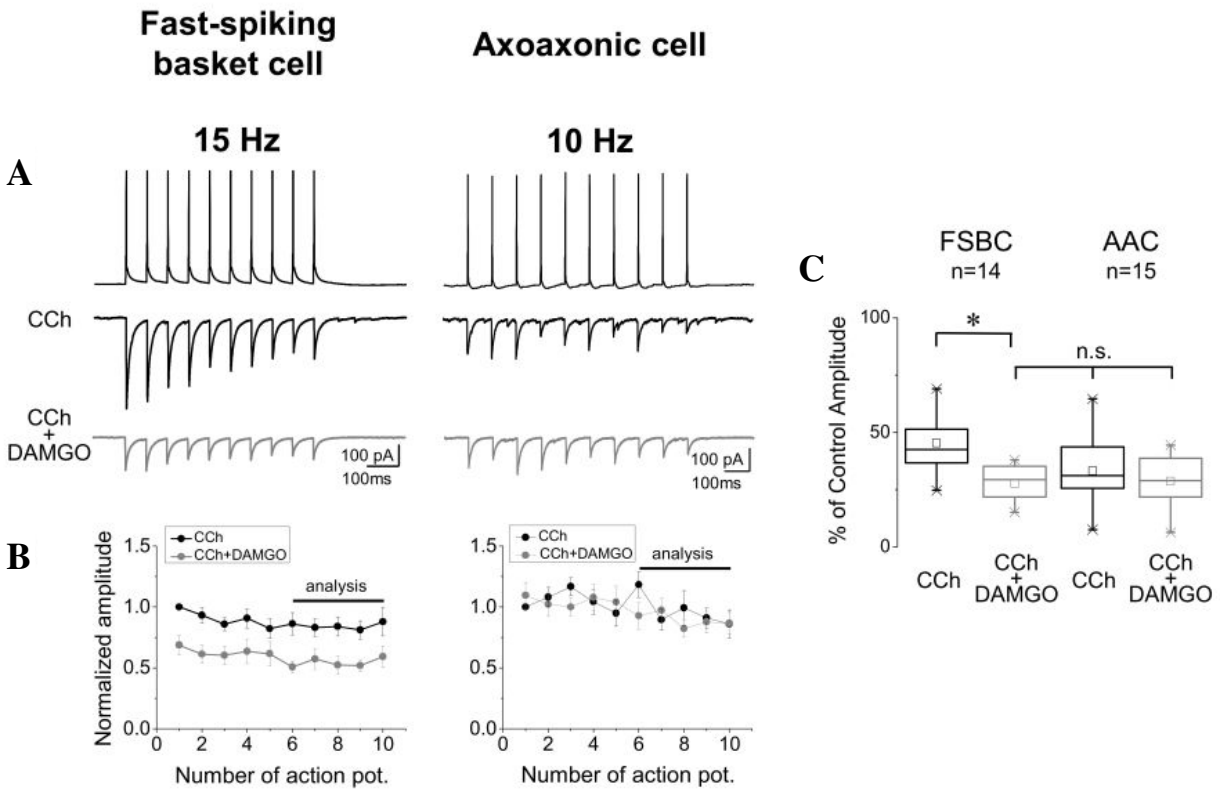

Figure 27. μ-opioid receptor activation selectively reduces the residual inhibition of FSBCs, but not of AACs, in the presence of CCh. A,B) DAMGO application did not cause a noticeable decrease in synaptic inhibition of the AAC, but further suppressed the unitary IPSC amplitude of the FSBC. **C)** While the addition of DAMGO has not significantly reduced further the amplitude of IPSCs in AAC-pyramidal cell pairs (90.4 ± 6.0 % of the amplitude in CCh, n=15, p = 0.15), there was a significant reduction in the amplitude in FSBC–pyramidal cell pairs (62.3 ± 3.9% of the amplitude in CCh, n = 14, p = 0.001), decreasing the current amplitudes down to the level of AAC–pyramidal cell pairs (p = 0.15).

The question arises whether DAMGO would be able to suppress the CCh-induced oscillation, if the GABA release was normal from the axon terminals of RSBCs (i.e., when the firing of RSBCs would give rise to IPSCs during oscillations). To clarify this issue, we induced oscillations with CCh in hippocampal slices prepared from CB1R knock-out mice, where CCh does not alter the GABA release of RSBCs (Neu et al., 2007). Comparable to those results obtained in wild type mice, DAMGO could reduce, or even eliminate the carbachol-induced oscillations in slices from these knock-outs (Fig. 28). This finding shows that eliminating the contribution of fast-spiking basket cells to the CA3 network results the collapse of oscillation even if the function of RSBCs remain intact.

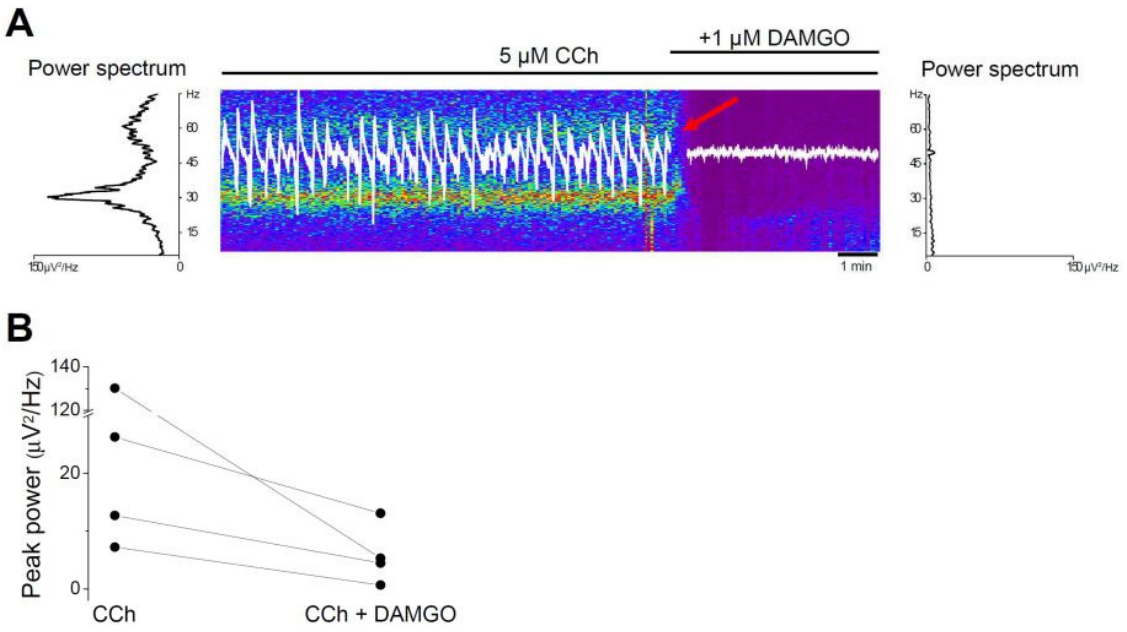

Figure 28. CCh-induced oscillations in hippocampal slices prepared from CB1 cannabinoid receptor knockout mice are also suppressed by bath application of the µ-opioid receptor agonist DAMGO. Field oscillation was monitored in the pyramidal cell layer of CA3 at 32-34 ºC. **A)** The color figure shows the changes in the power spectra as a function of time, which were calculated from 10-s-long epochs. Warmer colors indicate the magnitude of the peak on the power spectra. Example traces from before and after DAMGO application (in white) are overlaid on the spectrogram. Left and right graphs indicate the power spectra under control conditions and after the drug treatment. The red arrow shows the rapid drop in the oscillation power. **B)** Summary plot of results obtained in four different experiments. In the control, oscillations had a mean frequency of 28.8 ± 1.3 Hz and their max. gamma power was 44.1 ± 28.9 μV^2/Hz (n=4), which significantly differed from those values calculated in the presence of DAMGO 5.8 ± 2.6 μV^2/Hz (p=0.03).

V. DISCUSSION

The main goal of experiments shown in the present thesis was to get deeper insights into the mechanisms underlying cholinergically induced fast network oscillations. Being aware of that perisomatic inhibition plays a key role in the generation of oscillatory activities, in the first part of the thesis we investigated the output properties of the cells giving rise to perisomatic inhibition, i.e. the characteristics of GABA release from axon endings of distinct types of perisomatic region targeting interneurons during control conditions and in the presence of CCh. Regarding oscillations, one of the most important findings of these approaches is that although all investigated cell types are sensitive to cholinergic receptor activation, in the presence of 5μM CCh RSBCs release a very little, if any GABA, which excludes their participation in the maintenance of CCh-induced fast network oscillation.

The role of the remaining two cell types in the oscillogenesis was clarified in the second study. Field potential experiments unequivocally demonstrated that the activation of μ-opioid receptors effectively disrupts CCh-induced fast network oscillations. Paired recordings indicated that this effect is due to the FSBCs, suggesting that these cells are endowed with such properties that make them capable of generating oscillation.

V/1. Special properties of perisomatic inhibition (Study I.)

Experiments of the first part revealed the different characteristics of interneurons synapsing on the soma-near membranes of pyramidal cells. The finding that different types of these interneurons have distinct output properties that could be variously affected by CCh suggests that these cell types may fulfill different roles in the control of pyramidal cell firing, and additionally, they provide an indirect way to influence the pyramidal cell functions by cholinergic inputs. We found that AACs produced the largest uIPSCs compared to the other two groups. Although it was suggested that the terminals originating from different perisomatic region targeting neurons form synapses with $GABA_A$ receptors enriched with certain subunits (Nusser et al., 1996; Nyíri et al., 2001), other studies showed that in the CA1 region all somatic synapses similarly contain α1, α2, β3 and γ2,3 subunits

(Kasugai et al., 2010; Somogyi et al., 1996). Therefore, neither the larger amplitude nor the longer decay of uIPSCs in AAC– pyramidal cell pairs compared to those recorded in basket cell–pyramidal cell pairs could be the result of distinct subunit compositions. In addition to the similar subunit composition, the area of synapses formed by basket cells and AACs was found to be similar (Nusser et al., 1998). Thus, the larger amplitude of these uIPSCs might be attributable to the higher number of synaptic contacts formed by AACs compared to basket cells, although the number of axon terminals of AACs contacting CA3 pyramidal cells has not been studied specifically in CA3. Basket cells preferentially innervate pyramidal cells in CA3 via two to six synapses (Miles et al., 1996; Biró et al., 2006). This number is lower than the observations obtained in other regions, for instance in CA1, where 10–12 synaptic contacts were identified between basket cells and pyramidal cells (Buhl et al., 1994; Cobb et al., 1997). In this region, AACs have been shown to innervate their targets via similar numbers of synapses (Maccaferri et al., 2000), which is in agreement with physiological measurements showing that basket cells and AACs in CA1 produce uIPSCs with similar amplitude. If we assume that the sum of $GABA_A$ receptor conductances at a given synapse that originate from perisomatic region targeting inhibitory cells are similar in different regions, then in CA3 more synaptic contacts should be responsible for the larger IPSC amplitude in AAC–pyramidal cell pairs than in basket cell–pyramidal cell connections.

Beside larger amplitudes, uIPSCs from AAC terminals showed salient decay values as well. Our experiments suggest that this finding may be due to the different probability of GABA spillover at the different release sites as it was introduced by Overstreet and Westbrook (2003) in the dentate gyrus. By using CCh to reduce the probability of release we could apparently increase the distance between individual release sites hence we decreased the chance to synaptic cross-talk (Fig. 14). The observation that this phenomenon predominantly occurs at AAC-pyramidal cell synapses and in a much lesser extent at FSBC-pyramidal cell synapses is probably attributable to the different synapse density. Nevertheless, it should be taken into account that our experiences were achieved at room temperature, at which the neurotransmitter transporters are largely altered (Binda et al., 2001). Under physiological conditions (i.e. at higher temperature), GABAergic synapses of AACs are probably not subject to cross-talk because they produce IPSCs with similar kinetics to basket cells (Maccaferri et al., 2000; Overstreet and Westbrook, 2003).

Nevertheless the present observations might gain significance in pathological states in which the GABA uptake system is compromised (Volk et al., 2001; Liu et al., 2007).

We found that the uIPSC response follows the action potential in the RSBCs with a significantly longer latency compared to either FSBC - or AAC - pyramidal cell synapses. Furthermore, we found RSBCs to produce uIPSCs with lower release probability compared to the other two cell types, and additionally, RSBCs were found to be able to release transmitter in an asynchronous manner. Together these properties, at least partly, might be due to the different types of presynaptic voltage sensitive Ca^{2+} channels. In the dentate gyrus it has been shown by pharmacological approaches that whereas the parvalbumin-containing basket cells express P/Q-type Ca^{2+} channels, the CCK positive basket cells express N-type Ca^{2+} channels at their axon terminals (Hefft and Jonas, 2005). It is very likely that similarly to the dentate gyrus and CA1, RSBCs and FSBCs are equipped with N-type and P/Q type Ca^{2+} channels, respectively. The presence of P/Q-type Ca^{2+} channels at the active zone of PV-containing basket cell terminals was also proved by electron microscopic investigations (Bucurenciu et al., 2008), but no data are available about which type of Ca^{2+} channel mediates transmitter release from AAC terminals. It was shown that the evoked IPSCs originating from the depolarization-induced suppression of inhibition (DSI) sensitive fibers could be blocked by the N-type Ca^{2+} channel inhibitor ω-conotoxin, whereas the evoked IPSCs coming from the DSI-insensitive fibers could be blocked by the P/Q-type Ca^{2+} channel inhibitor ω-agatoxin (Wilson et al., 2001). Since in the former study the DSI-insensitive IPSCs originating from the AACs and from the FSBCs were not distinguished, it can be supposed with high likelihood that transmitter release from the AAC terminals is also carried out by P/Q-type Ca^{2+} channels. This idea is supported by the similar kinetic properties and similarly depressing feature of the synapses of AACs and FSBCs (Figures 9; 11).

The tight coupling of P/Q-type Ca^{2+} channels to the Ca^{2+} sensors can be responsible for the faster and more precise response at FSBC and probably AAC terminals, whereas the loose coupling of N-type Ca^{2+} channels to the Ca^{2+} sensors at RSBC terminals may result longer latency and rise time (Hefft and Jonas, 2005). This loose coupling between the Ca^{2+} sources and sensors also results that the CCK expressing perisomatic boutons may release GABA in an asynchronous manner in the rat dentate gyrus (Hefft and Jonas, 2005), as well as in the cornu Ammonis (Daw et al., 2009). In agreement with these results we showed that in the mouse hippocampal CA3 region RSBC terminals may also release GABA

asynchronously, whereas the other two perisomatic region targeting inhibitory cell types did not show this phenomenon. Asynchronous release from RSBC terminals proved to be frequency dependent: its proportion lowered markedly by decreasing the frequency from 30Hz, at 10Hz and below no asynchronous release was observed. These findings indicate that firing of RSBCs at high frequencies can be translated to a prolonged inhibition of CA3 pyramidal cells.

Beside the different Ca^{2+} channels involved in transmitter release the observed high failure rates at RSBC-pyramidal cell synapses is likely to be due to the tonic activation of CB1R as it was demonstrated in the study of Neu et al. (2007). Our finding that the CB1R antagonist AM251 reversed the amplitude of uIPSCs above the control levels after cholinergic receptor activation further supports this idea (Fig. 10).

We investigated the effect of CCh on the IPSCs at the different types of perisomatic region targeting inhibitory cell-pyramidal cell synapses and found that the peak amplitudes of uIPSCs markedly decreased in a different extent at the three types of synapses. The most significant decrement, often a full block could be observed at RSBC-pyramidal cell synapses. In the presence of CCh at FSBC- and AAC-pyramidal cell pairs the uIPSC responses never disappeared, instead endured remarkable decrease in the amplitude, whereas at RSBC-pyramidal cell synapses the failure rate drastically elevated leading to the total block of release in most cases. These different responses to cholinergic receptor activation indicate diverse locus of action. Indeed, we found that at FSBC- and AAC-pyramidal cell pairs the decreased uIPSC amplitudes could be reversed to control values by application of the M2-type specific cholinergic receptor antagonist AF/DX 116, whereas the muting of transmission at RSBC- pyramidal cell pairs could be reversed by the CB1R antagonist AM251. These results together with other observations (Hájos et al., 1998; Ohno-Shosaku et al., 2003; Fukudome et al., 2004; Neu et al., 2007) strongly suggest that at FSBC and AAC terminals CCh exerted its effect presynaptically via activating M2 receptors, whereas at RSBC terminals cholinergic receptor activation triggered release of endocannabinoids via activating M1 and M3 receptors postsynaptically, which then bound to the CB1Rs muted neurotransmission.

We found that the synaptic depression at PV-containing interneuron-pyramidal cell connections observed under control conditions was largely reduced or even eliminated in the presence of CCh. These results seemingly contradict to those findings obtained in the dentate gyrus, where CCh suppressed but did not abolish the depression (Hefft et al., 2002).

The major difference that could explain the disagreement between these two studies was the recording temperature. While we performed our experiments at room temperature, the study in the dentate gyrus was done at 34°C. As the vast majority of physiological processes, including the affinity of muscarinic acetylcholine receptors to their agonists (Aronstam and Narayanan, 1988) have been found to be altered by lowering the temperature, the higher affinity of CCh with their receptors, causing more stable receptor–G-protein complex at room temperature, might produce a larger reduction in the release probability in parallel with the elimination of the depression (Brenowitz et al., 1998). In agreement with this hypothesis, we observed a 70% reduction in the peak amplitude after CCh application at room temperature, whereas at 34°C this agonist suppressed the first uIPSC amplitude by only 30% (Hefft et al., 2002). This temperature-dependent difference in the efficacy of CCh in decreasing the initial release probability could account for its distinct effects on synaptic depression. Similarly, the slower decay of uIPSCs in our study compared to those values found at 33–34°C (Bartos et al., 2002) is probably due to the difference in the recording temperature (Otis and Mody, 1992). While both FSBCs and AACs form typical depressing synapses with pyramidal cells, at RSBC-pyramidal cell synapses such type of plasticity does not occur (Fig. 11). We also demonstrated that short term depression at FSBC- and AAC-pyramidal cell pairs shows strong frequency dependency (Fig. 11). The decrease in the extent of depression at both FSBC- and AAC-pyramidal cell synapses suggests that cholinergic receptor activation not just allow pyramidal cells to fire by disinhibition but the changes in short-term plasticity at these synapses may cause retuning of perisomatic inhibition by converting a synapse functioning as a “low pass filter” (Abbott and Regehr, 2004) to a synapse possessing a less effective but consistent ability to inhibit pyramidal cell firing.

V/2. Involvement of perisomatic inhibition in generating fast network oscillations (Study II)

In the second study we aimed to reveal the behavior of perisomatic region targeting neurons and their contribution to the fast network oscillation in the CA3 region. The results of Study I revealed that RSBCs are not likely to participate in generating CCh-induced oscillation because of the negligible amount of GABA released from their axon terminals. However, a study of Makara and her colleagues showed that an endocannabinoid mediated depolarization induced suppression of inhibition (DSI, see above) occurs with particularly high magnitude in the presence of CCh. Their results indicate that pyramidal cells receive large amplitude perisomatic IPSCs originating from endocannabinoid sensitive fibers in slices treated with CCh (Makara et al., 2007). One explanation to this discrepancy would be that these IPSCs originate from a very few number of active RSBCs, which neurons avoided our sampling. Indeed, examining the spontaneous IPSCs arriving to pyramidal cells in the presence of CCh revealed that these DSI sensitive IPSCs are quite similar to each other suggesting that they come from only one or at least very few RSBCs (unpublished observations of the authors). Although we did not find such RSBCs that produced significant IPSCs in the presence of CCh, since the authors used similar conditions during recordings to the experiments achieved by us, we considered RSBCs to be important to involve to the investigation of their behavior during CCh-induced fast network oscillation.

The three types of perisomatic region targeting inhibitory neurons fire within the same time window, but with different phase-coupling precision, during CCh-induced fast network oscillation

Analyzing of the firing phases of cells (Figs 17; 18) revealed a considerable variation in the preferred firing phase of individual neurons within each type and thus an overlapping activity of the populations. Most of the cells fire 0–60° after the negative peak

of the oscillations (i.e., in the ascending phase, measured in stratum pyramidale), following the discharge of pyramidal cells, consistent with the synaptic feedback model of pharmacologically induced oscillations in CA3 either in hippocampal slices (Hájos et al., 2004; Gloveli et al., 2005; Mann et al., 2005; Hájos and Paulsen, 2009) or in *in vivo* gamma oscillation (Csicsvári et al., 2003; Atallah and Scanziani, 2009). Based on population averages, FSBCs fired somewhat earlier, but the differences did not reach significance level. While the phase of firing did not differ among the three cell groups, their phase locking was distinct. FSBCs showed the strongest phase locking (0.8 ± 0.04), and RSBCs the weakest (0.49 ± 0.06). These differences found in the spiking accuracy of the two basket cell types match earlier findings. PV-containing basket cells (FSBCs) have a narrow input integration window, a precise input–output relationship, and synchronized transmitter release, in contrast to CCK-immunopositive basket cells (RSBCs), which have a wider input integration window and less accurate firing, and show asynchronous, delayed GABA release (Hefft and Jonas, 2005; Glickfeld and Scanziani, 2006; Daw et al., 2009).

These properties together with the weak phase locking and the lack of transmitter release in the presence of CCh further strengthen our hypothesis that RSBCs may not play a role in the generation of CCh-induced fast network oscillation. This suggestion is consistent with the idea that the imprecise input–output function of RSBCs is poorly suited to operate at high frequencies (Glickfeld and Scanziani, 2006). Nevertheless, it has been shown that activation of CB1Rs both *in vitro* and *in vivo* massively disrupts synchronous neural activity (Hájos et al., 2000; Robbe et al., 2006), which raise the involvement of RSBCs in oscillations since CB1Rs occur at a particularly high concentration in their nerve terminals. Yet, a recent study has demonstrated that during *in vitro* gamma oscillation and SPWs the target of cannabinoid action is the synaptic excitation received by FSBCs and pyramidal neurons, instead of the output of RSBCs (Holderith et al., 2011; Maier et al., 2011).

We found that the phase coupling of the three types of perisomatic inhibitory interneurons in CA3 was considerably higher (0.80–0.49) than measured in the CA1 area *in vivo* during gamma oscillations (0.23–0.07) (Tukker et al., 2007; Klausberger and Somogyi, 2008). Still, the relative modulation depth of firing of these cell types is similar *in vivo* and *in vitro*, since FSBCs had the highest modulation, while RSBCs the lowest. Several explanations can be proposed for the difference in the modulation depths, as follows: (1) *in vitro*, the strength of gamma modulation of interneuronal firing in the CA1 area is weaker than in the CA3 area (R. Zemankovics, JM. Veres, I. Oren, and N. Hájos, in

preparation), most probably because gamma activity is generated in CA3 and only spreads into CA1 (Csicsvári et al., 2003); (2) differences in the recording and signal-processing methods used in *in vivo* and in this study; (3) *in vivo*, there are several network activity patterns embedded in each other that might result in weaker modulation of neuronal activity in the gamma band, since subsequent gamma cycles are occurring at different phases of the carrier activities; and (4) though we induced CCh-evoked network oscillations with a lower concentration of agonist than in earlier studies, in our slices the synchrony of oscillations, and therefore the accuracy of cell firing, can still be higher than that achieved *in vivo*.

In the presence of CCh activation of MORs regulates synaptic inhibition originating only from FSBCs

Our data obtained from paired recordings showed that MOR activation by DAMGO reduced the GABA release from FSBCs but did not influence the release of AACs in the presence of CCh. These electrophysiological data agree with the results obtained with immunocytochemistry, showing the presence of MORs at the axon terminals of FSBCs but their apparent lack at the axon endings of AACs (Drake and Milner, 2002). The fact that DAMGO potently blocks network oscillation, by selectively reducing GABA release from the axon terminals of FSBCs in the presence of CCh, supports the key role of FSBCs in the generation of rhythmic inhibitory currents that temporally structure the oscillation in CCh-induced synchronous activities in CA3. The finding that DAMGO is able to suppress the CCh-induced oscillation even though the GABA release is normal from the axon terminals of RSBCs (i.e., in slices prepared from CB1R knockout mice (Fig. 28)) further strengthens our main conclusion that FSBCs alone can generate oscillatory rhythm in the cholinergic model of oscillations.

As DAMGO suppressed the oscillation, the pyramidal cell firing and consequently the EPSCs became desynchronized as a result of the elimination of phasic inhibition originating from FSBCs. Thus, DAMGO did not diminish activity in the CA3 network, only let pyramidal cells discharge without rhythmic entrainment (i.e., out of synchrony). This observation suggests that endogenously released opioids might set the level of synchrony and thereby the mode of information processing in the hippocampus. Since

dynorphin is present in the mossy terminals of dentate granule cells (Torres-Reveron et al., 2009), which are located adjacent to the MOR-expressing axon terminals of FSBCs, one might speculate that dynorphin release during highly synchronized activities in the dentate gyrus might contribute to the feedforward suppression of oscillations in CA3 (Bragin et al., 1995b; Bragin et al., 1995a).

Agreeing with *in vitro* results shown in the thesis, MOR activation was shown to markedly reduce the power of gamma oscillation also *in vivo*, as it was directly tested by bilateral infusion of DAMGO into the mouse hippocampus (Gulyás et al., 2010, not shown in the thesis). In addition to the finding a pharmacological tool to selectively suppress GABA release from FSBC terminals, our experiments also revealed a possible mechanism for how opiates interfere with oscillogenesis and thus with cognitive processes (Smith et al., 1962; Braida et al., 1994; Whittington et al., 1998) Taken together, in Study II we provided several lines of evidence converging to the conclusion that FSBCs, but not RSBCs or AACs, play central role in the generation of rhythmic field activities induced by carbachol in hippocampal slices, as follows: (1) during CCh-induced network oscillations FSBCs fired the most with the highest accuracy compared with the discharge of AACs and RSBCs; (2) the MOR agonist DAMGO, which co-applied with CCh effectively blocked oscillations, selectively reduced inhibitory currents of FSBCs, but not of AACs; and (3) in CB1R knockouts, in which release from RSBC terminals remain intact even in the presence of CCh, activation by MORs with DAMGO disrupts fast network oscillations.

V/3. Functional implications

We compared the output properties of the three key participants of perisomatic inhibition and aimed to clarify their role in CCh-induced fast network oscillation. Based on the pure morphology of these cells similar functions would be predicted, namely the effective control of firing of principal cells with their perisomatic contacts (Cobb et al., 1995; Miles et al., 1996). By targeting the action potential-generating sites each of these neurons is able to block firing of thousands of principal cells at the same time allowing of synchronized firing at a moment (Freund and Buzsáki, 1996). However, the different neurochemical repertoire and the different output properties shown in this study predict further special roles of perisomatic inhibition. And indeed, in the hippocampus, AACs and FSBCs fire at distinct phases of the theta cycles, suggesting different functions in oscillatory activity. Furthermore, AACs specifically fire transiently at the beginning of SWRs (Klausberger et al., 2003), foreshadowing the involvement of AACs in the generation of SWRs. Additionally, the massive IPSCs originating from AACs may be capable of keeping network excitability from going out of control, thus protecting the circuitry from epileptic discharges (Zhu et al., 2004).

As AACs specifically target AISs of principal cells, their role might be to regulate action potential generation directly. The fact that AACs are excitatory in cortex in certain states or inhibitory in others, as in the hippocampus (Glickfeld et al., 2009), does not influence the conclusion that they can play a role in rhythmic or intermittent synchronization of large pyramidal cell populations.

We showed that GABA release of RSBCs is robustly controlled by the CB1Rs located on their terminals. Endocannabinoids, which activate these receptors, have been shown to be released at various conditions, for instance, in response to activation of metabotropic glutamate receptors (mGluR1/5)(Chevaleyre and Castillo, 2003), activation of mAChRs (Ohno-Shosaku et al., 2003; Neu et al., 2007; present study) or during the depolarization of pyramidal cells (DSI, Pitler and Alger, 1992b; Di Marzo et al., 1998; Wilson and Nicoll, 2002). GABA release from perisomatic region targeting cells that express PV is not sensitive to endocannabinoids (Hájos et al., 2000). Why are the distinct elements of perisomatic inhibition differently equipped with the capability of suppressing GABA release by endocannabinoids? Considering the behavior of interneurons during network oscillations might help answering this question. *In vivo* studies of Klausberger and

his colleagues in the CA1 region have shown that firing of the PV- and the CCK-positive basket cells is preferentially distributed into time windows that are shifted in phase relative to each other during the same rhythmic network activity pattern (Klausberger et al., 2003; Klausberger et al., 2005). These experiments suggest that the two basket cell types fill different functional niches in the organization of cortical network activity (Losonczy et al., 2010). During theta activity, both basket cell types fire during the peak of the theta waves, but the activity of RSBCs is shifted toward the ascending phase, whereas FSBCs fire preferentially during the descending phase (Klausberger et al., 2003, 2005). The firing preference of the RSBCs at the ascending phase of theta has been demonstrated in the CA3 region as well (Lásztóczi et al., 2011). The early firing of RSBCs relative to FSBCs may be explained by the fact that they have long membrane time constants and do not seem to receive disynaptic inhibition following Schaffer collateral stimulation. These special features endow RSBCs with a unique ability to summate excitatory input from several different sources within a relatively broad time window (Glickfeld and Scanziani, 2006). RSBCs firing at the ascending phase of theta periodically inhibit pyramidal cells, resulting a delay in the timing of their discharges. When the animal enters to a place field, the corresponding pyramidal cell will start to fire. The burst firing of pyramidal cells provides ideal circumstances to endocannabinoid release (DSI, mGluR activation, see above), which molecules reduce the IPSCs originating from RSBCs, causing the gradual disinhibition of pyramidal cell, which then fire earlier and earlier in subsequent theta cycles, a phenomenon called phase precession (see more detailed in the introduction chapter). This idea (Freund et al., 2003) may serve as a plausible answer to the question raised above.

Taken together, distinct perisomatic region targeting inhibitory neurons endowed with various output properties may contribute to different cognitive functions, which contribution may be specifically fine-tuned by cholinergic receptor activation originating from the septal afferents of the hippocampus.

It has been shown the oscillatory activity that can be recorded in the field potential recorded in the CA3 region that the currents that generate the alternating current-sink transitions (dipoles) during fast network oscillations, which manifest as oscillatory pattern in the field potential, originate predominantly from the inhibitory drive of pyramidal neurons in the perisomatic region (Oren et al., 2010, Atallah&Scanziani, 2009). Among the three perisomatic region targeting neurons investigated in this study only the FSBCs proved to be indispensable for generating CCh-induced fast network oscillation. Based on these

results, we can conclude that the current generator of the fast network oscillations is the amplitude of IPSCs originating from FSBCs, whereas the rhythm generator is the decay time of these currents. But what makes the FSBCs fire? The answer to this question lies in the structure of the CA3 region. A unique property of the CA3 network is the extended recurrent collateral system (Li et al., 1994). In the generation of gamma rhythm this feature might be critical, because this may allow of the emergence of synchronous neural activities. During fast network oscillations the firing of inhibitory neurons is induced by the recurrent excitation of pyramidal cells, while the discharging of pyramidal cells is timed by perisomatic inhibition (Oren et al., 2006; 2010). The synchronization of the firing of pyramidal cells, at least during CCh-induced fast network oscillation, is therefore achieved clearly by the function of FSBCs.

Although the fast network oscillations investigated in this study do not matches all the properties of oscillations recorded in the gamma frequency range *in vivo*, our experiments showed that at more physiological temperatures the frequency of cholinergically induced oscillation felt to the gamma frequency band. The continuous transition of frequency during the switching from room temperature to the more physiological values indicates the same mechanisms behind generating oscillatory activity (Figs 15-16). Therefore, we can conclude that the CCh-induced network oscillation might be an appropriate model of theta-nested gamma oscillations, when the cholinergic tone is high (Marrosu et al., 1995; Buzsáki et al., 2003).

In conclusion, these data indicate that FSBCs represent the most important inhibitory component of the network that generates oscillation in the presence of CCh. Consequently, since CCh-induced fast network oscillations probably shares the underlying mechanisms with the theta nested gamma rhythm in the hippocampus, and the participation of FSBCs in the generation of gamma oscillation has also been emphasized by significant studies carried out *in vivo* (Cardin et al., 2009; Sohal et al., 2009), it is not a premature conclusion that this interneuron type similarly plays a crucial role in the *in vivo* recorded gamma oscillatory pattern, thus participating in the related hippocampal memory functions (Fuchs et al., 2007).

VI. SUMMARY

Hippocampal network activities are related to different memory processes. To understand hippocampal function the detailed knowledge of cellular and network mechanisms underlying these network activities is essential. The main goal of this thesis was to characterize and reveal the elements of perisomatic inhibition that is known to be required for the generation of fast network oscillation induced by the cholinergic receptor agonist carbachol. This type of oscillation can be recorded in acute hippocampal slices, and it might be a realistic model of the gamma oscillation, which can be recorded *in vivo* embedded in the theta rhythm, when the cholinergic tone is high.

In the first part of the thesis we investigated the synaptic properties of perisomatic inhibitory cells as well as their sensitivity to carbachol. These experiments revealed that perisomatic inhibition originating from the three investigated types of interneurons shows marked differences regarding the amplitude, decay kinetic, and latency of inhibitory postsynaptic currents as well as the probability of transmitter release and its asynchronous nature. Furthermore, we found that cholinergic receptor activation differently decrease the release of transmitter from the three types of terminals owing to the participation of different receptors at distinct locations. In terms of carbachol induced fast network oscillation, an important conclusion of these results is that since *regular spiking basket cells* do not release the inhibitory transmitter GABA in the presence of carbachol, they are not likely to contribute to the generation of this type of oscillation.

The results presented in the second part of the thesis revealed further details of the mechanism of oscillation. We observed that during carbachol induced fast network oscillation the firing of fast spiking basket cells was the most coupled to the given phase of the oscillation cycle, whereas the discharge of regular spiking basket cells showed poor phase locking, supporting the idea that these latter cells do not participate in oscillogenesis. We found that activation of μ-opioid receptors abolished the oscillation, which effect was proven to be due to the reduction of transmitter release from fast spiking basket cells but not from the terminals originating from *axo-axonic cells* in the presence of carbachol.

These findings collectively suggest the crucial role of the fast spiking basket cells in carbachol induced fast network oscillation, which neurons periodically discharge during gamma cycles, thus produce synchronized inhibitory currents through the pyramidal cell membrane. This synchronous inhibition gives rise to the oscillatory activity that can be detected in the field potential recorded in the CA3 region of the hippocampus.

VII. ÖSSZEFOGLALÁS

A hippokampális hálózati aktivitásmintázatok szoros korrelációt mutatnak a hippokampusz jellemző memóriafunkcióival. Ezen aktivitásmintázatok hátterében álló celluláris és hálózati mechanizmusok részletes ismerete szükséges a hippokampusz működésének megértéséhez. A disszertáció fő célja a kolinerg receptor agonista karbakollal kiváltott gyors hálózati oszcilláció geneziséért felelős periszomatikus gátlás feltérképezése volt. Ez a típusú oszcilláció túlélő agyszeletben elvezethető, és a theta ritmusba ágyazott gamma oszcillációnak lehet a modellje, melyre a magas kolinerg tónus jellemző.

Kísérleteink első felében a periszomatikus gátlósejtek szinaptikus tulajdonságait vizsgáltuk, valamint, hogy milyen hatással van rájuk a megnövekedett kolinerg tónus. Ezen kísérletek feltárták, hogy a három vizsgált sejttípustól eredő periszomatikus gátlás markáns különbségeket mutat a gátló szinaptikus áramok amplitúdóját, hanyatlási kinetikáit, látenciáját, valamint a transzmitter felszabadulás valószínűségét, illetve aszinkron jellegét tekintve. Megállapítottuk továbbá, hogy a karbakol különböző mértékben csökkenti a transzmitter felszabadulást a három periszomatikus gátlósejt idegvégződéseiből, melynek hátterében eltérő molekuláris mechanizmusok állnak. A karbakollal kiváltott gyors hálózati oszcilláció szempontjából fontos megállapítás, hogy az oszcillációhoz szükséges koncentrációjú karbakol mellett a *szabályosan tüzelő kosársejtek* nem szabadítanak fel GABA transzmittert, így valószínűleg nem vesznek részt az oszcilláció kialakításában.

A disszertáció második felében bemutatott eredmények az oszcilláció mechanizmusának további részleteit tárták fel. Megfigyeltük, hogy az oszcilláció alatt a *gyorsan tüzelő kosársejtek* voltak a legnagyobb mértékben fáziskapcsoltak, míg a regulárisan tüzelő kosársejtek kevéssé mutatták ezt a tulajdonságot, alátámasztva feltételezésünket, miszerint utóbbi sejtek nem vesznek részt az oszcilláció kialakításában. A μ-opiát receptorok aktiválása megszüntette az oszcillációt, amiről párelvezetésben bemutattuk, hogy karbakol jelenlétében csak a gyorsan tüzelő kosársejtek terminálisaiból csökkenti le a GABA felszabadulást, az *axo-axonikus sejtekéből* nem.

Ezen eredmények együttesen arra utalnak, hogy a karbakollal kiváltott gyors hálózati oszcilláció genezisében a legfontosabb szerepet a gyorsan tüzelő kosársejtek játsszák, mely sejtek időben összehangolt periodikus tüzelése a piramissejtek membránján keresztülfolyó szinkron szinaptikus áramok formájában létrehozza a mezőpotenciálban mérhető oszcillatórikus aktivitást a hippokampusz CA3 régiójában.

VIII. LIST OF REFERENCES

Abbott LF, Regehr WG (2004) Synaptic computation. Nature 431:796-803.

Acsády L, Arabadzisz D, Freund TF (1996a) Correlated morphological and neurochemical features identify different subsets of vasoactive intestinal polypeptide-immunoreactive interneurons in rat hippocampus. Neuroscience 73:299-315.

Acsády L, Görcs TJ, Freund TF (1996b) Different populations of vasoactive intestinal polypeptide- immunoreactive interneurons are specialized to control pyramidal cells or interneurons in the hippocampus. Neuroscience 73:317-334.

Aggleton JP, Saunders RC (1997) The relationships between temporal lobe and diencephalic structures implicated in anterograde amnesia. Memory 5:49-71.

Aghajanian GK, Marek GJ (1999) Serotonin, via 5-HT2A receptors, increases EPSCs in layer V pyramidal cells of prefrontal cortex by an asynchronous mode of glutamate release. Brain Res 825:161-171.

Albuquerque EX, Pereira EF, Alkondon M, Rogers SW (2009) Mammalian nicotinic acetylcholine receptors: from structure to function. Physiol Rev 89:73-120.

Amaral DG, Kurz J (1985) An analysis of the origins of the cholinergic and noncholinergic septal projections to the hippocampal formation of the rat. J Comp Neurol 240:37-59.

Andersen P, Morris R, Amaral D, Bliss T, O'Keefe J (2007) The Hippocampus Book: Oxford University Press.

Aronstam RS, Narayanan TK (1988) Temperature effect on the detection of muscarinic receptor-G protein interactions in ligand binding assays. Biochem Pharmacol 37:1045-1049.

Atallah BV, Scanziani M (2009) Instantaneous modulation of gamma oscillation frequency by balancing excitation with inhibition. Neuron 62:566-577.

Baisden RH, Woodruff ML, Hoover DB (1984) Cholinergic and non-cholinergic septo-hippocampal projections: a double- label horseradish peroxidase-acetylcholinesterase study in the rabbit. Brain Res 290:146-151.

Bartos M, Vida I, Frotscher M, Meyer A, Monyer H, Geiger JR, Jonas P (2002) Fast synaptic inhibition promotes synchronized gamma oscillations in hippocampal interneuron networks. Proc Natl Acad Sci U S A 99:13222-13227.

Behrends JC, Ten Bruggencate G (1993) Cholinergic modulation of synaptic inhibition in the guinea pig hippocampus in vitro:Excitation of GABAergic interneurons and inhibition of GABA-relaese. JNeurophysiol 69:626-629.

Ben-Chaim Y, Tour O, Dascal N, Parnas I, Parnas H (2003) The M2 muscarinic G-protein-coupled receptor is voltage-sensitive. J Biol Chem 278:22482-22491.

Berry SD, Thompson RF (1978) Prediction of learning rate from the hippocampal electroencephalogram. Science 200:1298-1300.

Binda F, Bossi E, Giovannardi S, Forlani G, Peres A (2002) Temperature effects on the presteady-state and transport-associated currents of GABA cotransporter rGAT1. FEBS Lett 512:303-307.

Biró AA, Holderith NB, Nusser Z (2006) Release probability-dependent scaling of the postsynaptic responses at single hippocampal GABAergic synapses. The Journal of neuroscience 26:12487-12496.

Bliss TV, Lomo T (1973) Long-lasting potentiation of synaptic transmission in the dentate area of the anaesthetized rabbit following stimulation of the perforant path. J Physiol 232:331-356.

Bliss TV, Gardner-Medwin AR (1973) Long-lasting potentiation of synaptic transmission in the dentate area of the unanaestetized rabbit following stimulation of the perforant path. J Physiol 232:357-374.

Boddeke HW, Best R, Boeijinga PH (1997) Synchronous 20 Hz rhythmic activity in hippocampal networks induced by activation of metabotropic glutamate receptors in vitro. Neuroscience 76:653-658.

Bodizs R, Kantor S, Szabo G, Szucs A, Eross L, Halasz P (2001) Rhythmic hippocampal slow oscillation characterizes REM sleep in humans. Hippocampus 11:747-753.

Boiko T, Vakulenko M, Ewers H, Yap CC, Norden C, Winckler B (2007) Ankyrin-dependent and -independent mechanisms orchestrate axonal compartmentalization of L1 family members neurofascin and L1/neuron-glia cell adhesion molecule. J Neurosci 27:590-603.

Borhegyi Z, Freund TF (1998) Dual projection from the medial septum to the supramammillary nucleus in the rat. Brain Res Bull 46:453-459.

Boucetta S, Jones BE (2009) Activity profiles of cholinergic and intermingled GABAergic and putative glutamatergic neurons in the pontomesencephalic tegmentum of urethane-anesthetized rats. J Neurosci 29:4664-4674.

Bragin A, Penttonen M, Buzsáki G (1997) Termination of epileptic afterdischarge in the hippocampus. J Neurosci 17:2567-2579.

Bragin A, Jando G, Nadasdy Z, van Landeghem M, Buzsaki G (1995a) Dentate EEG spikes and associated interneuronal population bursts in the hippocampal hilar region of the rat. J Neurophysiol 73:1691-1705.

Bragin A, Engel J, Jr., Wilson CL, Fried I, Buzsaki G (1999) High-frequency oscillations in human brain. Hippocampus 9:137-142.

Bragin A, Jando G, Nadasdy Z, Hetke J, Wise K, Buzsaki G (1995b) Gamma (40-100 Hz) oscillation in the hippocampus of the behaving rat. J Neurosci 15:47-60.

Braida D, Gori E, Sala M (1994) Relationship between morphine and etonitazene-induced working memory impairment and analgesia. Eur J Pharmacol 271:497-504.

Brankack J, Stewart M, Fox SE (1993) Current source density analysis of the hippocampal theta rhythm: associated sustained potentials and candidate synaptic generators. Brain Res 615:310-327.

Brenowitz S, David J, Trussell L (1998) Enhancement of synaptic efficacy by presynaptic GABA(B) receptors. Neuron 20:135-141.

Bucurenciu I, Kulik A, Schwaller B, Frotscher M, Jonas P (2008) Nanodomain coupling between Ca2+ channels and Ca2+ sensors promotes fast and efficient transmitter release at a cortical GABAergic synapse. Neuron 57:536-545.

Buffalo EA, Reber PJ, Squire LR (1998) The human perirhinal cortex and recognition memory. Hippocampus 8:330-339.

Buhl EH, Halasy K, Somogyi P (1994) Diverse sources of hippocampal unitary inhibitory postsynaptic potentials and the number of synaptic release sites [see comments] [published erratum appears in Nature 1997 May 1;387(6628):106]. Nature 368:823-828.

Buzsáki G (2002) Theta oscillations in the hippocampus. Neuron 33:325-340.

Buzsáki G, Leung LW, Vanderwolf CH (1983) Cellular bases of hippocampal EEG in the behaving rat. Brain Res 287:139-171.

Buzsáki G, Buhl DL, Harris KD, Csicsvári J, Czeh B, Morozov A (2003) Hippocampal network patterns of activity in the mouse. Neuroscience 116:201-211.

Buzsáki G (1986) Hippocampal sharp waves: their origin and significance. Brain Res 398:242-252.

Buzsáki G (1989) Two-stage model of memory trace formation: A role for 'noisy' brain states. Neuroscience 310:551-570.

Buzsáki G (2006) Rhythms of the brain: Oxford University Press.

Buzsáki G, Chrobak JJ (1995) Temporal structure in spatially organized neuronal ensembles: a role for interneuronal networks. Curr Opinion Neurobiol 5:504-510.

Buzsáki G, Czopf J, Kondakor I, Kellenyi L (1986) Laminar distribution of hippocampal rhythmic slow activity (RSA) in the behaving rat:current-source density analysis, effects of urethane and atropine. Brain Res 365:125-137.

Buzsáki G, Horvath Z, Urioste R, Hetke J, Wise K (1992) High-frequency network oscillation in the hippocampus. Science 256:1025-1027.

Caplan JB, Madsen JR, Schulze-Bonhage A, Aschenbrenner-Scheibe R, Newman EL, Kahana MJ (2003) Human theta oscillations related to sensorimotor integration and spatial learning. J Neurosci 23:4726-4736.

Cardin JA, Carlen M, Meletis K, Knoblich U, Zhang F, Deisseroth K, Tsai LH, Moore CI (2009) Driving fast-spiking cells induces gamma rhythm and controls sensory responses. Nature 459:663-667.

Cea-del Rio CA, Lawrence JJ, Erdelyi F, Szabo G, McBain CJ (2011) Cholinergic modulation amplifies the intrinsic oscillatory properties of CA1 hippocampal cholecystokinin-positive interneurons. J Physiol 589:609-627.

Cea-del Rio CA, Lawrence JJ, Tricoire L, Erdelyi F, Szabo G, McBain CJ (2010) M3 muscarinic acetylcholine receptor expression confers differential cholinergic modulation to neurochemically distinct hippocampal basket cell subtypes. J Neurosci 30:6011-6024.

Chedotal A, Umbriaco D, Descarries L, Hartman BK, Hamel E (1994) Light and electron microscopic immunocytochemical analysis of the neurovascular relationships of choline acetyltransferase and vasoactive intestinal polypeptide nerve terminals in the rat cerebral cortex. JCN.

Chevaleyre V, Castillo PE (2003) Heterosynaptic LTD of hippocampal GABAergic synapses: a novel role of endocannabinoids in regulating excitability. Neuron 38:461-472.

Chevaleyre V, Siegelbaum SA (2010) Strong CA2 pyramidal neuron synapses define a powerful disynaptic cortico-hippocampal loop. Neuron 66:560-572.

Chrobak JJ, Buzsáki G (1996) High-frequency oscillations in the output networks of the hippocampal-entorhinal axis of the freely behaving rat. J Neurosci 16:3056-3066.

Chrobak JJ, Buzsaki G (1998) Gamma oscillations in the entorhinal cortex of the freely behaving rat. J Neurosci 18:388-398.

Chu HY, Yang Z, Zhao B, Jin GZ, Hu GY, Zhen X (2010) Activation of phosphatidylinositol-linked D1-like receptors increases spontaneous glutamate release in rat somatosensory cortical neurons in vitro. Brain Res 1343:20-27.

Clemens Z, Molle M, Eross L, Barsi P, Halasz P, Born J (2007) Temporal coupling of parahippocampal ripples, sleep spindles and slow oscillations in humans. Brain 130:2868-2878.

Cobb SR, Buhl EH, Halasy K, Paulsen O, Somogyi P (1995) Synchronization of neuronal activity in hippocampus by individual GABAergic interneurons. Nature 378:75-78.

Cobb SR, Halasy K, Vida I, Nyiri G, Tamas G, Buhl EH, Somogyi P (1997) Synaptic effects of identified interneurons innervating both interneurons and pyramidal cells in the rat hippocampus. Neuroscience 79:629-648.

Cohen GA, Doze VA, Madison DV (1992) Opioid inhibition of GABA release from presynaptic terminals of rat hippocampal interneurons. Neuron 9:325-335.

Cole AE, Nicoll RA (1984) The pharmacology of cholinergic excitatory responses in hippocampal pyramidal cells. Brain Res 305:283-290.

Colgin LL, Denninger T, Fyhn M, Hafting T, Bonnevie T, Jensen O, Moser MB, Moser EI (2009) Frequency of gamma oscillations routes flow of information in the hippocampus. Nature 462:353-357.

Colonnier M (1968) Synaptic patterns on different cell types in the different laminae of the cat visual cortex. An electron microscope study. Brain Res 9:268-287.

Cooke SF, Bliss TV (2006) Plasticity in the human central nervous system. Brain 129:1659-1673.

Cope DW, Maccaferri G, Marton LF, Roberts JD, Cobden PM, Somogyi P (2002) Cholecystokinin-immunopositive basket and Schaffer collateral-associated interneurones target different domains of pyramidal cells in the CA1 area of the rat hippocampus. Neuroscience 109:63-80.

Corkin S (2002) What's new with the amnesic patient H.M.? Nat Rev Neurosci 3:153-160.

Corkin S, Amaral DG, Gonzalez RG, Johnson KA, Hyman BT (1997) H. M.'s medial temporal lobe lesion: findings from magnetic resonance imaging. J Neurosci 17:3964-3979.

Csicsvári J, Hirase H, Mamiya A, Buzsaki G (2000) Ensemble patterns of hippocampal CA3-CA1 neurons during sharp wave-associated population events. Neuron 28:585-594.

Csicsvári J, Jamieson B, Wise KD, Buzsaki G (2003) Mechanisms of gamma oscillations in the hippocampus of the behaving rat. Neuron 37:311-322.

Dasari S, Gulledge AT (2011) M1 and M4 receptors modulate hippocampal pyramidal neurons. J Neurophysiol 105:779-792.

Daw MI, Tricoire L, Erdelyi F, Szabo G, McBain CJ (2009) Asynchronous transmitter release from cholecystokinin-containing inhibitory interneurons is widespread and target-cell independent. J Neurosci 29:11112-11122.

Deco G, Thiele A (2009) Attention: oscillations and neuropharmacology. Eur J Neurosci 30:347-354.

Descarries L, Mechawar N (2000) Ultrastructural evidence for diffuse transmission by monoamine and acetylcholine neurons of the central nervous system. Prog Brain Res 125:27-47.

Di Marzo V, Melck D, Bisogno T, De Petrocellis L (1998) Endocannabinoids: endogenous cannabinoid receptor ligands with neuromodulatory action. Trends Neurosci 21:521-528.

Drake CT, Milner TA (2002) Mu opioid receptors are in discrete hippocampal interneuron subpopulations. Hippocampus 12:119-136.

Ekstrom AD, Caplan JB, Ho E, Shattuck K, Fried I, Kahana MJ (2005) Human hippocampal theta activity during virtual navigation. Hippocampus 15:881-889.

Ellender TJ, Nissen W, Colgin LL, Mann EO, Paulsen O (2010) Priming of hippocampal population bursts by individual perisomatic-targeting interneurons. J Neurosci 30:5979-5991.

Fell J, Klaver P, Lehnertz K, Grunwald T, Schaller C, Elger CE, Fernandez G (2001) Human memory formation is accompanied by rhinal-hippocampal coupling and decoupling. Nat Neurosci 4:1259-1264.

Felleman DJ, Van Essen DC (1991) Distributed hierarchical processing in the primate cerebral cortex. Cereb Cortex 1:1-47.

Ferezou I, Cauli B, Hill EL, Rossier J, Hamel E, Lambolez B (2002) 5-HT3 receptors mediate serotonergic fast synaptic excitation of neocortical vasoactive intestinal peptide/cholecystokinin interneurons. J Neurosci 22:7389-7397.

Ferraguti F, Klausberger T, Cobden P, Baude A, Roberts JD, Szucs P, Kinoshita A, Shigemoto R, Somogyi P, Dalezios Y (2005) Metabotropic glutamate receptor 8-expressing nerve terminals target subsets of GABAergic neurons in the hippocampus. J Neurosci 25:10520-10536.

Fisahn A, Pike FG, Buhl E, Paulsen O (1998) Cholinergic induction of network oscillations at 40 Hz in the hippocampus in vitro. Nature 394:186-189.

Frazier CJ, Strowbridge BW, Papke RL (2003) Nicotinic receptors on local circuit neurons in dentate gyrus: a potential role in regulation of granule cell excitability. J Neurophysiol 89:3018-3028.

Frazier CJ, Buhler AV, Weiner JL, Dunwiddie TV (1998a) Synaptic potentials mediated via alpha-bungarotoxin-sensitive nicotinic acetylcholine receptors in rat hippocampal interneurons. J Neurosci 18:8228-8235.

Frazier CJ, Rollins YD, Breese CR, Leonard S, Freedman R, Dunwiddie TV (1998b) Acetylcholine activates an alpha-bungarotoxin-sensitive nicotinic current in rat hippocampal interneurons, but not pyramidal cells. J Neurosci 18:1187-1195.

Freund TF (1992) GABAergic septal and median raphe afferents preferentially innervate inhibitory interneurons in the hippocampus and dentate gyrus. The dentate gyrus and its role in seizures:79-91.

Freund TF (2003) Rhythm and mood in perisomatic inhibition. TINS.

Freund TF, Antal M (1988) GABA-containing neurons in the septum control inhibitory interneurons in the hippocampus. Nature 336:170-173.

Freund TF, Buzsáki G (1996) Interneurons of the hippocampus. Hippocampus 6:347-470.

Freund TF, Katona I (2007) Perisomatic inhibition. Neuron 56:33-42.

Freund TF, Katona I, Piomelli D (2003) The role of endogenous cannabinoids in synaptic signaling. Physiological Reviews 83:1017-1066.

Freund TF, Gulyás AI, Acsády L, Görcs T, Tóth K (1990a) Serotonergic control of the hippocampus via local inhibitory interneurons. Proc Natl Acad Sci U S A 87:8501-8505.

Freund TF, Gulyás AI, Acsády L, Görcs T, Bickford RG, Tóth K (1990b) Selective serotonergic innervation of specialized type of GABAergic interneuron in the hippocampus. SocNeurosciAbs(Suppl) 16.

Fries P, Nikolic D, Singer W (2007) The gamma cycle. Trends Neurosci 30:309-316.

Fries P, Reynolds JH, Rorie AE, Desimone R (2001) Modulation of oscillatory neuronal synchronization by selective visual attention. Science 291:1560-1563.

Frotscher M, Léránth C (1985) Cholinergic innervation of the rat hippocampus as revealed by choline acetyltransferase immunocytochemistry: a combined light and electron microscopic study. JCompNeurol 239:237-246.

Frotscher M, Léránth C (1986) The cholinergic innervation of the rat fascia dentata: identification of target structures on granule cells by combining choline acetyltransferase immunocytochemistry and Golgi impregnation. JCompNeurol 243.

Frotscher M, Schlander M, Leranth C (1986) Cholinergic neurons in the hippocampus. A combined light- and electron- microscopic immunocytochemical study in the rat. Cell Tissue Res 246:293-301.

Fuchs EC, Zivkovic AR, Cunningham MO, Middleton S, Lebeau FE, Bannerman DM, Rozov A, Whittington MA, Traub RD, Rawlins JN, Monyer H (2007) Recruitment of parvalbumin-positive interneurons determines hippocampal function and associated behavior. Neuron 53:591-604.

Fuentealba P, Begum R, Capogna M, Jinno S, Marton LF, Csicsvari J, Thomson A, Somogyi P, Klausberger T (2008) Ivy cells: a population of nitric-oxide-producing, slow-spiking GABAergic neurons and their involvement in hippocampal network activity. Neuron 57:917-929.

Fukudome Y, Ohno-Shosaku T, Matsui M, Omori Y, Fukaya M, Tsubokawa H, Taketo MM, Watanabe M, Manabe T, Kano M (2004) Two distinct classes of muscarinic action on hippocampal inhibitory synapses: M2-mediated direct suppression and M1/M3-mediated indirect suppression through endocannabinoid signalling. The European journal of neuroscience 19:2682-2692.

Glickfeld LL, Scanziani M (2006) Distinct timing in the activity of cannabinoid-sensitive and cannabinoid-insensitive basket cells. Nat Neurosci 9:807-815.

Glickfeld LL, Atallah BV, Scanziani M (2008) Complementary modulation of somatic inhibition by opioids and cannabinoids. The Journal of neuroscience 28:1824-1832.

Glickfeld LL, Roberts JD, Somogyi P, Scanziani M (2009) Interneurons hyperpolarize pyramidal cells along their entire somatodendritic axis. Nat Neurosci 12:21-23.

Gloveli T, Dugladze T, Saha S, Monyer H, Heinemann U, Traub RD, Whittington MA, Buhl EH (2005) Differential involvement of oriens/pyramidale interneurones in hippocampal network oscillations in vitro. The Journal of physiology 562:131-147.

Good M, Honey RC (1991) Conditioning and contextual retrieval in hippocampal rats. Behav Neurosci 105:499-509.

Goshen I, Brodsky M, Prakash R, Wallace J, Gradinaru V, Ramakrishnan C, Deisseroth K (2011) Dynamics of retrieval strategies for remote memories. Cell 147:678-689.

Grastyán E, Lissak K, Madarasz I, Donhoffer H (1959) Hippocampal electrical activity during the development of conditioned reflexes. Electroencephalogr Clin Neurophysiol 11:409-430.

Gray R, Rajan AS, Radcliffe KA, Yakehiro M, Dani JA (1996) Hippocampal synaptic transmission enhanced by low concentrations of nicotine. Nature 383:713-716.

Guerineau NC, Gahwiler BH, Gerber U (1994) Reduction of resting K+ current by metabotropic glutamate and muscarinic receptors in rat CA3 cells: mediation by G-proteins. J Physiol 474:27-33.

Gulledge AT, Kawaguchi Y (2007) Phasic cholinergic signaling in the hippocampus: functional homology with the neocortex? Hippocampus 17:327-332.

Gulledge AT, Bucci DJ, Zhang SS, Matsui M, Yeh HH (2009) M1 receptors mediate cholinergic modulation of excitability in neocortical pyramidal neurons. J Neurosci 29:9888-9902.

Gulyás AI, Hájos N, Katona I, Freund TF (2003) Interneurons are the local targets of hippocampal inhibitory cells which project to the medial septum. Eur J Neurosci 17:1861-1872.

Gulyás AI, Hajos N, Freund TF (1996) Interneurons containing calretinin are specialized to control other interneurons in the rat hippocampus. J Neurosci 16:3397-3411.

Gulyás AI, Miettinen R, Jacobowitz DM, Freund TF (1991) Calretinin-immunoreacti cells in the rat hippocampus. I. A new type of neuron - specifically associated with the mossy fibre system - revealed. EurJNeurosciSuppl 4:158.

Gulyás AI, Miles R, Hájos N, Freund TF (1993) Precision and variability in postsynaptic target selection of inhibitory cells in the hippocampal CA3 region. Eur J Neurosci 5:1729-1751.

Hájos N, Mody I (1997) Synaptic communication among hippocampal interneurons: properties of spontaneous IPSCs in morphologically identified cells. J Neurosci 17:8427-8442.

Hájos N, Paulsen O (2009) Network mechanisms of gamma oscillations in the CA3 region of the hippocampus. Neural Netw 22:1113-1119.

Hájos N, Papp EC, Acsády L, Levey AI, Freund TF (1998) Distinct interneuron types express m2 muscarinic receptor immunoreactivity on their dendrites or axon terminals in the hippocampus. Neuroscience 82:355-376.

Hájos N, Pálhalmi J, Mann EO, Németh B, Paulsen O, Freund TF (2004) Spike timing of distinct types of GABAergic interneuron during hippocampal gamma oscillations in vitro. The Journal of neuroscience 24:9127-9137.

Hájos N, Katona I, Naiem SS, MacKie K, Ledent C, Mody I, Freund TF (2000) Cannabinoids inhibit hippocampal GABAergic transmission and network oscillations. Eur J Neurosci 12:3239-3249.

Hajos N, Ellender TJ, Zemankovics R, Mann EO, Exley R, Cragg SJ, Freund TF, Paulsen O (2009) Maintaining network activity in submerged hippocampal slices: importance of oxygen supply. Eur J Neurosci 29:319-327.

Hájos N, Papp EC, Acsády L, Levey AI, Freund TF (1998) Distinct interneuron types express m2 muscarinic receptor immunoreactivity on their dendrites or axon terminals in the hippocampus. Neuroscience 82:355-376.

Hájos N, Katona I, Naiem SS, MacKie K, Ledent C, Mody I, Freund TF (2000) Cannabinoids inhibit hippocampal GABAergic transmission and network oscillations. Eur J Neurosci 12:3239-3249.

Hamlyn LH (1962) The fine structure of the mossy fibre endings in the hippocampus of the rabbit. J Anat 96:112-120.

Hangya B, Borhegyi Z, Szilagyi N, Freund TF, Varga V (2009) GABAergic neurons of the medial septum lead the hippocampal network during theta activity. J Neurosci 29:8094-8102.

Hasselmo ME (2006) The role of acetylcholine in learning and memory. Curr Opin Neurobiol 16:710-715.

Hefft S, Jonas P (2005) Asynchronous GABA release generates long-lasting inhibition at a hippocampal interneuron-principal neuron synapse. Nat Neurosci 8:1319-1328.

Hefft S, Kraushaar U, Geiger JR, Jonas P (2002) Presynaptic short-term depression is maintained during regulation of transmitter release at a GABAergic synapse in rat hippocampus. J Physiol 539:201-208.

Heister DS, Hayar A, Garcia-Rill E (2009) Cholinergic modulation of GABAergic and glutamatergic transmission in the dorsal subcoeruleus: mechanisms for REM sleep control. Sleep 32:1135-1147.

Holderith N, Németh B, Papp OI, Veres JM, Nagy GA, Hájos N (2011) Cannabinoids attenuate hippocampal gamma oscillations by suppressing excitatory synaptic input onto CA3 pyramidal neurons and fast spiking basket cells. J Physiol 589:4921-4934.

Hopfield JJ (1995) Pattern recognition computation using action potential timing for stimulus representation. Nature 376:33-36.

Jenkins SM, Bennett V (2001) Ankyrin-G coordinates assembly of the spectrin-based membrane skeleton, voltage-gated sodium channels, and L1 CAMs at Purkinje neuron initial segments. J Cell Biol 155:739-746.

Jensen O, Lisman JE (1996) Hippocampal CA3 region predicts memory sequences: accounting for the phase precession of place cells. Learn Mem 3:279-287.

Jensen O, Lisman JE (1998) An oscillatory short-term memory buffer model can account for data on the Sternberg task. J Neurosci 18:10688-10699.

Jinno S, Kosaka T (2002) Immunocytochemical characterization of hippocamposeptal projecting GABAergic nonprincipal neurons in the mouse brain: a retrograde labeling study. Brain Res 945:219-231.

Jinno S, Klausberger T, Marton LF, Dalezios Y, Roberts JD, Fuentealba P, Bushong EA, Henze D, Buzsaki G, Somogyi P (2007) Neuronal diversity in GABAergic long-range projections from the hippocampus. J Neurosci 27:8790-8804.

Jones BE, Moore RY (1977) Ascending projections of the locus coeruleus in the rat.II. autoradiographic study. Brain Res 127:23-53.

Jones MW, McHugh TJ Updating hippocampal representations: CA2 joins the circuit. Trends Neurosci 34:526-535.

Jones S, Yakel JL (1997) Functional nicotinic ACh receptors on interneurones in the rat hippocampus. J Physiol 504 (Pt 3):603-610.

Káli S, Acsády L (2003) A hippokampusz-függő memória neurobiológiai alapjai. In: Kognitív idegtudomány (Pléh C, Kovács G, Gulyás B, eds), pp 359-388. Budapest: Osiris Kiadó.

Kamondi A, Acsády L, Buzsáki G (1998) Dendritic spikes are enhanced by cooperative network activity in the intact hippocampus. J Neurosci 18:3919-3928.

Kasugai Y, Swinny JD, Roberts JD, Dalezios Y, Fukazawa Y, Sieghart W, Shigemoto R, Somogyi P (2010) Quantitative localisation of synaptic and extrasynaptic GABAA receptor subunits on hippocampal pyramidal cells by freeze-fracture replica immunolabelling. Eur J Neurosci 32:1868-1888.

Katsumaru H, Kosaka T, Heizmann CW, Hama K (1988) Immunocytochemical study of GABAergic neurons containing the calcium-binding protein parvalbumin in the rat hippocampus. ExpBrain Res 72:347-362.

Kim JJ, Fanselow MS (1992) Modality-specific retrograde amnesia of fear. Science 256:675-677.

Kirk IJ (1998) Frequency modulation of hippocampal theta by the supramammillary nucleus, and other hypothalamo-hippocampal interactions: mechanisms and functional implications. Neurosci Biobehav Rev 22:291-302.

Klausberger T, Somogyi P (2008) Neuronal diversity and temporal dynamics: the unity of hippocampal circuit operations. Science (New York, NY 321:53-57.

Klausberger T, Marton LF, Baude A, Roberts JD, Magill PJ, Somogyi P (2004) Spike timing of dendrite-targeting bistratified cells during hippocampal network oscillations in vivo. Nat Neurosci 7:41-47.

Klausberger T, Magill PJ, Marton LF, Roberts JD, Cobden PM, Buzsaki G, Somogyi P (2003) Brain-state- and cell-type-specific firing of hippocampal interneurons in vivo. Nature 421:844-848.

Klausberger T, Marton LF, O'Neill J, Huck JH, Dalezios Y, Fuentealba P, Suen WY, Papp E, Kaneko T, Watanabe M, Csicsvari J, Somogyi P (2005) Complementary roles of cholecystokinin- and parvalbumin-expressing GABAergic neurons in hippocampal network oscillations. J Neurosci 25:9782-9793.

Kocsis B, Bragin A, Buzsaki G (1999) Interdependence of multiple theta generators in the hippocampus: a partial coherence analysis. J Neurosci 19:6200-6212.

Kramis R, Vanderwolf CH, Bland BH (1975) Two types of hippocampal rhythmical slow activity in both the rabbit and the rat: relations to behavior and effects of atropine, diethyl ether, urethane, and pentobarbital. Exp Neurol 49:58-85.

Krnjevic K, Pumain R, Renaud L (1971) The mechanism of excitation by acetylcholine in the cerebral cortex. J Physiol 215:247-268.

Lásztóczi B, Tukker JJ, Somogyi P, Klausberger T (2011) Terminal field and firing selectivity of cholecystokinin-expressing interneurons in the hippocampal CA3 area. J Neurosci 31:18073-18093.

Lawrence JJ, Statland JM, Grinspan ZM, McBain CJ (2006) Cell type-specific dependence of muscarinic signalling in mouse hippocampal stratum oriens interneurones. J Physiol 570:595-610.

Lawrence JJ (2007) Homosynaptic and heterosynaptic modes of endocannabinoid action at hippocampal CCK+ basket cell synapses. J Physiol 578:3-4.

Lawrence JJ (2008) Cholinergic control of GABA release: emerging parallels between neocortex and hippocampus. Trends Neurosci 31:317-327.

Lawson VH, Bland BH (1993) The role of the septohippocampal pathway in the regulation of hippocampal field activity and behavior: analysis by the intraseptal microinfusion of carbachol, atropine, and procaine. Exp Neurol 120:132-144.

Levey AI, Edmunds SM, Koliatsos V, Wiley RG, Heilman CJ (1995) Expression of m1-m4 muscarinic acetylcholine receptor proteins in rat hippocampus and regulation by cholinergic innervation. J Neurosci 15:4077-4092.

Li XG, Somogyi P, Ylinen A, Buzsáki G (1994) The hippocampal ca3 network - an in vivo intracellular labeling study. Journal of Comparative Neurology 339:181-208.

Lisman J, Buzsaki G (2008) A neural coding scheme formed by the combined function of gamma and theta oscillations. Schizophr Bull 34:974-980.

Lisman JE, Idiart MA (1995) Storage of 7 +/- 2 short-term memories in oscillatory subcycles. Science 267:1512-1515.

Liu GX, Cai GQ, Cai YQ, Sheng ZJ, Jiang J, Mei Z, Wang ZG, Guo L, Fei J (2007) Reduced anxiety and depression-like behaviors in mice lacking GABA transporter subtype 1. Neuropsychopharmacology 32:1531-1539.

Lopez-Bendito G, Sturgess K, Erdelyi F, Szabo G, Molnar Z, Paulsen O (2004) Preferential origin and layer destination of GAD65-GFP cortical interneurons. Cereb Cortex 14:1122-1133.

Lopez JC, Gomez Y, Vargas JP, Salas C (2003) Spatial reversal learning deficit after medial cortex lesion in turtles. Neurosci Lett 341:197-200.

Losonczy A, Biro AA, Nusser Z (2004) Persistently active cannabinoid receptors mute a subpopulation of hippocampal interneurons. Proc Natl Acad Sci U S A 101:1362-1367.

Losonczy A, Zemelman BV, Vaziri A, Magee JC (2010) Network mechanisms of theta related neuronal activity in hippocampal CA1 pyramidal neurons. Nat Neurosci 13:967-972.

Losonczy A, Zhang L, Shigemoto R, Somogyi P, Nusser Z (2002) Cell type dependence and variability in the short-term plasticity of EPSCs in identified mouse hippocampal interneurones. J Physiol 542:193-210.

Lovett-Barron M, Turi GF, Kaifosh P, Lee PH, Bolze F, Sun XH, Nicoud JF, Zemelman BV, Sternson SM, Losonczy A (2012) Regulation of neuronal input transformations by tunable dendritic inhibition. Nat Neurosci 15:423-430, S421-423.

M'Harzi M, Palacios A, Monmaur P, Willig F, Houcine O, Delacour J (1987) Effects of selective lesions of fimbria-fornix on learning set in the rat. Physiol Behav 40:181-188.

Maccaferri G, McBain CJ (1996) The hyperpolarization-activated current (Ih) and its contribution to pacemaker activity in rat CA1 hippocampal stratum oriens-alveus interneurones. J Physiol 497 (Pt 1):119-130.

Maccaferri G, Roberts JD, Szucs P, Cottingham CA, Somogyi P (2000) Cell surface domain specific postsynaptic currents evoked by identified GABAergic neurones in rat hippocampus in vitro. J Physiol 524 Pt 1:91-116.

Magloczky Z, Acsády L, Freund TF (1994) Principal cells are the postsynaptic targets of supramammillary afferents in the hippocampus of the rat. Hippocampus 4:322-334.

Maguire EA, Frackowiak RS, Frith CD (1997) Recalling routes around london: activation of the right hippocampus in taxi drivers. J Neurosci 17:7103-7110.

Maguire EA, Woollett K, Spiers HJ (2006) London taxi drivers and bus drivers: a structural MRI and neuropsychological analysis. Hippocampus 16:1091-1101.

Maguire EA, Gadian DG, Johnsrude IS, Good CD, Ashburner J, Frackowiak RS, Frith CD (2000) Navigation-related structural change in the hippocampi of taxi drivers. Proc Natl Acad Sci U S A 97:4398-4403.

Maier N, Nimmrich V, Draguhn A (2003) Cellular and network mechanisms underlying spontaneous sharp wave-ripple complexes in mouse hippocampal slices. The Journal of physiology 550:873-887.

Maier N, Morris G, Schuchmann S, Korotkova T, Ponomarenko A, Bohm C, Wozny C, Schmitz D (2011) Cannabinoids disrupt hippocampal sharp wave-ripples via inhibition of glutamate release. Hippocampus.

Makara JK, Katona I, Nyiri G, Nemeth B, Ledent C, Watanabe M, de Vente J, Freund TF, Hajos N (2007) Involvement of nitric oxide in depolarization-induced suppression of inhibition in hippocampal pyramidal cells during activation of cholinergic receptors. The Journal of neuroscience 27:10211-10222.

Mann EO, Suckling JM, Hajos N, Greenfield SA, Paulsen O (2005) Perisomatic feedback inhibition underlies cholinergically induced fast network oscillations in the rat hippocampus in vitro. Neuron 45:105-117.

Marrosu F, Portas C, Mascia MS, Casu MA, Fa M, Giagheddu M, Imperato A, Gessa GL (1995) Microdialysis measurement of cortical and hippocampal acetylcholine release during sleep-wake cycle in freely moving cats. Brain Res 671:329-332.

Masukawa LM, Prince DA (1982) Enkephalin inhibition of inhibitory input to CA1 and CA3 pyramidal neurons in the hippocampus. Brain Res 249:271-280.

Matthes HW, Maldonado R, Simonin F, Valverde O, Slowe S, Kitchen I, Befort K, Dierich A, Le Meur M, Dolle P, Tzavara E, Hanoune J, Roques BP, Kieffer BL (1996) Loss of morphine-induced analgesia, reward effect and withdrawal symptoms in mice lacking the mu-opioid-receptor gene. Nature 383:819-823.

Maurer AP, McNaughton BL (2007) Network and intrinsic cellular mechanisms underlying theta phase precession of hippocampal neurons. Trends Neurosci 30:325-333.

McBain CJ, DiChiara TJ, Kauer JA (1994) Activation of metabotropic glutamate receptors differentially affects two classes of hippocampal interneurons and potentiates excitatory synaptic transmission. J Neurosci 14:4433-4445.

McQuiston AR, Madison DV (1999a) Muscarinic receptor activity has multiple effects on the resting membrane potentials of CA1 hippocampal interneurons. J Neurosci 19:5693-5702.

McQuiston AR, Madison DV (1999b) Nicotinic receptor activation excites distinct subtypes of interneurons in the rat hippocampus. J Neurosci 19:2887-2896.

Mechawar N, Cozzari C, Descarries L (2000) Cholinergic innervation in adult rat cerebral cortex: a quantitative immunocytochemical description. J Comp Neurol 428:305-318.

Megiás M, Emri Z, Freund TF, Gulyas AI (2001) Total number and distribution of inhibitory and excitatory synapses on hippocampal CA1 pyramidal cells. Neuroscience 102:527-540.

Melzer S, Michael M, Caputi A, Eliava M, Fuchs EC, Whittington MA, Monyer H (2012) Long-range-projecting GABAergic neurons modulate inhibition in hippocampus and entorhinal cortex. Science 335:1506-1510.

Mercer A, Eastlake K, Trigg HL, Thomson AM (2010) Local circuitry involving parvalbumin-positive basket cells in the CA2 region of the hippocampus. Hippocampus 22:43-56.

Mercer A, Botcher NA, Eastlake K, Thomson AM (2012) SP-SR interneurones: A novel class of neurones of the CA2 region of the hippocampus. Hippocampus.

Meyer AH, Katona I, Blatow M, Rozov A, Monyer H (2002) In vivo labeling of parvalbumin-positive interneurons and analysis of electrical coupling in identified neurons. J Neurosci 22:7055-7064.

Miles R, Wong RKS (1987) Inhibitory control of local excitatory circuits in the guinea-pig hippocampus. JPhysiol 388:611-629.

Miles R, Toth K, Gulyás AI, Hajos N, Freund TF (1996) Differences between somatic and dendritic inhibition in the hippocampus. Neuron 16:815-823.

Mitchell SJ, Ranck JB, Jr. (1980) Generation of theta rhythm in medial entorhinal cortex of freely moving rats. Brain Res 189:49-66.

Mizuseki K, Sirota A, Pastalkova E, Buzsaki G (2009) Theta oscillations provide temporal windows for local circuit computation in the entorhinal-hippocampal loop. Neuron 64:267-280.

Montgomery SM, Buzsaki G (2007) Gamma oscillations dynamically couple hippocampal CA3 and CA1 regions during memory task performance. Proc Natl Acad Sci U S A 104:14495-14500.

Moore RY, Bloom FE (1979) Central catecholamine neuron systems: anatomy and physiology of the norepinephrine and epinephrine systems. Annu Rev Neurosci 2:113-168.

Morales M, Bloom FE (1997) The 5-HT3 receptor is present in different subpopulations of GABAergic neurons in the rat telencephalon. J Neurosci 17:3157-3167.

Morris RG, Garrud P, Rawlins JN, O'Keefe J (1982) Place navigation impaired in rats with hippocampal lesions. Nature 297:681-683.

Mosko S, Lynch G, Cotman CW (1973) The distribution of septal projections to the hippocampus of the rat. J Comp Neurol 152:163-174.

Nadasdy Z, Hirase H, Czurko A, Csicsvari J, Buzsaki G (1999) Replay and time compression of recurring spike sequences in the hippocampus. J Neurosci 19:9497-9507.

Nakajima Y, Nakajima S, Leonard RJ, Yamaguchi K (1986) Acetylcholine raises excitability by inhibiting the fast transient potassium current in cultured hippocampal neurons. Proc Natl Acad Sci U S A 83:3022-3026.

Nelson S, Toth L, Sheth B, Sur M (1994) Orientation selectivity of cortical neurons during intracellular blockade of inhibition. Science 265:774-777.

Neu A, Foldy C, Soltesz I (2007) Postsynaptic origin of CB1-dependent tonic inhibition of GABA release at cholecystokinin-positive basket cell to pyramidal cell synapses in the CA1 region of the rat hippocampus. J Physiol 578:233-247.

Northcutt RG (1981) Evolution of the telencephalon in nonmammals. Annu Rev Neurosci 4:301-350.

Nusser Z, Hajos N, Somogyi P, Mody I (1998) Increased number of synaptic GABA(A) receptors underlies potentiation at hippocampal inhibitory synapses. Nature 395:172-177.

Nusser Z, Sieghart W, Benke D, Fritschy J-M, Somogyi P (1996) Differential synaptic localization of two major gamma-aminobutyric acid type A receptor alfa subunits on hippocampal pyramidal cells. PNAS 93:11939-11944.

Nyíri G, Freund TF, Somogyi P (2001) Input-dependent synaptic targeting of alpha(2)-subunit-containing GABA(A) receptors in synapses of hippocampal pyramidal cells of the rat. Eur J Neurosci 13:428-442.

O'Keefe J, Dostrovsky J (1971) The hippocampus as a spatial map. Preliminary evidence from unit activity in the freely-moving rat. Brain Res 34:171-175.

O'Keefe J, Nadel L, eds (1978) The Hippocampus as a Cognitive Map: Oxford University Press.

O'Keefe J, Recce ML (1993) Phase relationship between hippocampal place units and the EEG theta rhythm. Hippocampus 3:317-330.

Olah S, Fule M, Komlosi G, Varga C, Baldi R, Barzo P, Tamas G (2009) Regulation of cortical microcircuits by unitary GABA-mediated volume transmission. Nature 461:1278-1281.

Oren I, Hajos N, Paulsen O (2010) Identification of the current generator underlying cholinergically induced gamma frequency field potential oscillations in the hippocampal CA3 region. J Physiol 588:785-797.

Oren I, Mann EO, Paulsen O, Hajos N (2006) Synaptic currents in anatomically identified CA3 neurons during hippocampal gamma oscillations in vitro. The Journal of neuroscience 26:9923-9934.

Otis TS, Mody I (1992) Modulation of decay kinetics and frequency of GABAA receptor-mediated spontaneous inhibitory postsynaptic currents in hippocampal neurons. Neuroscience 49:13-32.

Overstreet LS, Westbrook GL (2003) Synapse density regulates independence at unitary inhibitory synapses. J Neurosci 23:2618-2626.

Pálhalmi J, Paulsen O, Freund TF, Hájos N (2004) Distinct properties of carbachol- and DHPG-induced network oscillations in hippocampal slices. Neuropharmacology 47:381-389.

Pálhalmi J, Paulsen O, Freund TF, Hájos N (2004) Distinct properties of carbachol- and DHPG-induced network oscillations in hippocampal slices. Neuropharmacology 47:381-389.

Panula P, Pirvola U, Auvinen S, Airaksinen MS (1989) Histamine-immunoreactive nerve fibers in the rat brain. Neuroscience 28:585-610.

Papp EC, Hajos N, Acsady L, Freund TF (1999) Medial septal and median raphe innervation of vasoactive intestinal polypeptide-containing interneurons in the hippocampus. Neuroscience 90:369-382.

Parra P, Gulyás AI, Miles R (1998) How many subtypes of inhibitory cells in the hippocampus? Neuron 20:983-993.

Paulsen O, Moser EI (1998) A model of hippocampal memory encoding and retrieval: GABAergic control of synaptic plasticity. Trends Neurosci 21:273-278.

Pawelzik H, Hughes DI, Thomson AM (2002) Physiological and morphological diversity of immunocytochemically defined parvalbumin- and cholecystokinin-positive interneurones in CA1 of the adult rat hippocampus. J Comp Neurol 443:346-367.

Petsche H, Stumpf C, Gogolak G (1962) [The significance of the rabbit's septum as a relay station between the midbrain and the hippocampus. I. The control of hippocampus arousal activity by the septum cells]. Electroencephalogr Clin Neurophysiol 14:202-211.

Pitler TA, Alger BE (1992a) Cholinergic excitation of GABAergic interneurons in the rat hippocampal slice. J Physiol 450:127-142.

Pitler TA, Alger BE (1992b) Postsynaptic spike firing reduces synaptic GABA(a) responses in hippocampal pyramidal cells. Journal of Neuroscience 12:4122-4132.

Pouille F, Scanziani M (2004) Routing of spike series by dynamic circuits in the hippocampus. Nature 429:717-723.

Price CJ, Scott R, Rusakov DA, Capogna M (2008) GABA(B) receptor modulation of feedforward inhibition through hippocampal neurogliaform cells. J Neurosci 28:6974-6982.

Price CJ, Cauli B, Kovacs ER, Kulik A, Lambolez B, Shigemoto R, Capogna M (2005) Neurogliaform neurons form a novel inhibitory network in the hippocampal CA1 area. J Neurosci 25:6775-6786.

Raisman G (1966) The connexions of the septum. Brain 89:317-348.

Rawlins JN, Feldon J, Gray JA (1979) Septo-hippocampal connections and the hippocampal theta rhythm. Exp Brain Res 37:49-63.

Rempel-Clower NL, Zola SM, Squire LR, Amaral DG (1996) Three cases of enduring memory impairment after bilateral damage limited to the hippocampal formation. J Neurosci 16:5233-5255.

Riedel G, Micheau J, Lam AG, Roloff EL, Martin SJ, Bridge H, de Hoz L, Poeschel B, McCulloch J, Morris RG (1999) Reversible neural inactivation reveals hippocampal participation in several memory processes. Nat Neurosci 2:898-905.

Robbe D, Montgomery SM, Thome A, Rueda-Orozco PE, McNaughton BL, Buzsaki G (2006) Cannabinoids reveal importance of spike timing coordination in hippocampal function. Nat Neurosci 9:1526-1533.

Rodriguez F, Lopez JC, Vargas JP, Broglio C, Gomez Y, Salas C (2002) Spatial memory and hippocampal pallium through vertebrate evolution: insights from reptiles and teleost fish. Brain Res Bull 57:499-503.

Rosenbaum RS, Priselac S, Kohler S, Black SE, Gao F, Nadel L, Moscovitch M (2000) Remote spatial memory in an amnesic person with extensive bilateral hippocampal lesions. Nat Neurosci 3:1044-1048.

Sarter M, Parikh V, Howe WM (2009) Phasic acetylcholine release and the volume transmission hypothesis: time to move on. Nat Rev Neurosci 10:383-390.

Scanziani M, Gahwiler BH, Thompson SM (1993) Presynaptic inhibition of excitatory synaptic transmission mediated by alpha-adrenergic receptors in area-CA3 of the rat hippocampus invitro. Journal of Neuroscience 13:5393-5401.

Scatton B, Simon H, Le Moal M, Bischoff S (1980) Origin of dopaminergic innervation of the rat hippocampal formation. Neurosci Lett 18:125-131.

Scoville WB, Milner B (1957) Loss of recent memory after bilateral hippocampal lesions. J Neurol Neurosurg Psychiatry 20:11-21.

Sederberg PB, Kahana MJ, Howard MW, Donner EJ, Madsen JR (2003) Theta and gamma oscillations during encoding predict subsequent recall. J Neurosci 23:10809-10814.

Sík A, Ylinen A, Penttonen M, Buzsaki G (1994) Inhibitory CA1-CA3-hilar region feedback in the hippocampus. Science 265:1722-1724.

Sík A, Penttonen M, Ylinen A, Buzsáki G (1995) Hippocampal CA1 interneurons: An in vivo intracellular labeling study. Neurosci 15:6651-6665.

Simon A, Olah S, Molnar G, Szabadics J, Tamas G (2005) Gap-junctional coupling between neurogliaform cells and various interneuron types in the neocortex. J Neurosci 25:6278-6285.

Singer W (1993) Synchronization of cortical activity and its putative role in information processing and learning. Annu Rev Physiol 55:349-374.

Skaggs WE, McNaughton BL (1996) Replay of neuronal firing sequences in rat hippocampus during sleep following spatial experience. Science 271:1870-1873.

Smith GM, Semke CW, Beecher HK (1962) Objective evidence of mental effects of heroin, morphine and placebo in normal subjects. J Pharmacol Exp Ther 136:53-58.

Sohal VS, Zhang F, Yizhar O, Deisseroth K (2009) Parvalbumin neurons and gamma rhythms enhance cortical circuit performance. Nature 459:698-702.

Soltész I, Deschénes M (1993) Low- and high-frequency membrane potential oscillations during theta activity in CA1 and CA3 pyramidal neurons of the rat hippocampus under ketamine-xylazine anesthesia. Journal of Neurophysiology 70:97-116.

Somogyi P (1977) A specific 'axo-axonal' interneuron in the visual cortex of the rat. Brain Res 136:345-350.

Somogyi P, Freund TF, Cowey A (1982) The axo-axonic interneuron in the cerebral cortex of the rat, cat and monkey. Neuroscience 7:2577-2607.

Somogyi P, Tamás G, Lujan R, Buhl EH (1998) Salient features of synaptic organisation in the cerebral cortex. Brain Res Rev 26:113-135.

Somogyi P, Fritschy JM, Benke D, Roberts JD, Sieghart W (1996) The gamma 2 subunit of the GABAA receptor is concentrated in synaptic junctions containing the alpha 1 and beta 2/3 subunits in hippocampus, cerebellum and globus pallidus. Neuropharmacology 35:1425-1444.

Squire LR (1992) Memory and the hippocampus: a synthesis from findings with rats, monkeys, and humans. Psychol Rev 99:195-231.

Squire LR, Zola SM (1998) Episodic memory, semantic memory, and amnesia. Hippocampus 8:205-211.

Staba RJ, Wilson CL, Bragin A, Jhung D, Fried I, Engel J, Jr. (2004) High-frequency oscillations recorded in human medial temporal lobe during sleep. Ann Neurol 56:108-115.

Sternberg S (1966) High-speed scanning in human memory. Science 153:652-654.

Szabadics J, Soltész I (2009) Functional specificity of mossy fiber innervation of GABAergic cells in the hippocampus. J Neurosci 29:4239-4251.

Szabadics J, Tamás G, Soltész I (2007) Different transmitter transients underlie presynaptic cell type specificity of GABAA,slow and GABAA,fast. Proc Natl Acad Sci U S A 104:14831-14836.

Szabadics J, Varga C, Molnár G, Oláh S, Barzó P, Tamás G (2006) Excitatory effect of GABAergic axo-axonic cells in cortical microcircuits. Science 311:233-235.

Takács VT, Freund TF, Gulyás AI (2008) Types and synaptic connections of hippocampal inhibitory neurons reciprocally connected with the medial septum. Eur J Neurosci 28:148-164.

Taxidis J, Coombes S, Mason R, Owen MR (2011) Modeling sharp wave-ripple complexes through a CA3-CA1 network model with chemical synapses. Hippocampus 22:995-1017.

Teng E, Squire LR (1999) Memory for places learned long ago is intact after hippocampal damage. Nature 400:675-677.

Tiitinen H, Sinkkonen J, Reinikainen K, Alho K, Lavikainen J, Naatanen R (1993) Selective attention enhances the auditory 40-hz transient response in humans. Nature 364:59-60.

Torres-Reveron A, Khalid S, Williams TJ, Waters EM, Jacome L, Luine VN, Drake CT, McEwen BS, Milner TA (2009) Hippocampal dynorphin immunoreactivity increases in response to gonadal steroids and is positioned for direct modulation by ovarian steroid receptors. Neuroscience 159:204-216.

Tóth K, Freund TF (1992) Calbindin D28k-containing nonpyramidal cells in the rat hippocampus: their immunoreactivity for GABA and projection to the medial septum. Neuroscience 49:793-805.

Tóth K, Borhegyi Z, Freund TF (1993) Postsynaptic targets of GABAergic hippocampal neurons in the medial septum-diagonal band of broca complex. JNeurosci 13:3712-3724.

Totterdell S, Hayes L (1987) Non-pyramidal hippocampal projection neurons: a light and electron microscopic study. J Neurocytol 16:477-485.

Traub RD, Miles R, Wong RK (1989) Model of the origin of rhytmic population oscillations in the hippocampal slice. Science 243:1319-1325.

Traub RD, Whittington MA, Colling SB, Buzsaki G, Jefferys JG (1996) Analysis of gamma rhythms in the rat hippocampus in vitro and in vivo. J Physiol (Lond) 493:471-484.

Traub RD, Whittington MA, Buhl EH, LeBeau FE, Bibbig A, Boyd S, Cross H, Baldeweg T (2001) A possible role for gap junctions in generation of very fast EEG oscillations preceding the onset of, and perhaps initiating, seizures. Epilepsia 42:153-170.

Tsodyks MV, Skaggs WE, Sejnowski TJ, McNaughton BL (1996) Population dynamics and theta rhythm phase precession of hippocampal place cell firing: a spiking neuron model. Hippocampus 6:271-280.

Tukker JJ, Fuentealba P, Hartwich K, Somogyi P, Klausberger T (2007) Cell type-specific tuning of hippocampal interneuron firing during gamma oscillations in vivo. J Neurosci 27:8184-8189.

Tulving E, Markowitsch HJ (1998) Episodic and declarative memory: role of the hippocampus. Hippocampus 8:198-204.

Umbriaco D, Watkins KC, Descarries L, Cozzari C, Hartman BK (1994) Ultrastructural and morphometric features of the acetylcholine innervation in adult rat parietal cortex: an electron microscopic study in serial sections. J Comp Neurol 348:351-373.

Van Groen T, Wyss JM (2003) Connections of the retrosplenial granular b cortex in the rat. J Comp Neurol 463:249-263.

Vanderwolf CH (1969) Hippocampal electrical activity and voluntary movement in the rat. Electroencephalogr Clin Neurophysiol 26:407-418.

Vann SD (2009) Re-evaluating the role of the mammillary bodies in memory. Neuropsychologia 48:2316-2327.

Varga V, Losonczy A, Zemelman BV, Borhegyi Z, Nyíri G, Domonkos A, Hangya B, Holderith N, Magee JC, Freund TF (2009) Fast synaptic subcortical control of hippocampal circuits. Science 326:449-453.

Vargha-Khadem F, Gadian DG, Watkins KE, Connelly A, Van Paesschen W, Mishkin M (1997) Differential effects of early hippocampal pathology on episodic and semantic memory. Science 277:376-380.

Vertes RP, Kocsis B (1997) Brainstem-diencephalo-septohippocampal systems controlling the theta rhythm of the hippocampus. Neuroscience 81:893-926.

Vida I, Frotscher M (2000) A hippocampal interneuron associated with the mossy fiber system. Proc Natl Acad Sci U S A 97:1275-1280.

Volk D, Austin M, Pierri J, Sampson A, Lewis D (2001) GABA transporter-1 mRNA in the prefrontal cortex in schizophrenia: decreased expression in a subset of neurons. Am J Psychiatry 158:256-265.

Wainer BH, Levey AI, Rye DB, Mesulam MM, Mufson EJ (1985) Cholinergic and non-cholinergic septohippocampal pathways. Neurosci Lett 54:45-52.

Wenk H, Ritter J, Meyer U (1975) [Histochemistry of cholinergic systems in the CNS. I. Topochemical and quantitative changes in acetylcholinesterase activity in the limbic cortex after septal lesions in the rat (author's transl)]. Acta Histochem 53:77-92.

Whishaw IQ, Vanderwolf CH (1973) Hippocampal EEG and behavior: changes in amplitude and frequency of RSA (theta rhythm) associated with spontaneous and learned movement patterns in rats and cats. Behav Biol 8:461-484.

Whittington MA, Traub RD, Jefferys JG (1995) Synchronized oscillations in interneuron networks driven by metabotropic glutamate receptor activation. Nature 373:612-615.

Whittington MA, Traub RD, Faulkner HJ, Jefferys JG, Chettiar K (1998) Morphine disrupts long-range synchrony of gamma oscillations in hippocampal slices. Proc Natl Acad Sci U S A 95:5807-5811.

Wilson RI, Nicoll RA (2002) Endocannabinoid signaling in the brain. Science 296:678-682.

Winson J (1978) Loss of hippocampal theta rhytm results in spatial memory deficit in the rat. Science 201:160-163.

Woodruff AR, Anderson SA, Yuste R (2010) The enigmatic function of chandelier cells. Front Neurosci 4:201.

Yamasaki M, Matsui M, Watanabe M (2010) Preferential localization of muscarinic M1 receptor on dendritic shaft and spine of cortical pyramidal cells and its anatomical evidence for volume transmission. J Neurosci 30:4408-4418.

Ylinen A, Bragin A, Nadasdy Z, Jando G, Szabo I, Sik A, Buzsaki G (1995) Sharp wave-associated high-frequency oscillation (200 Hz) in the intact hippocampus: network and intracellular mechanisms. J Neurosci 15:30-46.

Young KW, Billups D, Nelson CP, Johnston N, Willets JM, Schell MJ, Challiss RA, Nahorski SR (2005) Muscarinic acetylcholine receptor activation enhances hippocampal neuron excitability and potentiates synaptically evoked Ca(2+) signals via phosphatidylinositol 4,5-bisphosphate depletion. Mol Cell Neurosci 30:48-57.

Zaborszky L, Pang K, Somogyi J, Nadasdy Z, Kallo I (1999) The basal forebrain corticopetal system revisited. Ann N Y Acad Sci 877:339-367.

Zhu Y, Stornetta RL, Zhu JJ (2004) Chandelier cells control excessive cortical excitation: characteristics of whisker-evoked synaptic responses of layer 2/3 nonpyramidal and pyramidal neurons. J Neurosci 24:5101-5108.

Zsiros V, Maccaferri G (2005) Electrical coupling between interneurons with different excitable properties in the stratum lacunosum-moleculare of the juvenile CA1 rat hippocampus. J Neurosci 25:8686-8695.

Zsiros V, Aradi I, Maccaferri G (2007) Propagation of postsynaptic currents and potentials via gap junctions in GABAergic networks of the rat hippocampus. J Physiol 578:527-544.

IX. ACKNOWLEDGEMENTS

First of all I am deeply indebted to my supervisor Dr. Norbert Hájos, for the patient guidance, encouragement and advice he has provided throughout my time as a research assistant and subsequently as a PhD student. I have been extremely lucky to have a supervisor who cared so much about my work, who answered to my questions so willingly and patiently and who read the manuscript so many times as possible to weed out the mistakes.

I would like to thank Prof. Tamás Freund for providing me the possibility to work in the Institute of Experimental Medicine of the Hungarian Academy of Sciences, and also for his continuous support and encouragement during the years spent there.

I would like to express my gratitude to Dr. Attila Gulyás, who performed some of experiments of the second part of the thesis, and wrote the custom-made softwares which made my job much easier with data analysis.

I also wish to thank Dr. Noémi Holderith for performing the majority of anatomical experiments for both parts of the study.

I am also grateful to Dr. Ferenc Erdélyi and Dr. Gábor Szabó for the transgenic animal supply. I also wish to thank Gregori Erzsébet and Katalin Lengyel for their excellent technical assistance.

Also, I am grateful to my former colleague, Dr. Rita Zemankovics, who spent her time to read the manuscript thoroughly and provided it with useful comments and stimulating suggestions.

I thank to all the members of the Laboratory of Network Neurophysiology in the Institute of Experimental Medicine, for their everyday help in my work. Additionally, this dissertation could not have been written without the joyful and inspiring working atmosphere provided by them.

And finally I would like to express my deepest gratitude to my family in supporting me.

X. LIST OF PUBLICATIONS

Publications related to the dissertation

Szabó GG, Holderith N, Gulyás AI, Freund TF, Hájos N (2010) Distinct synaptic properties of perisomatic inhibitory cell types and their different modulation by cholinergic receptor activation in the CA3 region of the mouse hippocampus. Eur J Neurosci 31(12): 2234-2246.

Gulyás AI, **Szabó GG**, Ulbert I, Holderith N, Monyer H, Erdélyi F, Szabó G, Freund TF, Hájos N (2010) Parvalbumin-containing fast-spiking basket cells generate the field potential oscillations induced by cholinergic receptor activation in the hippocampus. J Neurosci 30(45): 15134-15145.

Other publication

Hájos N, Holderith N, Németh B, Papp OI, **Szabó GG**, Zemankovics R, Freund TF, Haller J (2012) The Effects of an Echinacea Preparation on Synaptic Transmission and the Firing Properties of CA1 Pyramidal Cells in the Hippocampus. Phytother Res. 26 (3): 354-362.